

5-7-1993

Gravity Sedimentation: A One-Dimensional Numerical Model

Joanna Robin Karl
Portland State University

Follow this and additional works at: https://pdxscholar.library.pdx.edu/open_access_etds



Part of the [Civil Engineering Commons](#)

Let us know how access to this document benefits you.

Recommended Citation

Karl, Joanna Robin, "Gravity Sedimentation: A One-Dimensional Numerical Model" (1993). *Dissertations and Theses*. Paper 4594.

<https://doi.org/10.15760/etd.6478>

This Thesis is brought to you for free and open access. It has been accepted for inclusion in Dissertations and Theses by an authorized administrator of PDXScholar. Please contact us if we can make this document more accessible: pdxscholar@pdx.edu.

AN ABSTRACT OF THE THESIS OF Joanna Robin Karl for the Master of Science in Civil Engineering presented May 7, 1993.

Title: Gravity Sedimentation: A One-Dimensional Numerical Model

APPROVED BY THE MEMBERS OF THE THESIS COMMITTEE:



Scott Wells, Chair



Shu-Guang Li



Gerald Rectenwald

A large fraction of the current cost of wastewater treatment is from the treatment and disposal of wastewater sludge. Improved design, energy efficiency, and performance of dewatering facilities could significantly decrease transport and disposal costs.

Dewatering facilities are designed based on field experience, trial and error, pilot plant testing, and/or full scale testing. Design is generally time-consuming and expensive. A full-scale test typically consists of side-by-side operation of 4 to 5 full-scale dewatering units for several weeks to more than 6 months. Theoretical modeling of the physics of dewatering units such as the belt filter press, based on laboratory determined sludge properties, would better predict dewatering performance.

This research developed a numerical computer model of the physics of gravity sedimentation. The model simulated the gravity sedimentation portion of the belt filter press. The model was

developed from a physically-based numerical computer model of cake filtration by Wells (1990).

As opposed to the cake filtration model, the inertial and gravity terms were retained in the gravity sedimentation model. Although in the cake filtration model, the inertial terms were shown to be negligible, according to Dixon, Souter, and Buchanan (1985), inertial effects in gravity sedimentation cannot generally be ignored. The region where inertia is important is the narrow interface between suspension and sediment. In the cake filtration model the gravity term was negligible due to the relatively large magnitude of the applied pressure; but in the gravity sedimentation model, since there was no applied pressure, it was necessary to consider the effect of gravity.

Two final governing equations were developed - solid continuity and total momentum with continuity ("momentum"). The finite difference equations used a "space-staggered" mesh. The solid continuity equation was solved using an explicit formulation, with a forward difference in time and central difference in space. The "momentum" equation used a fully implicit formulation with a forward difference in time. The modeler could choose either a central difference or forward difference in space. Non-linear terms were linearized. Boundary conditions and constitutive relationships were determined. Numerical errors in the numerical model were analyzed.

The model was calibrated to known data and verified with additional data. The model was extremely sensitive to the constitutive relationships used, but relatively unaffected by the Δt or the use of central difference or forward difference for the spatial derivative term in the "momentum" equation. Correlations of the calibrated model to data with a low initial concentration show that the constitutive parameters approximate the data, but not very well. Model runs with low initial concentration required the addition of artificial viscosity to remain stable.

The gravity term was always significant, whereas the inertial terms were many orders of magnitude less than gravity. However, the lower the initial concentration, the larger the inertial terms.

In addition to the belt filter press, the model can also be applied to cake filtration and design of gravity sedimentation tanks as well.

GRAVITY SEDIMENTATION: A ONE-DIMENSIONAL NUMERICAL MODEL

by

JOANNA ROBIN KARL

A thesis submitted in partial fulfillment of the
requirements for the degree of

**MASTER OF SCIENCE
in
CIVIL ENGINEERING**

**Portland State University
1993**

TO THE OFFICE OF GRADUATE STUDIES:

The members of the Committee approve the thesis of Joanna Robin Karl presented May 7, 1993.



Scott Wells, Chair



Shu-Guang Li



Gerald Rectenwald

APPROVED:



Franz Rad, Chair, Department of Civil Engineering



Roy W. Koch, Vice Provost for Graduate Studies and Research

TABLE OF CONTENTS

	PAGE
LIST OF TABLES	v
LIST OF FIGURES	vi
LIST OF SYMBOLS USED	viii
CHAPTER	
I INTRODUCTION	1
Background	1
Problem Description	5
II REVIEW OF THE LITERATURE	7
Introduction	7
General Theory	7
Sedimentation/Consolidation	7
One-Dimensional Nonlinear Finite Strain Consolidation Theory	12
Constitutive Relationships	14
Applied Theory	16
Gravity Thickening	16
Cake Filtration	20
III DEVELOPMENT OF THE GRAVITY SEDIMENTATION MODEL	22
Two Phase Flow Governing Equations	22
Summary - Two Phase Flow Governing Equations	22
Final Form of Governing Equations - Model Formulation	31

	Numerical Solution Technique	33
	Computational Strategy	36
	Boundary Conditions for ε and V_s	36
	Finite Difference Form of Continuity Equation	36
	Finite Difference Form of "Momentum" Equation	38
	An Analysis of the Modified "Momentum" Equation	43
	Artificial Diffusion (or Artificial Viscosity)	55
	Comparing the Numerical Model to an Analytical Solution by Soo	56
	Constitutive Relationships	57
IV	MODEL RESULTS	63
	Calibration to Gravity Sedimentation Data	63
	Model Verification	66
	Model Sensitivity	73
	Constitutive Relationships	73
	Central Difference vs. Upwind	73
	Time Step, Δt	76
	Effect of Artificial Diffusion	76
	Degree of Explicitness/Implicitness	76
	Magnitude of Terms	76
V	CONCLUSIONS AND RECOMMENDATIONS FOR FURTHER RESEARCH	83
	REFERENCES	85
	APPENDICES	
	A GRAVITY SEDIMENTATION - FORTRAN COMPUTER CODE	93
	B SAMPLE INPUT FILE	106
	C FORTRAN COMPUTER CODES FOR PROCESSING DATA AND MODEL OUTPUT	109

LIST OF TABLES

TABLE		PAGE
I	Milestones in the History of the Theory of Consolidation	10
II	Liquid Momentum: Comparison of Different Researchers' Equations - Initial Form	27
III	Liquid Momentum: Comparison of Different Researchers' Equations in Comparable Nomenclature	28
IV	Solid Momentum: Comparison of Different Researchers' Equations - Initial Form	29
V	Solid Momentum: Comparison of Different Researchers' Equations in Comparable Nomenclature	30
VI	Summary of Development of Governing Equations	34
VII	Discretization of Equation 3.9	39
VIII	Summary of Development of Equation 3.9 (Central Difference Scheme)	44
IX	Summary of Development of Equation 3.9 (Upwind Scheme)	46
X	Formulation of Modified Equation	49
XI	The Modified Equation (Central Difference)	50
XII	The Modified Equation (Upwind)	53
XIII	Statistics from Model Results for Suspended Solids Concentration Compared to Gravity Sedimentation Data for Kaolin Clay Suspensions	67

LIST OF FIGURES

FIGURE		PAGE
1.	Belt filter press schematic diagram (Viessman and Hammer, 1985)	4
2.	Liquid and solid continuity balance over a control volume	24
3.	Liquid momentum balance over a control volume	25
4.	Solid momentum balance over a control volume	26
5.	Grid layout used in the computer program, with the porosity array (EE) evaluated at the control volume center and the solid velocity array (US) evaluated at the control volume edges	37
6.	Comparison of explicit and implicit numerical strategies	40
7.	Comparison of central and upwind differencing.	41
8.	Comparison of Soo's (1989) analytical solution to the numerical model results . .	58
9.	Plot of data obtained from Wells (1990) and constitutive relationships for porosity, ϵ , vs. the effective stress, σ' , from Plaskett (1992) and Wells (1990) . .	60
10.	Plaskett's (1992) and Wells' (1990) relationships between porosity, ϵ , and the coefficient of volume compressibility, m_v	62
11.	Plot of porosity vs. permeability from cake filtration data for kaolin clay suspensions (Wells, 1990)	61
12.	Comparison of model predictions for suspended solids (solid lines) to data set SEDM1K (D2)	64
13.	Comparison of model predictions for solid velocity (solid lines) to data set SEDM1K (D2)	65
14.	Plot of mass vs. time for the model simulation which was calibrated to the SEDM1K (D2) data set	66
15.	Comparison of model predictions to data set SEDL2K (D7)	68
16.	Comparison of model predictions to data set SEDL3K (D10)	69
17.	Comparison of model predictions to data set DPK6 (D11)	70

18.	Comparison of model predictions to data set KDM10 (D13)	71
19.	Comparison of model predictions to data set LKD4 (D14)	72
20.	Comparison of constitutive relationships for permeability	74
21.	Sensitivity of constitutive relationships	75
22.	Sensitivities of central difference vs. upwind and time step	76
23.	Sensitivities of artificial diffusion and degree of explicitness/implicitness	78
24.	Order of magnitude of terms of Equation 3.9 at low initial concentrations at 3 minutes and 20 minutes	80
25.	Order of magnitude of terms of Equation 3.9 at medium initial concentrations at 3 minutes and 20 minutes	81
26.	Order of magnitude of terms of Equation 3.9 at high initial concentrations at 3 minutes and 20 minutes	82

LIST OF SYMBOLS USED

SYMBOL	DEFINITION
c	= concentration (M/L^3)
e	= void ratio
F	= $\varepsilon\mu/k$, averaged interfacial interaction term between the solid and the liquid phases [M/L^3-T]
g	= acceleration due to gravity [L/T^2]
k	= coefficient of permeability, intrinsic permeability [L^2]
m_v	= coefficient of volume compressibility [T^2-L/M]
p	= fluid static pressure [$M/L-T^2$]
n	= time level
P	= applied pressure [$M/L-T^2$]
P_1	= local pressure of the liquid [$M/L-T^2$]
P_s	= local pressure of the solid [$M/L-T^2$]
t	= time [T]
u	= excess pore water pressure [$M/L-T^2$]
u_w	= pore water pressure (defined as partial pressure) [$M/L-T^2$]
V_1	= true liquid velocity (in contrast to the Darcy velocity [L/T])
V_0	= true liquid velocity at $z=0$ [L/T]
V_s	= velocity of the solid particles [L/T]
v_w	= velocity of the fluid [L/T]
z	= distance from filtration medium [L]
α	= empirical constant [L^2]
β	= empirical constant [-]; a monotonic function of the void ratio, e [-]
θ	= explicit-/implicit-ness ($\theta=0$ fully implicit; $\theta=1$ fully explicit)
μ	= dynamic (or absolute) viscosity [$M/L-T$]
ε	= porosity (volume liquid/total volume) [-]
ε_0	= terminal porosity at $z=0$ [-]
ε_1	= empirical constant corresponding to limiting porosity [-]

- ζ = empirical constant [M/L-T²]
 ξ = "convective" coordinate [L²/T²]
 ν = coefficient for dimensional consistency [L-T²/M]
 ρ_l = liquid density [M/L³]
 ρ_s = solid density [M/L³]
 ρ_w = density of water (weight per unit of its own volume) [M/L³]
 σ = Total stress applied to the system; [M/L-T²]
 σ' = effective stress (interparticle pressure) [M/L-T²]
 σ'_1 = empirical constant corresponding to limiting effective stress [M/L-T²]
 ω' = artificial diffusion coefficient [L²/T]

CHAPTER I

INTRODUCTION

BACKGROUND

Production of sewage sludge, the residual from municipal wastewater treatment plants, has increased two-fold over the past 20 years in the United States (Morse, 1989). The current annual sludge production is over 8 million dry tons (EPA, 1990, as cited by Ravenscroft, 1992). Wastewater treatment costs are currently increasing, with sludge treatment and disposal representing a large fraction of the overall treatment cost. Since sludges typically consist of approximately 95% water (Villiers and Farrell, 1977), costs are significantly decreased by dewatering. Dewatering effectively minimizes the volume and mass of the sludge. Resultant transportation cost savings can be dramatic, as noted in Villiers and Farrell's (1977) example of a 50% decrease in cost resulting from increasing the sludge solids content from 20% to 30%.

Sludge disposal, which is regulated by a combination of state agencies and the Environmental Protection Agency (EPA), primarily consists of landfilling (64%), incineration (14%), land application (9%), distribution and marketing (6%), and ocean dumping (5%) - (EPA, 1990, as cited by Ravenscroft, 1992). The Federal Ocean Dumping Ban Act of 1988 prohibited ocean dumping of sludge. In January 1992, New York City became the last major city to halt its ocean dumping practices (Ravenscroft, 1992).

Landfilling of wet sludge, which may result in leachate problems, are discouraged or banned. Greater amounts of landfill space are required for wetter sludges, due to its increased volume. With landfill siting tending to be further from the population centers (due to the Not-in-my-Backyard, or NIMBY, syndrome) and with new environmental regulations for landfill construction and closure,

transportation and disposal costs for landfilling are rising.

Incineration is not possible if the sludge is too wet for combustion. Land application of extremely wet sludge cakes has more probability of odors, insects, or liquid runoff (Smith et al, 1989), and greatly increases the required land area (Villiers and Farrell, 1977). And composting of sludge with wet cakes is far less economical due to the costs of maintaining a specific moisture and temperature range (Smith and Semon, 1989). According to Smith and Semon (1989), the acceptable minimum solids content may vary for different means of disposal, i.e, 18% for narrow trench landfilling, 24% for combustion, and 28-30% for economical operation of an incineration facility. Due to economic, social, and environmental pressures regarding sludge disposal, an increased emphasis is being placed on the need for improved efficiency and performance of the wastewater treatment plant's sludge dewatering treatment process.

Development of processes for dewatering of wastewater sludge began toward the end of the 19th and beginning of the 20th century (Dick and Ball, 1980). Equipment for dewatering wastewater sludge include vacuum filters, filter presses, belt filter presses, gravity filters, and centrifuges. Vacuum filtration is intrinsically limited by the available vacuum, and centrifugation has been limited by practical machine speeds, such that neither can develop sufficient force on the cake to move the free water from the interior of the cake as it is formed (Villiers and Farrell, 1977). Nevertheless, recent advances in centrifugation technology have made this process more efficient in sludge dewatering. The belt filter press squeezes the water out of a sludge layer compressed between two porous woven fiber belts, and thus can remove more of the residual water (Villiers and Farrell, 1977).

Belt filter presses, initially designed to dewater paper pulp, were modified in the early 1960s in Germany by Klein to dewater sewage sludge (Villiers and Farrell, 1977). Although the belt filter press was introduced into the United States by Carter in 1971 (Villiers and Farrell, 1977), the difference between U.S. and European sludge led to low cake solids and poor solids capture (EPA, 1987). Early belt filter presses demonstrated poor performance and durability, as compared to vacuum filters and centrifuges, and often required large dosages of conditioning chemicals (EPA, 1986). These

early problems led to American manufacture of the belt filter press. The first American belt filter presses were based on the design of belt conveyors and were much lighter than their European counterparts, and thus were plagued with mechanical failures of rollers and bearings (EPA, 1987). By the late 1970s, American manufacturers made significant improvements, considerably reducing failures, and leading to an increased popularity of the belt filter press (EPA, 1987). Furthermore, compared to other mechanical dewatering equipment, belt filter presses have very low power requirements and are quite energy conservative (EPA, 1987). Thus, although the belt filter press is a relatively new addition in the variety of commercially available sludge dewatering equipment, it is now marketed by ten to fifteen different manufacturers in the U.S. (Searle and Bennett, 1987).

Design of dewatering equipment, such as the belt filter press, is based on field experience, trial and error, pilot plant testing, and/or full scale testing. Time-consuming and expensive, full-scale dewatering tests might include four to five side-by-side full-scale dewatering units for time periods ranging from several weeks to over 6 months (EPA, 1982; as cited in Wells, 1988).

Use of dewaterability tests in the lab, such as the specific resistance test, have not been able to predict full-scale equipment performance (EPA, 1987; as cited in Wells, 1988). Although small-scale dewatering units may provide more accuracy than the lab tests, obtaining operational data may be expensive and time-consuming (Wells, 1988).

Better prediction of dewatering performance could be provided by use of theoretical modeling of the physics of the belt filter press based on laboratory determined sludge properties. Thus, optimal design and operations of a belt filter press could be determined without the necessity of full-scale testing. This is in contrast to empirical models of sludge dewatering processes, which are each applicable only to specific sludges. Because each sludge must be verified independently, a relatively large experimental effort is required. And since physical properties of sludge change with time, such empirical data and models derived from them may have limited value.

To date, no numerical studies of dewatering for the belt filter press have been developed which incorporate all the physical phenomena of the process. An operating belt filter press continuously

dewaters sludge (after chemical conditioning) by gravity drainage and mechanically-applied pressure in both a low pressure "wedge" zone and high pressure "shear" zone, as shown in Figure 1.

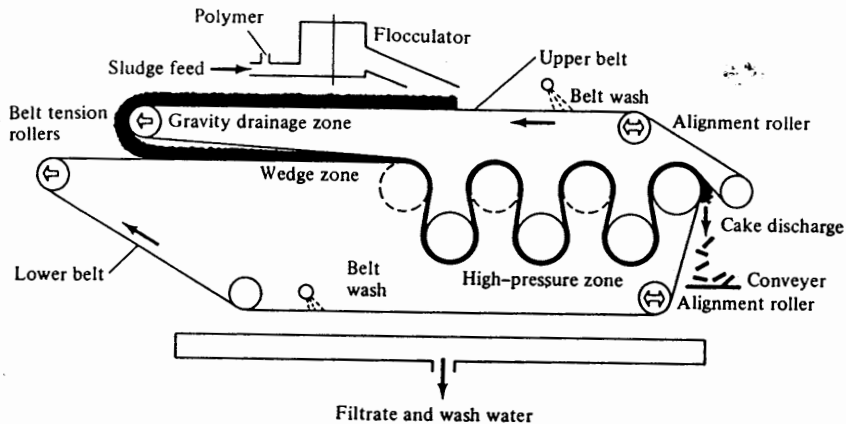


Figure 1. Belt filter press schematic diagram (Viessman and Hammer, 1985).

In the gravity drainage zone, approximately one-half or more of the water is removed, and suspended solids content is doubled (Viessman and Hammer, 1985), or even tripled (EPA, 1986; and EPA, 1987). Gravity drainage is essential to create a great enough solids concentration for the sludge to be squeezed between the belts (Task Committee on Belt Filter Presses, 1988). Within the low pressure "wedge" zone, the sludge is gradually compressed between the upper and lower belts, forming a firm sludge cake able to withstand the shear forces within the high pressure zone. Within the high pressure "shear" zone, the confined sludge layer is subjected to both compression and shearing action caused by the outer belt being a greater distance from the center of the roller than the inner belt (Viessman and Hammer, 1985).

PROBLEM DESCRIPTION

This study focuses on the physical modeling of the gravity drainage (or sedimentation) portion of the belt filter press operation. The model was developed from a physically based numerical computer model of cake filtration developed by Wells (1990), which solved a non-linear, partial differential equation with an explicit finite difference procedure.

Both the gravity sedimentation and cake filtration models were based on the same governing equations for two-phase flow: liquid continuity, solid continuity, liquid momentum, and solid momentum. Whereas cake filtration may occur due to either a gravity head or applied pressure, gravity sedimentation is driven only by gravity. Thus, in Wells' (1990) cake filtration model the gravity term was negligible due to the relatively large magnitude of the applied pressure, but in the gravity sedimentation model, since there was no applied pressure it was necessary to consider the effect of gravity.

Although in the cake filtration model the inertial terms were shown to be negligible, according to Dixon, Souter, and Buchanan (1985), inertial effects in gravity sedimentation cannot be generally ignored. The region where inertia is important is the narrow interface between suspension and sediment.

The strategy in developing the gravity sedimentation model involved the following:

- (1) Determination of the solid and liquid continuity and momentum equations;
- (2) Derivation of the final equations to be solved numerically;
- (3) Development of a numerical solution strategy;
- (4) Determination of boundary conditions and constitutive relationships;
- (5) Analysis of numerical errors in the numerical model; and
- (6) Comparison of model predictions to known data.

The governing equations used in this study were compared to those developed by other investigators. Two final equations were developed: (1) solid continuity, and (2) total momentum with continuity (derived based on a technique used by Soo in 1989, and referred to as the "momentum" equation). First, the solid continuity equation was solved to determine porosity at the next time step. Then the "momentum" equation was solved for the solid velocity, also at the next time step.

Boundary conditions were required for the equations being solved. Constitutive relationships were developed for "k" (intrinsic permeability) and "m," (coefficient of volume compressibility), both functions of porosity, which accounted for the sedimentation zone and the transition zone (between free settling and the cake).

Different computational strategies were used for each of the two final equation included in the numerical solution. A finite difference equation was developed with a "space-staggered mesh", such that porosity was evaluated at the control volume center and solid velocity was evaluated at the control volume edges. An explicit formulation was used to solve the solid continuity equation with a forward difference in time and a centered difference in space. A fully implicit formulation (which required linearization of the non-linear terms) was used for the "momentum" equation, with a forward difference in time. Both upwinding and central differences were used for the spatial derivatives. As the model was developed and refined, a number of other computational schemes were tried for the "momentum" equation. The computer code was developed to be as general as possible with the ability to toggle between alternate schemes.

Analysis of the modified "momentum" equation indicated which terms led to instability due to numerical dispersion. This was used to determine how much "artificial viscosity" was necessary to reduce these numerical errors (by adding numerical diffusion) and smooth out the solution.

And finally, the model physics were verified by comparison to gravity sedimentation porosity data collected by Wells and Dick (1988) at the Cornell High Energy Synchrotron Source (CHESS).

CHAPTER II

REVIEW OF THE LITERATURE

INTRODUCTION

Research in sedimentation and consolidation has been applied to environmental engineering, material science, marine geology, coastal engineering, biotechnology, chemical engineering, mining engineering, and geotechnical engineering (Schiffman, 1985). This research involves soil or soil-like materials, the compressibility and permeability properties of a porous material, and time effects. The applications differ in the time scale of interest. For example, the geologist is interested in millions of years, while the geotechnical engineer is generally concerned with the one- to fifty-year life of a constructed facility, and the chemical engineer involved with filtration processes is concerned with seconds (Schiffman et al., 1985).

The following literature review focuses on: (1) general theory, such as sedimentation/consolidation, one-dimensional nonlinear finite strain theory, and constitutive relationships; and (2) applied theory, such as gravity thickening and cake filtration.

GENERAL THEORY

Sedimentation/Consolidation

Hindered Settling. Although sedimentation processes were used in chemical engineering for many years, until 1950 most of the experimental work was based on Stokes law (1851; as cited by Richardson and Zaki, 1954) and assumed a steady-state process (Lamb, 1932; as cited in Schiffman et al., 1985). The settling velocity, a function of the Stoke's velocity and the particle concentration, was considered to be a "material" property of the mixture (Schiffman et al., 1985) and was based on the

motion of a single spherical particle in an infinite fluid (Richardson and Zaki, 1954).

The settling of slimes, containing particles with a wide range of sizes, were studied by Coe and Clevenger in 1916 (Richardson and Zaki, 1954). Although sedimentation usually began at a constant rate, they noted a progressive decrease in the rate of sedimentation as thickening occurred.

A modification of the Stokes' law was suggested in 1926 by Robinson (Richardson and Zaki, 1954) for predicting the settling rates of suspensions of fine uniformly sized particles.

Steinour studied the sedimentation of suspensions of uniform particles under conditions of streamline flow in 1944 (Richardson and Zaki, 1954). He assumed that the effect of concentration could be taken into account by using the density of the suspension and the viscosity of the liquid, and that a function of the porosity could be used to account for the shape and size of the flow spaces.

Hawksley expressed a rate of settling of concentrated suspensions based on the assumption that during the settling process an "equilibrium arrangement" of particles was established (Richardson and Zaki, 1954).

All three researchers - Robinson, Steinour, and Hawksley - assumed that the effective buoyancy force acting on the particles depends on the density of the suspension. Richardson and Zaki (1954) demonstrated that the falling velocity of a suspension relative to a fixed horizontal plane was equal to the upward velocity of liquid required to maintain a suspension at the same concentration. Their work showed that the earlier assumption - that the effective gravitational force acting on a particle in a suspension was determined by the density of the suspension and that the drag on the particles was a function of the apparent viscosity - could not be true for a suspension of uniform particles.

The theoretical background of sedimentation was established by Kynch (1952; as cited in Schiffman et al., 1985) and Richardson and Zaki (1954; as cited in Schiffman et al., 1985). Kynch realized that the settling process of uniform dispersions was a highly transient process. The theory of hindered settling - the downward motion of solid particles as they coalesce and their packing density increases - developed by Kynch primarily focused on the continuity of the solid phase. This simplifies

the problem because effective stresses in the sediment formed at the bottom of the dispersion were ignored, and the velocity of the solid particles was a function solely of the porosity (Schiffman et al., 1985). Thus, the particulate suspension is characterized over the entire concentration range by a single relationship between settling velocity and concentration of solids, implying the existence of a flux curve for each slurry (Kos, 1985). Schiffman et al. (1985) noted that as the concentration of solids tended to zero, Kynch's theory reduces to Stokes' theory.

Kynch's concept was used by nearly all of the disciplines concerned with settling phenomena (Schiffman et al., 1985). This theory was elaborated by chemical engineering literature, and applied to continuous thickening processes of sludges (Schiffman et al., 1985). In 1980, Shin and Dick noted that Kynch's assumption that the settling velocity of a suspension was a function of the particle concentration only may not be valid for flocculent suspensions, and thus the initial settling velocity data might not accurately represent the settleability of a suspension as it was formed during thickening. Because the Kynch theory applied only to sedimentation of particulate suspensions, it assumed no interparticle contacts and postulated the existence of only one settling velocity for each solids concentration (Kos, 1985). Sedimentation of flocculated suspensions could not be described by Kynch theory because a certain quantity of water, kept by the flocks, could be expelled from the sediment except by means of compression (Concha and Bustos, 1985). The various shapes of batch settling curves for flocculent suspensions, which are the result of the consolidation of the interconnected matrix of solids, thus cannot be described by the Kynch theory (Kos, 1985).

Consolidation. According to Schiffman et al. (1985), "The theory of consolidation is a continuum theory designed to predict the progress of deformation of an element of a porous material when this element is subjected to an imposed disturbance. The porous medium is defined, in the general case, as a system of interacting continua where each component continuum is governed by its constitutive (stress-strain and flow) relationships."

Five milestones in the history of the theory of consolidation are shown in Table I (Schiffman et al., 1985):

TABLE I
MILESTONES IN THE HISTORY OF THE THEORY OF CONSOLIDATION

RESEARCHER (YEAR)	TYPE OF THEORY OF CONSOLIDATION	DESCRIPTION
1. Terzaghi (1923), Znidarcic and Schiffman, 1982)	One-dimensional theory of consolidation (Terzaghi) formulated in a finite strain theory assuming that compressibility and the reduced coefficient of permeability are constant (Znidarcic and Schiffman)	The reduced coefficient of permeability is defined as $k/(1+e)$ where k is the conventionally measured coefficient of permeability and e is the current void ratio.
2. Terzaghi (1942)	One-dimensional theory of consolidation reformulated in an infinitesimal strain theory with linear properties for constant compressibility and coefficient of permeability	This is conventional theory. A first attempt at the transformation of the 1923 theory to infinitesimal strains was provided by Terzaghi and Fronlich (1936); however, this work was somewhat ambiguous with regard to the definition of strain.
3. Mikasa (1963), Gibson, England and Hussey, 1967)	One-dimensional nonlinear finite strain theory of consolidation	Unrestricted with respect to the magnitude of strain and the variations of compressibility and permeability save that they are single-valued functions of the void ratio alone.
4. Biot (1941)	Coupled multi-dimensional infinitesimal strain theory of consolidation	In 1956, this theory was clarified by Biot by defining Darcy's law in terms of the relative velocity between the fluid and solids.
5. Biot (1972), Carter, Small and Booker (1977)	Multi-dimensional nonlinear finite strain theory of consolidation where both the deformations and the fluid flow occur in more than one-dimension	Mathematical complexity and the lack of verifiable information on multi-dimensional constitutive models applicable to soft clay have limited development of such models.

One-dimensional nonlinear finite strain consolidation theory developed in both the geotechnical (Mikasa, 1963; Gibson, England and Hussey, 1967; as cited in Schiffman et al., 1985) and chemical engineering fields (Shirato et al., 1970; Kos, 1977; Dixon, 1979; Tiller, 1981; as cited in Schiffman et al., 1985) are reviewed below.

More recently, Kynch's theory has been generalized to take account of a zone of consolidation below the suspension (Tiller, 1981; as cited in Schiffman et al., 1985; Fitch, 1983; as cited in Schiffman et al., 1985). The new equations by Tiller (1981) take account of the sediment rising from the bottom of the settling chamber.

A Linked Theory. Been (1980; as cited in Pane et al., 1985) has demonstrated that consolidation and hindered settling derive from the same basic principles, and that by setting the effective stress to zero, hindered settling can be deduced from consolidation. Schiffman et al. (1985)

explain that when the concentration was defined as the volume fraction (i.e. $c = 1-n$, where n is the porosity of the suspension and c is the volumetric concentration of particles) the equation for hindered settlement led to the solid continuity equation. This equation was also the Gibson, England and Hussey (1967; as cited in Schiffman, et al., 1985) consolidation equation, with the void ratio as the dependent variable in which the vertical effective stress was everywhere zero. Thus, Been was able to show that Kynch's theory of hindered settlement (1952) was one component of the more general Gibson, England, and Hussey non-linear finite strain theory of consolidation (1967) - logically linking sedimentation (hindered settling) and consolidation.

This single theoretical basis for sedimentation and consolidation processes of solid-water mixtures was provided by modifying the effective stress principle (Schiffman, Pane and Gibson, 1984; as cited in Schiffman et al., 1985) and by extending the concept of the permeability to the dispersed state (Pane, 1985; as cited in Schiffman et al., 1985). However, the use of the concept of hindered settling and the qualitative linkage between sedimentation and consolidation has long been recognized by environmental (or sanitary) engineers (Mohlman, 1934; as cited in Schiffman et al., 1985).

Harris, Somasundaran and Jensen (1975; as cited in Schiffman et al., 1985) and Somasundaran (1981; as cited in Schiffman et al., 1985) have studied the process of sedimentation and consolidation primarily from an experimental and phenomenological viewpoint. Tiller (1981; as cited in Schiffman et al., 1985) developed consistent equations for both sedimentation and consolidation phases and linked the two by matching the boundary condition at the interface between phases.

Schiffman et al. (1985) noted that the study of coupled sedimentation and consolidation had been limited to an abrupt change from a dispersion to a soil. Within a transition zone there was a wide range of void ratios where even relatively inert clay dispersions exhibited fabric changes and intrinsic time dependency. Pane and Schiffman (1985) noted that studies by Michaels and Bolger (1962) and by Been and Sills (1981) have shown the existence of a transition zone between the dispersion and soil (i.e., the pelagic deposition of a sediment column) characterized by large concentration gradients with depth.

Two aspects of the sedimentation/consolidation theory - the constitutive relationships of the medium and the finite strain nature of the deformations are discussed below.

One-Dimensional Nonlinear Finite Strain Consolidation Theory

One-dimensional finite strain consolidation theory was independently developed by Mikasa in 1963, and Gibson, England, and Hussey in 1967 (Townsend and Hernandez, 1985).

Gibson, et al. (Gibson, Schiffman, and Cargill, et al.; 1981, as cited in Benson; 1987) derived their finite-strain consolidation equation by applying the continuity equation, force equilibrium, porewater equilibrium, Darcy equation, and effective stress principle to a differential element of the compressible media. Their model considered the value of the hydraulic conductivity at each point in the consolidating layer for all times during the consolidation process. Their model showed that as the material near the filter compacted due to the very large effective stress gradient, the resistance to the flow of water through this thin compacting layer increased causing a slowing of the consolidation process (Benson, 1987).

According to Townsend and Hernandez (1985), the theory of Gibson et al. (1967) had the following advantages over previous theories: incorporation of the nonlinearity of both permeability and compressibility with depth, inclusion of the influence of self-weight of the consolidating layer, and removal of limitation to infinitesimal strains.

According to Townsend and Hernandez (1985), Gibson et al.'s (1981) one-dimensional finite strain equation was reformulated by Somgyi (1980) using a material coordinate system such that it described the excess pore pressure during consolidation; an alternating direction explicit finite difference procedure was used for its solution. As a result of this reformulation of the finite strain consolidation equation, the conventional coefficient of consolidation was seen to be a highly non-linear function of the void ratio. Both Somogyi and Gibson et al. incorporated this nonlinear function into their finite strain solutions, while others such as Yong and Ludwig (1984; as cited in Townsend and Hernandez, 1985) and Olson and Ladd (1979; as cited in Townsend and Hernandez, 1985) selected a piecewise linear consolidation model. The piecewise linear consolidation theory uses an assumption of

continuous loading, nonlinear soil properties and nonhomogeneity (Townsend and Hernandez, 1985).

The classical consolidation theory was formulated by Yong and Ludwig (1984; as cited in Townsend and Hernandez, 1985). Although "the overall solution of the problem was nonlinear, the coefficients of permeability (k) and compression (a_v) remained constant for each time step and were continually updated by taking small time steps."

Development of numerical procedures has been reported for a wide variety of field situations as cited by Schiffman et al. (1985): Shirato et al. (1970), Pane (1981), Somogyi, Keshian, and Bromwell (1981), and Mikasa and Takada (1984). Also, Townsend and Hernandez (1985) reported that finite strain numerical analyses and piecewise linear models have been used to provide design predictions for predicting the rates and magnitudes of settlement/consolidation in phosphate mining in Florida (Townsend and Hernandez, 1985).

Townsend and Hernandez (1985) determined that numerical models based upon effective stresses were only appropriate for consolidation phases. They found that physical models (such as by using a centrifuge to evaluate consolidation properties) were a viable technique for validating numerical models and programs. Also, Townsend and Hernandez (1985) concluded that the physical models could represent the sedimentation/consolidation phases, provided the appropriate time scaling component was used. According to Schiffman et al. (1985) centrifuge validation of nonlinear finite strain consolidation for soft and very soft materials was presented by Bloomquist and Townsend (1984), Croce, et al. (1984), Leung, et al. (1984), Mikasa and Takada (1984), and Scully et al. (1984).

To a large extent, existing theory of nonlinear finite strain consolidation was limited to one-dimension. Some work published by Somogyi et al. (1981; as cited by Schiffman, 1985) used a simplified theory incorporating multi-dimensional flow but maintaining one-dimensional compression. Some work has been undertaken to develop a fully coupled theory of multi-dimensional finite strain by Carter, Small, and Booker (1977; as cited by Schiffman, 1985).

Schiffman, Pane, and Sunara (1985) summarized their research by stating that nonlinear finite strain consolidation theory was an accurate predictor of field performance and that it should replace the

use of conventional theory. Their research of nonlinear finite strain theory indicated the following in comparison to conventional theory: (1) progress of settlement was substantially faster; (2) dissipation of excess pore water pressure of a loaded clay layer was substantially slower than the progress of settlement; (3) the vertical effective stresses was generated faster in many cases - especially those involving slow accumulation of material; and (4) the measured values of the change in compressibility and permeability as function of the void ratio replaced the use of a single value of the coefficient of consolidation.

Constitutive Relationships

In order to define the physical properties of a porous medium, a constitutive model describing filtration and deformation properties must be developed (Kos, 1985).

These constitutive relationships were:

- (1) an interrelationship between the component stresses (i.e., the effective stress principle), and
- (2) a definition of flow of fluid through the porous medium.

Effective Stress Principle. Effective stress is a measure of the soil or intergranular pressure. The effective stress principle states that there is a state of stress σ' , which is responsible for the deformation of the porous deformable mineral skeleton. The porous medium is a two-phase system consisting of a deformable mineral skeleton filled with an incompressible liquid (water), such that the effective stress principle can be formulated as:

$$\sigma = \sigma' + u_w \quad (2.1)$$

σ = total stress applied to the system [M/L-T²]
 σ' = effective stress (inter-particle pressure) [M/L-T₂]
 u_w = porewater pressure [M/L-T₂]

The effective stress principle governs the deformation of a porous medium, such as in the consolidation zone. At the top of the settling zone, the total stress and the pore water pressure were equal when as measured in a sedimentation column by Michaels and Bolger (1962; as cited in Schiffman et al., 1985), Been (1980; as cited in Schiffman et al., 1985), and Been and Sills (1981; as

cited in Schiffman et al., 1985). Schiffman, et al. (1985) note that this indicates the particles have not aggregated and thus the effective stresses are zero. According to Michaels and Bolger (1962) and Been (1980), a thin transition zone separating the settling and consolidation zones exists where the effective stresses are non-zero, but do not follow the Equation 1 (Schiffman et al., 1985). As a result of these observations, the effective stress equation was restated in a more general form as follows (Schiffman, Pane, and Gibson, 1984; Pane, 1985; Pane and Schiffman, 1985; as cited in Schiffman et al., 1985):

$$\sigma = \beta(e)\sigma' + u_w \quad (2.2)$$

- σ = Total stress applied to the system [M/L-T²]
- β = A monotonic function of the void ratio, e [-]
- σ' = Effective stress (inter-particle pressure) [M/L-T²]
- u_w = Porewater pressure [M/L-T²]

Kos investigated a model for constitutive theory which deviated from the work of previous investigations of compression during gravity thickening. While the earlier investigations had counterparts in soil consolidation and modern cake filtration theory, Kos' models were developed on the basis of a detailed measurement of filtration and consolidation properties of flocculent suspensions during continuous thickening. Thus, Kos' models reflect changes of structure of the flocculent porous medium during compression.

Flow Relationships. In both sedimentation and consolidation there were two absolute velocities - that of the solid particles and that of the fluid. The coefficient of permeability of the system, k , is the proportionality factor which relates the relative seepage velocity and the excess pore water pressure gradient, according to the Darcy-Gersevanov law (Darcy, 1856; Gersevanov, 1934; Verruijt, 1969; as cited in Schiffman et al., 1985):

$$k = \varepsilon \frac{(v_l - v_s)}{\frac{\partial u_w}{\partial \xi}} \rho_w \quad (2.3)$$

- k = coefficient of permeability [L^2]
 ε = porosity [-]
 v_l = velocity of the fluid [L/T]
 v_s = velocity of the solid particles [L/T]
 u_w = excess pore water pressure [$M/L-T^2$]
 ξ = "convective" coordinate [L^2/T^2]
 ρ_w = density of water [M/L^3]

Tiller and Green (1973; as cited in Tiller et al., 1985) in the theory of flow through compressible cakes, demonstrated that the flow rate of a highly compressible material reached a constant value when the pressure drop exceeded some relatively low value. Resistance to flow increased at that point in direct proportion to the pressure drop, and no increase in flow rate took place with increasing pressure and the average porosity reached an essentially constant value at the same point (Tiller et al., 1985).

APPLIED THEORY

Gravity Thickening

Introduction. Gravity thickening is a solid-liquid separation process. Because the particles are more dense than the liquid, the gravitational force per unit volume of particles is greater than that per unit volume of liquid, causing particles to move downwards relative to the liquid. The bottom of the container restricts particle movement, resulting in an increase in average particle concentration in the lower parts of the container (Dixon, 1979).

Suspensions of fine particles are usually treated with coagulants, to cause particles to form aggregates before they can be successfully separated by gravity. The forces opposing the downward motion of flocs are: (1) inter-particle forces, resisting increase in particle concentration, and (2) liquid-drag forces from the relative motion of flocs and liquid (Dixon, 1979). In a "thickening" process, the

particles move closer together, resulting in increased particle concentrations such that the inter-particle force is the primary force which opposes the gravitational force. The drag force which occurs due to the relative motion between the particles and liquid during thickening is a secondary force opposing the gravitational force (Dixon, 1979).

In comparison, clarification - which precedes thickening - involves the relative motion between flocs and liquid. Thus, the drag force is the primary force which opposes the gravity. Therefore, clarification only occurs at a sufficient distance above the bottom of the container that thickening from inter-particle forces transmitted from the bottom is negligible. In the clarification region, the velocity varies with the particle concentration since the drag force varies with the relative velocity of flocs and liquid and with the particle concentration (Dixon, 1979).

History. The earliest work on gravity thickening was carried out at the Tigre Mining Company in Sonora, Mexico, as reported by Mishler in 1912 (Okey, 1989). This study demonstrated a bench-scale technique, which was used to define the inter-relationship between solids concentration, settling velocity, tank depth, tank area and thickening capacity. In 1916, Coe and Clevenger introduced the concept of thickener capacity - that each concentration layer of a suspension in a continuous thickening tank has a certain capacity to transmit solids - as follows (Kos, 1985):

$$CAP = \frac{u_i}{\frac{1}{c_i} - \frac{1}{c_u}} \quad (2.4)$$

- CAP = capacity of a suspension at concentration c_i to transmit solids
 u_i = the zone settling velocity obtained from the linear portion at the beginning of the sedimentation curve [L/T]
 c_u = underflow concentration [M/L³]

Coe and Clevenger (1916), and later Kynch (1952), provided methods for obtaining sedimentation rates from static, batch tests used for designing continuous thickeners (Wakeman and Holdich, 1984).

Thickeners were first reported for environmental applications by Comings (1940) and Kammermeyer (1941). Works were published by Torpey and co-workers on the co-thickening of primary with waste activated and primary with digested sludge (Torpey, 1954; Torpey and Melbinger, 1967). Torpey optimized the operation of gravity thickeners by strict attention to the critical operational factors (Okey, 1989).

During the latter portion of the '60s and into the '70s, substantial contributions to the theory of the thickening of flocculent and compressible solids were made (Dick and Ewing, 1967; Edde and Eckenfelder, 1968; Vesilind, 1968; Dick, 1970; Dick and Young, 1972; Cole et al., 1973; Kos, 1977; and Fitch, 1979). However, gravity methods seldom produced solids concentrations greater than 1.5%-2.5% solids by weight in operating facilities (Okey, 1989).

Flotation thickening was investigated in the mid-fifties, and 1.0%-4.0% solids were obtained without polymer (Eckenfelder et al., 1958 and Howe, 1958). By the mid-sixties, data were presented showing that primary and activated sludge mixtures could be flotation thickened to 4.0%-8.0% with the use of polymers (Wahl et al., 1964). A comprehensive thickening study, appearing in the literature by Mulbarger and Huffman (1970), showed that flotators could thicken waste activated sludge to 4.0%-5.0% solids (Okey, 1989).

Dixon, Souter, and Buchanan (1976) concluded that inertial effects in sedimentation could not be generally ignored in all cases. While most researchers ignored the inertial effects, they concluded that the region where inertia was important was the narrow interface between suspension and sediment where rapid velocity change was occurring. Above the thickening region interface, the particles settled at the terminal velocity corresponding to the initial concentration and did not experience acceleration or retardation. Below the thickening interface, the solid velocity was approximately zero. The inertial effects in the narrow region at the interface were due to retardation of the particles as they struck the top of the sediment (Dixon, Souter, and Buchanan, 1976).

Dixon (1979) also studied batch thickening of an initially uniform suspension. He concluded that when the suspension was initially in free settling, the inertial effects could not normally be

neglected because the initial subsidence rate would be maintained until nearly all the particles had entered the compression zone. When the suspension was initially in compression, inertial effects were normally negligible.

In 1984, Wakeman and Holdich considered the distributions and magnitudes of weight, drag, inertial, and solids compressive stresses in sedimentation. The inertial effects in different parts of the column were found to be very small everywhere.

Settling Properties of Sludges. Gravity thickening can be carried out as a batch or a continuous process. In the batch process, a tank with a dilute material is allowed to settle for a desired period of time, after which the clear liquid (supernatant) is decanted and the thickened suspension is removed from the bottom of the tank. The continuous process of gravity thickening has continuous feed and continuous or periodic withdrawal of the thickened suspension from the tank bottom. Historically, the batch settling process has been studied more intensively than the continuous thickening process (Kos, 1985).

Settlement of suspended particles depends on the concentration of the suspension and the particle characteristics, such as density, shape, and size. Four distinct types of sedimentation, reflecting the concentration of the suspension and the flocculating properties of the particles, include (Fitch, 1958; as cited in Weber, 1972):

- (1) Class-1 clarification - the settling of a dilute suspension of particles which have little or no tendency to flocculate;
- (2) Class-2 clarification - the removal of a dilute suspension of flocculent particles;
- (3) Zone settling - subsidence of particles as a large mass rather than as discrete particles (due to the particles being sufficiently close such that interparticle forces are able to hold them in fixed positions relative to each other); and
- (4) Compression - restriction of further consolidation.

According to Weber (1972), sludges normally exhibit zone settling characteristics, as shown by the appearance of a distinct horizontal interface between the solids and the liquid.

Work with activated sludge (Dick, 1970a; as cited in Weber, 1972) has shown that fluid resistance and inter-particle drag need to be considered simultaneously and that a significant amount of "compression" may accompany sedimentation at comparatively dilute concentrations. For example, interparticle forces may reduce the subsidence rate of activated sludge at ordinary mixed-liquor suspended solids concentrations (Weber, 1972).

Conditioning of Sludges. Sludge conditioning refers to chemical and physical methods for altering sludge properties to remove water more readily. Conditioning technology is based on trial-and-error experimentation. The efficacy of alternate conditioning methods is evaluated by the many laboratory-derived parameters - such as specific resistance, coefficient of compressibility, yield, rise rate, and subsidence velocity - depending on the dewatering or thickening process to be used (Weber, 1972).

Cake Filtration

Models of one-dimensional cake filtration have been developed, based on two-phase flow theory and constitutive relationships, by: Smiles (1970), Atsumi and Akiyama (1975), Kos and Adrian (1975), Wakeman (1978), Tosun (1986), and Wells (1990).

A similarity transformation was used by Smiles (1970), Atsumi and Akiyama (1975), and Wakeman (1978) to change the governing partial differential equation into an ordinary differential equation. Due to the use of the similarity transformation, the applications of these models were restricted to situations where the average cake concentration was independent of time (Atsumi and Akiyama, 1975).

Tosun (1986) used a solution technique developed by Kehoe (1972) to approximate the non-linear governing equation with a moving boundary, and obtained similar results to those of Atsumi and Akiyama's (1975) similarity transformation. The results of Wakeman's (1978) model compared well to porosity data (obtained by electrical resistivity measurements after fitting model coefficients to the data by a least squares technique) even though Tosun (1986) showed that Wakeman did not have the correct moving boundary condition.

Wells (1990) solved the full non-linear, partial differential equation (using an explicit finite difference procedure) to predict cake development with time, shrinkage, and filtrate production. His model used porosity data from the Cornell High Energy Synchrotron Source (CHESS) and porewater pressure measurements within the kaolin cakes to determine constitutive relationships. Wells and Dick (1988) showed that the numerical model accurately described the effect of presedimentation on filtration. However, Wells' (1988) model used an initial known porosity profile as an initial condition, and did not account for gravity sedimentation.

ε	= porosity [-] = volume liquid/total volume
t	= time [T]
z	= distance from filtration medium [L]
V_1	= true liquid velocity (in contrast to Darcy velocity, εV_D) [L/T]
V_s	= velocity of the solid particles [L/T]
F	= $\varepsilon\mu/k$, Averaged interfacial interaction term between the solid and the liquid phases [M/L ³ -T]
μ	= dynamic (or absolute) viscosity [M/L-T]
k	= intrinsic permeability [L ²]
p	= fluid static pressure [M/L-T ²]
g	= acceleration due to gravity [L/T ²]
ρ_l	= liquid density [M/L ³]
ρ_s	= solid density [M/L ³]
σ'	= effective stress [M/LT]

The liquid continuity equation describes the difference in liquid flux into and out of the control volume, which is equal to the change in the mass of fluid within the control volume. Similarly, the solid continuity equation describes the difference in solid flux into and out of the control volume. A schematic of the solid and liquid flux into and out from a control volume is shown in Figure 2.

Control volumes are also shown in Figures 3 and 4 for the liquid and solid momentum balances. The sum of all body and surface forces acting on the body of fluid within the control volume are equated to the rate of change of momentum (McCormack and Crane, 1973) within the control volume.

Many researchers have investigated and derived equations for the conservation of mass (continuity) and momentum in two-phase flow. The continuity equations can be easily compared between researchers and are accepted as presented in this paper.

The momentum equations presented by researchers are more difficult to compare because of the variety of terms and the varied nomenclature. To confirm the correctness of the momentum equations presented here, a comparison was made of other researchers' equations, as shown in Tables II-V. Wells' (1990) governing equations for cake filtration before his scaling analysis determining negligible terms (i.e., gravity and inertial terms), Soo's (1989) equations for batch settling, and Gidaspow and Ettehadleh's (1983) 2-dimensional hydrodynamic modeling of fluidization

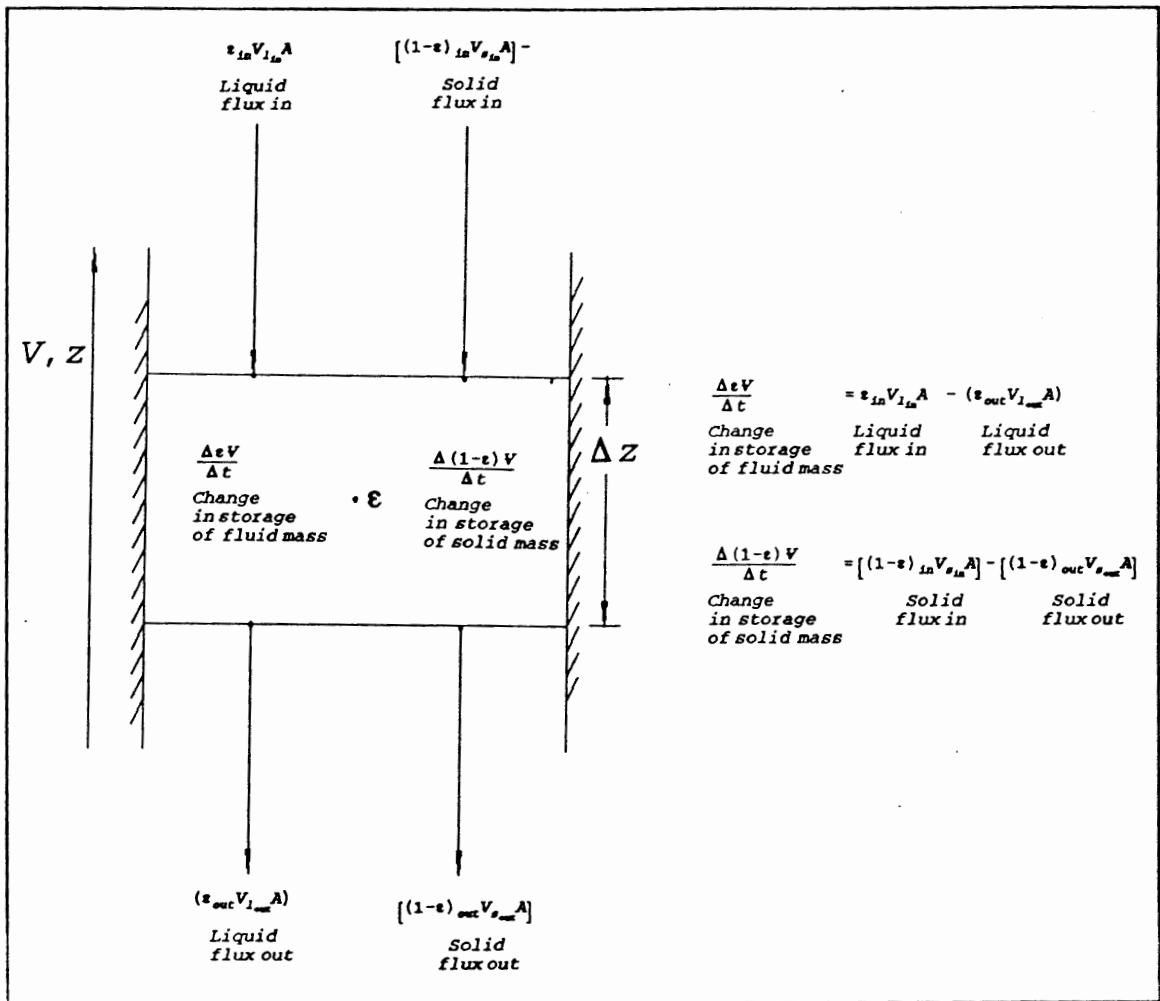


Figure 2. Liquid and solid continuity balance over a control volume.

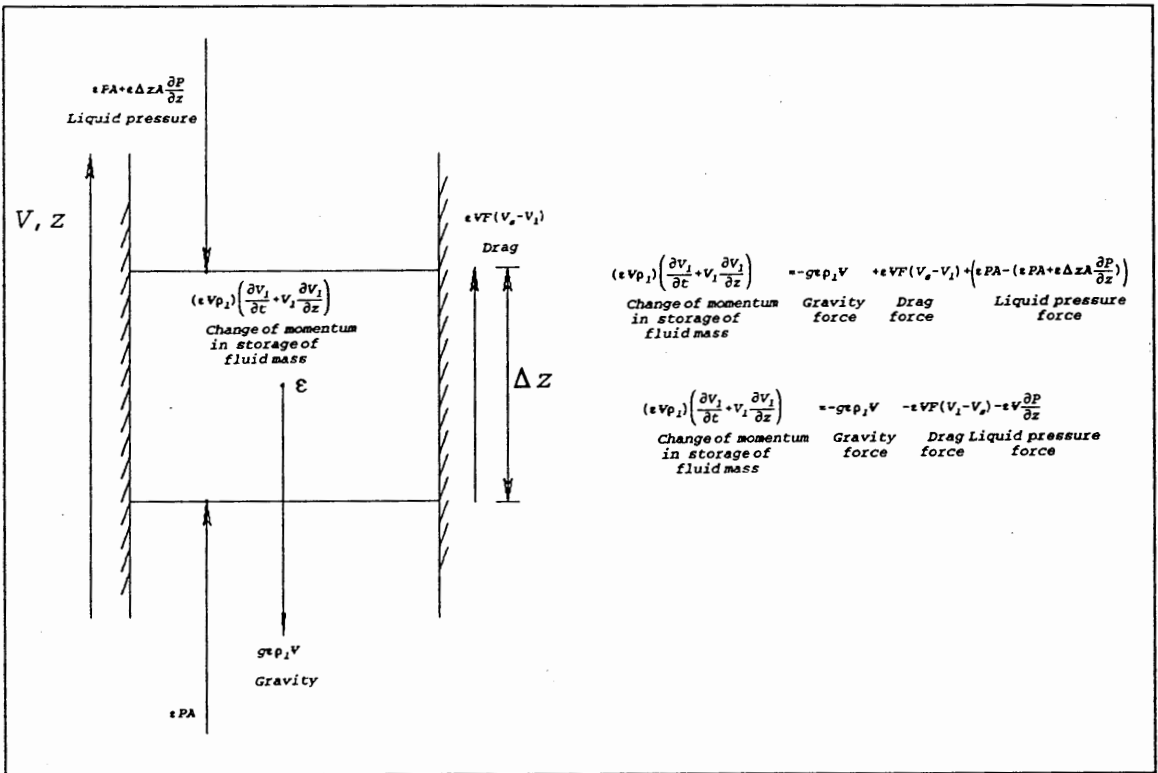


Figure 3. Liquid momentum balance over a control volume. Equation is a sum of all the forces: body forces include gravity, and surface forces include the liquid pressure (shown with a Taylor series expansion) and the drag (shear).

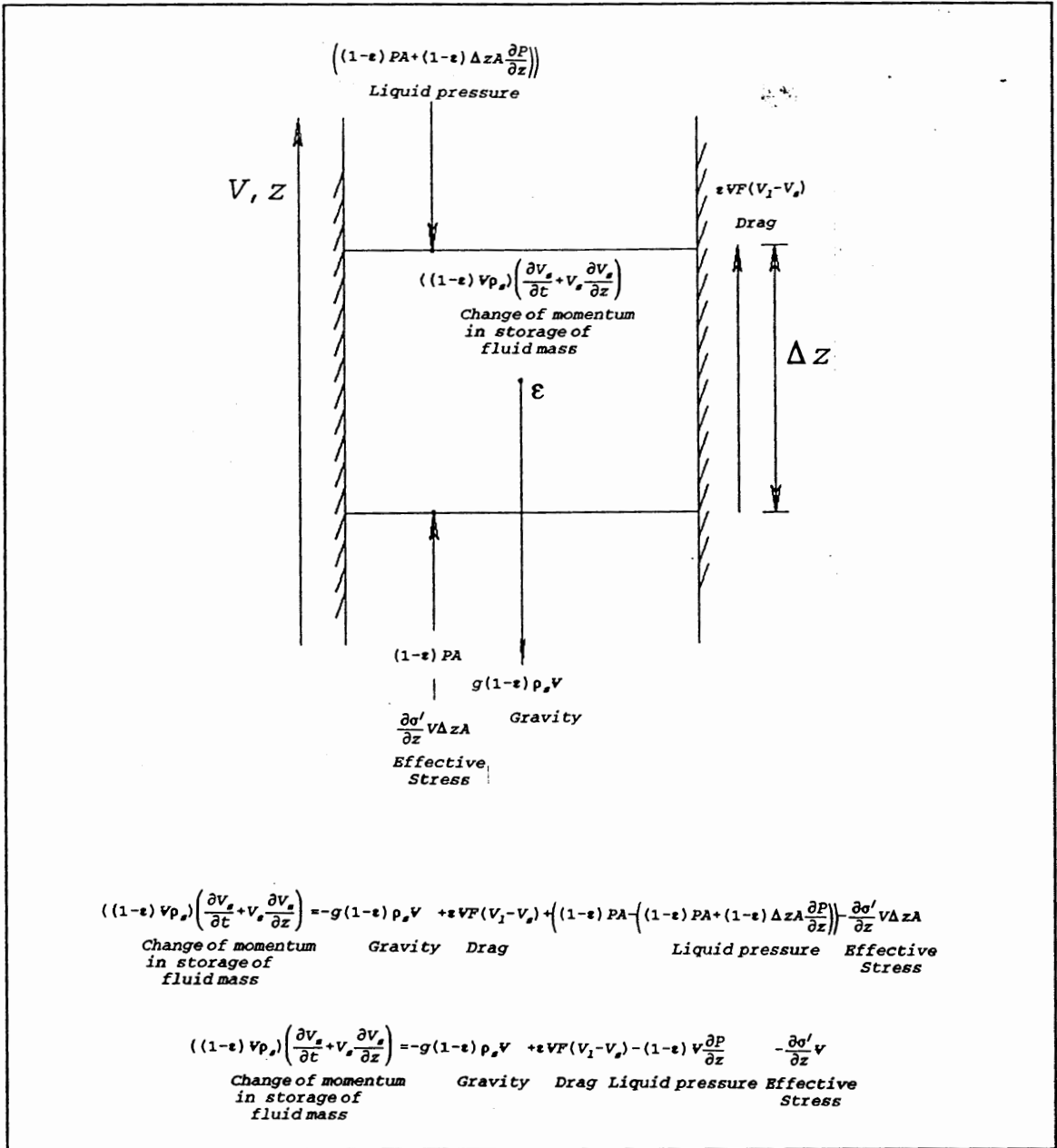


Figure 4. Solid momentum balance over a control volume. Equation is a sum of all the forces: body forces include gravity, and surface forces include the liquid pressure (shown with a Taylor series expansion), the effective stress, and the drag (shear).

TABLE II
LIQUID MOMENTUM:
COMPARISON OF DIFFERENT RESEARCHERS' EQUATIONS - INITIAL FORM

LIQUID MOMENTUM (Initial Equation)						
Researcher	Inertial Forces		= Gravity	+ Drag	+ Liquid Pressure	Substitutions (nomenclature)
	Unsteady Accelerat'n ^a	+ Convectv Accelerat'n ^b				
Wells (1990)	$\frac{\partial v_1}{\partial t}$	$v_1 \frac{\partial v_1}{\partial z}$	$-g$	$-\epsilon F(V_1 - V_p)$	$-\frac{1}{\rho_1} \frac{\partial p}{\partial z}$	Wells Wells $v = \frac{\mu}{\rho_1}$ $F_{Wells} = \epsilon \frac{\mu}{k}$
Soo ¹ (1989)	$\rho \frac{\partial W}{\partial t}$	$\rho W \frac{\partial W}{\partial z}$	$+\rho g$	$+\rho_p F(W - W_p)$	$+\frac{\rho_p}{\rho_p} \frac{\partial p}{\partial z}$	Soo Wells $\rho_p = (1 - \epsilon) \rho_s$ $\rho_p = \rho_s$ $W_p = V_s$ $W = V_1$ $\bar{\rho} = \rho_1$ $\rho = \epsilon \rho_1$ $F_{Soo} = \frac{F_{Wells}}{(1 - \epsilon) \rho_s}$
Giadspow/ Ettehadin (1983)	$\frac{\partial}{\partial t} (\rho_s \epsilon V_s)$	$\frac{\partial}{\partial x} [\rho_s \epsilon U_s V_s] + \frac{\partial}{\partial y} [\rho_s \epsilon V_s V_s]$	$-\rho_s \epsilon g$	$+B_y (V_s - V_p)$	$-\epsilon \frac{\partial p}{\partial y}$	Giadspow Wells $y = z$ $\tau = \sigma'$ $B_y = \epsilon F?$ $V_s = V_1$

^aRate of change of particle momentum

^bNet rate of convection of momentum of the particles

¹The liquid momentum equation is not actually presented by Soo. The solid momentum equation is subtracted from the total momentum, both given by Soo:

$$\text{Total Momentum: } \rho \frac{\partial W}{\partial t} + \rho W \frac{\partial W}{\partial z} + \rho_p \frac{\partial W_p}{\partial t} + \rho_p W_p \frac{\partial W_p}{\partial z} = -\frac{\partial P}{\partial z} - (\rho_p + \rho) g$$

$$\text{Solid Momentum: } \rho_p \frac{\partial W_p}{\partial t} + \rho_p W_p \frac{\partial W_p}{\partial z} = -\rho_p g + \rho_p F(W - W_p) - \frac{\rho_p}{\rho_p} \frac{\partial P}{\partial z}$$

TABLE III
LIQUID MOMENTUM:
COMPARISON OF DIFFERENT RESEARCHERS' EQUATIONS
IN COMPARABLE NOMENCLATURE

LIQUID MOMENTUM (Comparable Nomenclature)					
Researcher	Inertial Forces		= Gravity	+ Drag	+ Liquid Pressure
	Unsteady Acceleration ^a	+ Convective Acceleration ^b			
Wells (1990)	$\epsilon \rho_1 \frac{\partial V_1}{\partial t}$	$\epsilon \rho_1 V_1 \frac{\partial V_1}{\partial z}$	$-\epsilon \rho_1 g$	$-\epsilon F(V_1 - V_s)$	$-\epsilon \frac{\partial p}{\partial z}$
Soo (1989)	$\epsilon \rho_1 \frac{\partial V_1}{\partial t}$	$\epsilon \rho_1 V_1 \frac{\partial V_1}{\partial z}$	$-\epsilon \rho_1 g$	$-F(V_1 - V_s)$	$-\epsilon \frac{\partial p}{\partial z}$
Gidaspow/ Ettehadin ² (1983)	$\epsilon \rho_1 \frac{\partial V_1}{\partial t}$	$\epsilon \rho_1 V_1 \frac{\partial V_1}{\partial z}$	$-\epsilon \rho_1 g$	$-\beta_y (V_1 - V_s)$	$-\epsilon \frac{\partial p}{\partial z}$

^aRate of change of particle momentum

^bNet rate of convection of momentum of the particles

²To compare to the other equations, this 2-dimensional equation is written one-dimensionally. The inertial terms (left-hand side of the equation) can be re-written as follows:

$$\frac{\partial}{\partial t} (\rho_s \epsilon V_s) + \frac{\partial}{\partial x} (\rho_s \epsilon u_s V_s) + \frac{\partial}{\partial y} (\rho_s \epsilon v_s V_s)$$

Writing as a 1-D equation: $\rho_s \frac{\partial}{\partial t} (\epsilon V_s) + \rho_s \frac{\partial}{\partial y} [(\epsilon V_s) v_s]$

$$\text{Expanding: } \rho_s \left[\epsilon \frac{\partial v_s}{\partial t} + v_s \frac{\partial \epsilon}{\partial t} \right] + \rho_s \left[\epsilon v_s \frac{\partial v_s}{\partial y} + v_s \frac{\partial (\epsilon v_s)}{\partial y} \right]$$

The sum of the second and fourth terms can be equated to zero, due to liquid continuity:

$$\begin{aligned} \frac{\partial \epsilon}{\partial t} + \frac{\partial (\epsilon v_s)}{\partial y} &= 0 \\ \rightarrow \epsilon \rho_s \frac{\partial v_s}{\partial t} + \epsilon \rho_s v_s \frac{\partial v_s}{\partial y} &= 0 \end{aligned}$$

TABLE IV

**SOLID MOMENTUM:
COMPARISON OF DIFFERENT RESEARCHERS' EQUATIONS - INITIAL FORM**

SOLID MOMENTUM (Initial Equation)							
Researcher	Inertial Forces		= Gravity	+ Drag	+ Liquid Pressure	+ ef f strss	Substitutions nomenclature
	Unsteady Accelerat'n ^a	+ Convectv Accelerat'n ^b					
Wells (1990)	$(1-\varepsilon) \rho_p \frac{\partial V_p}{\partial t}$	$(1-\varepsilon) \rho_p V_p \frac{\partial V_p}{\partial z}$	$-(1-\varepsilon) \rho_p g$	$+\varepsilon F(V_I - V_p)$	$-(1-\varepsilon) \frac{\partial p}{\partial z}$	$-\frac{\partial \sigma}{\partial z}$	
Soo (1989)	$\rho_p \frac{\partial W_p}{\partial t}$	$\rho_p W_p \frac{\partial W_p}{\partial z}$	$-\rho_p g$	$+\rho_p F(W - W_p)$	$-\frac{\rho_p}{\rho_p} \frac{\partial p}{\partial z}$		<u>Soo Wells</u> $\rho_p = (1-\varepsilon) \rho_s$ $\bar{\rho}_p = \rho_p$ $W_p = V_p$ $W = V_I$ $\bar{\rho} = \rho_I$ $\rho = \varepsilon \rho_I$ $F_{soo} = \frac{F_{wells}}{(1-\varepsilon) \rho_p}$
Giadspow/ Ettehadin (1983)	$\frac{\partial}{\partial t} [\rho_p (1-\varepsilon) V_p]$	$\frac{\partial}{\partial x} [\rho_p (1-\varepsilon) U_p V_p]$ $\frac{\partial}{\partial y} [\rho_p (1-\varepsilon) V_p V_p]$	$-\rho_p (1-\varepsilon) g$	$+B_y (V_p - V_s)$	$-(1-\varepsilon) \frac{\partial p}{\partial y}$	$-\frac{\partial \tau}{\partial y}$	<u>GiadspowWells</u> $y = z$ $\tau = \sigma'$ $B_y = \varepsilon F?$ $V_s = V_I$

^aRate of change of particle momentum

^bNet rate of convection of momentum of the particles

TABLE V
SOLID MOMENTUM:
COMPARISON OF DIFFERENT RESEARCHERS' EQUATIONS
IN COMPARABLE NOMENCLATURE

SOLID MOMENTUM (Comparable Nomenclature)						
Researcher	Inertial Forces		= Gravity	+ Drag	+ Liquid Pressure	+ Inter-granular stress
	Unsteady Acceleration ^a	+ Convective Acceleration ^b				
Wells (1990)	$(1-\varepsilon) \rho_s \frac{\partial V_s}{\partial t}$	$(1-\varepsilon) \rho_s V_s \frac{\partial V_s}{\partial z}$	$-(1-\varepsilon) \rho_s g$	$+\varepsilon F (V_1 - V_s)$	$-(1-\varepsilon) \frac{\partial p}{\partial z}$	$-\frac{\partial \sigma'}{\partial z}$
Soo (1989)	$(1-\varepsilon) \rho_s \frac{\partial V_s}{\partial t}$	$(1-\varepsilon) \rho_s V_s \frac{\partial V_s}{\partial z}$	$-(1-\varepsilon) \rho_s g$	$+\varepsilon F (V_1 - V_s)$	$-(1-\varepsilon) \frac{\partial p}{\partial z}$	
Gidaspow/ Ettehadin (1983) ³	$(1-\varepsilon) \rho_s \frac{\partial V_s}{\partial t}$	$(1-\varepsilon) \rho_s V_s \frac{\partial V_s}{\partial z}$	$-(1-\varepsilon) \rho_s g$	$+\varepsilon F (V_1 - V_s)$	$-(1-\varepsilon) \frac{\partial p}{\partial z}$	$-\frac{\partial \sigma'}{\partial z}$

^aRate of change of particle momentum

^bNet rate of convection of momentum of the particles

³To compare to the other equations, this 2-dimensional equation is written one-dimensionally. The inertial terms (left-hand side of the equation) can be re-written as follows:

$$\frac{\partial}{\partial t} [\rho_s (1-\varepsilon) V_s] + \frac{\partial}{\partial x} [\rho_s (1-\varepsilon) U_s V_s] + \frac{\partial}{\partial y} [\rho_s (1-\varepsilon) V_s V_s]$$

Writing as a 1-D equation: $\rho_s \frac{\partial}{\partial t} [(1-\varepsilon) V_s] + \rho_s \frac{\partial}{\partial y} [(1-\varepsilon) V_s] V_s$

$$\text{Expanding: } \rho_s \left[(1-\varepsilon) \frac{\partial V_s}{\partial t} - V_s \frac{\partial \varepsilon}{\partial t} \right] + \rho_s \left[(1-\varepsilon) V_s \frac{\partial V_s}{\partial y} + V_s \frac{\partial (1-\varepsilon) V_s}{\partial y} \right]$$

The sum of the second and fourth terms can be equated to zero, due to solid continuity:

$$-\frac{\partial \varepsilon}{\partial t} + \frac{\partial (1-\varepsilon) V_s}{\partial y} = 0$$

$$(1-\varepsilon) \rho_s \frac{\partial V_s}{\partial t} + (1-\varepsilon) \rho_s V_s \frac{\partial V_s}{\partial y}$$

equations were compared. The liquid momentum equations were the same. The solid momentum equations were equivalent, except Soo's (1989) model did not consider the particle-to-particle interaction force (and thus has no effective stress or inter-granular stress term).

Wells' (1990) equations shown in Tables II-V were developed from the same governing equation he used for cake filtration, without neglecting the inertial or gravity terms. According to Dixon (1985), the inertial terms are important in the interface between suspension and sediment, where rapid velocity change is occurring. In this narrow interface zone the particles, which have been settling at the terminal velocity corresponding to the initial concentration, are retarded (the velocity is near zero in the sediment) as they strike the top of the sediment.

Wells' (1990) model assumed an applied pressure differential several orders of magnitude greater than gravity, making the gravity term negligible. However, no such (large) pressure term exists during gravity sedimentation. Thus, it is assumed that the gravity term is important, and is not neglected.

Final Form of Governing Equations - Model Formulation

The solid and liquid continuity equations can be equated as follows:

$$\frac{\partial \varepsilon}{\partial t} = - \frac{\partial (\varepsilon V_l)}{\partial z} = \frac{\partial [(1-\varepsilon) V_s]}{\partial z} \quad (3.5)$$

This equation was integrated from $z=0$, where $\varepsilon V_l = \varepsilon_0 V_0$ and $V_s = 0$, to z .

$$- \int_{\varepsilon_0 V_0}^{\varepsilon V_l} \partial (\varepsilon V_l) = \int_0^{V_s} \partial [(1-\varepsilon) V_s] \quad (3.6)$$

Simplifying, Equation 3.6 becomes:

$$V_l = \frac{\varepsilon_0 V_0 - (1-\varepsilon) V_s}{\varepsilon} \quad (3.7)$$

- V_l = true liquid velocity (in contrast to Darcy velocity, εV_l) [L/T]
- V_s = velocity of the solid particles [L/T]
- ε = porosity [-], volume liquid/total volume
- ε_0 = terminal porosity at $z=0$ [-]
- V_0 = true liquid velocity at $z=0$ [L/T]

It can be noted that these results differ from Soo's⁴ (1989) because of the boundary condition applied at the media ($z=0$).

Similarly, the two momentum equations can be added, resulting in a total momentum equation.

$$\rho_l \varepsilon \frac{\partial V_l}{\partial t} + \rho_l \varepsilon V_l \frac{\partial V_l}{\partial z} + (1-\varepsilon) \rho_s \frac{\partial V_s}{\partial t} + (1-\varepsilon) \rho_s V_s \frac{\partial V_s}{\partial z} = -\frac{\partial P}{\partial z} - [(1-\varepsilon) \rho_s + \varepsilon \rho_l] g - \frac{\partial \sigma}{\partial z} \quad (3.8)$$

The technique for simplifying the governing equations is similar to Soo's (1989) technique. By (1) equating the solid momentum, Equation 3.4, and the total momentum, Equation 3.8; (2) substituting V_l from the total continuity, Equation 3.7, into Equation 3.8; (3) combining like terms; and (4) substituting the constitutive relationship, $m_v = -\frac{\partial \varepsilon}{\partial \sigma}$ (Peck, et al., 1974, and Das, 1983; as cited by

Wells, 1988); Equation 3.8 becomes:

$$\begin{aligned} & [(1-\varepsilon) \rho_l + \varepsilon \rho_s] \frac{\partial V_s}{\partial t} + \left[\rho_l (\varepsilon_0 V_0 - (1-\varepsilon) V_s) \left(\frac{1-\varepsilon}{\varepsilon} \right) + \varepsilon \rho_s V_s \right] \frac{\partial V_s}{\partial z} + \left[-\rho_l \left(\frac{V_s - \varepsilon_0 V_0}{\varepsilon} \right) \right] \frac{\partial \varepsilon}{\partial t} \\ & + \left[\frac{\rho_l}{\varepsilon^2} (\varepsilon_0 V_0 - V_s) (\varepsilon_0 V_0 - (1-\varepsilon) V_s) \right] \frac{\partial \varepsilon}{\partial z} + \left[-\rho_l \frac{\partial}{\partial t} (\varepsilon_0 V_0) \right] \\ & = \varepsilon g (\rho_l - \rho_s) + \left(\frac{F}{1-\varepsilon} \right) (\varepsilon_0 V_0 - V_s) + \frac{\varepsilon}{(1-\varepsilon) m_v} \frac{\partial \varepsilon}{\partial z} \end{aligned} \quad (3.9)$$

ε = porosity [-], volume liquid/total volume

ρ_l = liquid density [M/L³]

ρ_s = solid density [M/L³]

V_s = velocity of the solid particles [L/T]

t = time [T]

ε_0 = terminal porosity at $z=0$ [-]

V_0 = true liquid velocity at $z=0$ [L/T]

z = distance from filtration medium [L]

g = acceleration due to gravity [L/T²]

F = $\varepsilon \mu / k$, averaged interfacial interaction term between the solid and the liquid phases [M/L³-T]

k = intrinsic permeability [L²]

⁴Soo (1989) obtained the following result for the less general case of no fluid loss, such as from a closed bottom (i.e., at $z=0$, $\varepsilon V_l=0$ and $V_s=0$):

$$V_s = \frac{-\varepsilon V_l}{(1-\varepsilon)} \quad \text{or, rearranging:} \quad V_l = \frac{-(1-\varepsilon) V_s}{\varepsilon}$$

$$m_v = \frac{\partial \varepsilon}{\partial \sigma'}, \text{ coefficient of volume compressibility } [T^2-L/M], \text{ where } \sigma' = \text{effective stress} \\ [M/LT^2]$$

$$p = \text{fluid static pressure } [M/L-T^2]$$

Details of the derivation of Equation 3.9 are shown in Table VI.

Equations 3.2 and 3.9 were used in the numerical computer model. The first equation was the solid continuity. The second equation was total momentum with continuity (referred to as the "momentum" equation throughout the modeling section). The formulation of the numerical model is discussed in more detail in the following section.

NUMERICAL SOLUTION TECHNIQUE

The final governing equations were put into a finite difference form and solved numerically using appropriate boundary conditions. The solid continuity equation (Equation 3.2) was first solved to determine ε at the new time level $n+1$. Using this result, the "momentum" equation (Equation 3.9) was used to solve for V_x , also at the new time level $n+1$.

The approach for developing the numerical solution strategy employed using simple techniques first (i.e., the explicit method was tried before the implicit), and then increasing the level of numerical refinement. The numerical code was written in the most general way, such that various techniques (such as explicit vs. implicit, central differencing vs. upwinding, added artificial viscosity, etc.) could be explored with one code. When the computer code was written, toggles allowed the modeler to choose at the start of each run between different conditions such as the central or the upwind difference for the convective terms. The modeler could choose degrees of explicitness or implicitness. The code automatically calculated a value for the artificial viscosity (to counter numerical dispersion) which the modeler could adjust during the run.

Many model simulations were made analyzing the behavior of the equation by varying the degree of explicitness/implicitness, differencing techniques, grid spacing, time step, artificial viscosity, and constitutive parameters.

TABLE VI

SUMMARY OF DEVELOPMENT OF GOVERNING EQUATIONS
(continued)

<p>(12) Substituting Equations 10 and 11 into Equation 9:</p> $\rho_s \frac{\partial V_s}{\partial t} + \rho_s V_s \frac{\partial V_s}{\partial z} + \rho_s g - \frac{\epsilon F}{1-\epsilon} (V_I - V_s) + \frac{1}{1-\epsilon} \frac{\partial \sigma'}{\partial z} - \rho_I \epsilon \left[\frac{-(1-\epsilon)}{\epsilon} \frac{\partial V_s}{\partial t} + \frac{(V_s - \epsilon_0 V_0)}{\epsilon^2} \frac{\partial \epsilon}{\partial t} + \frac{1}{\epsilon} \frac{\partial (\epsilon_0 V_0)}{\partial t} \right]$ $+ \rho_I \epsilon_0 V_0 - (1-\epsilon) V_s \left[\frac{V_s - \epsilon_0 V_0}{\epsilon^2} \frac{\partial \epsilon}{\partial z} - \frac{(1-\epsilon)}{\epsilon} \frac{\partial V_s}{\partial z} \right] + (1-\epsilon) \rho_s \frac{\partial V_s}{\partial t} + (1-\epsilon) \rho_s V_s \frac{\partial V_s}{\partial z} - \epsilon (1-\epsilon) \rho_s + \epsilon \rho_I \left[g + \frac{\partial \sigma'}{\partial z} \right]$
<p>(13) Organizing and simplifying terms:</p> $\left[(1-\epsilon) \rho_I + \epsilon \rho_s \right] \frac{\partial V_s}{\partial t} + \left[\rho_I \epsilon_0 V_0 - (1-\epsilon) V_s \left(\frac{1-\epsilon}{\epsilon} \right) + \epsilon \rho_s V_s \right] \frac{\partial V_s}{\partial z} + \left[-\rho_I \frac{(V_s - \epsilon_0 V_0)}{\epsilon} \right] \frac{\partial \epsilon}{\partial t} + \left[\frac{\rho_I}{\epsilon^2} (\epsilon_0 V_0 - V_s) (\epsilon_0 V_0 - (1-\epsilon) V_s) \right] \frac{\partial \epsilon}{\partial z}$ $- \rho_I \frac{\partial (\epsilon_0 V_0)}{\partial t} - \epsilon g (\rho_I - \rho_s) + \frac{\epsilon F}{(1-\epsilon)} \left(\frac{\epsilon_0 V_0 - (1-\epsilon) V_s - \epsilon V_s}{\epsilon} \right) + \left[-\frac{1}{(1-\epsilon)} + 1 \right] \frac{\partial \sigma'}{\partial z}$
<p>(14) Substituting the constitutive relationship (Equation 5) into Equation 13:</p> $\left[(1-\epsilon) \rho_I + \epsilon \rho_s \right] \frac{\partial V_s}{\partial t} + \left[\rho_I \epsilon_0 V_0 - (1-\epsilon) V_s \left(\frac{1-\epsilon}{\epsilon} \right) + \epsilon \rho_s V_s \right] \frac{\partial V_s}{\partial z} + \left[-\rho_I \frac{(V_s - \epsilon_0 V_0)}{\epsilon} \right] \frac{\partial \epsilon}{\partial t} + \left[\frac{\rho_I}{\epsilon^2} (\epsilon_0 V_0 - V_s) (\epsilon_0 V_0 - (1-\epsilon) V_s) \right] \frac{\partial \epsilon}{\partial z}$ $- \rho_I \frac{\partial (\epsilon_0 V_0)}{\partial t} - \epsilon g (\rho_I - \rho_s) + \left(\frac{F}{(1-\epsilon)} \right) (\epsilon_0 V_0 - V_s) + \frac{\epsilon}{(1-\epsilon) m_v} \frac{\partial \epsilon}{\partial z}$

Initially, the model was made to simulate sedimentation with no drainage out the bottom, so that this output could be compared to an analytical solution by Soo (1989) for a simple nontrivial solution. After satisfactorily simulating this condition, drainage could again be incorporated and cake filtration with gravity sedimentation could be modeled by a future investigator.

Computational Strategy

A "space-staggered mesh" was employed such that porosity, ϵ , was evaluated at the control volume center, and solid velocity, V_s , was evaluated at the control volume edges. This is shown in Figure 5 using the nomenclature of the computer program (i.e., EE is porosity and US is solid velocity). Note the location for "i" is different, contingent upon whether it is porosity or solid velocity (US) which is being evaluated.

Boundary Conditions for ϵ and V_s

Boundary conditions were determined as follows:

$$\text{Top: } \frac{\partial V_s}{\partial Z} = 0 \quad \text{or} \quad (V_s)_{k+2} = (V_s)_k \quad (3.10)$$

$$\epsilon_{k+1/2} = 1.0 \quad \text{or} \quad EE1 = 1.0 \quad (\text{at } I=K) \quad (3.11)$$

$$\text{Bottom: } V_s = 0 \quad (3.12)$$

V_s at $z=0$ was set equal to zero, and ϵ was set equal to 1 at the top of the domain. These boundary conditions reflect no flux of solids into the top or out from the bottom of the domain.

Finite Difference Form of Continuity Equation

An explicit formulation was used to solve the first equation (solid continuity), which had a forward difference in time and central difference in space.

$$\frac{\epsilon_i^{n+1} - \epsilon_i^n}{\Delta t} = \frac{[(1-\epsilon) V_s]_{i+\frac{1}{2}}^n - [(1-\epsilon) V_s]_{i-\frac{1}{2}}^n}{\Delta Z} \quad (3.13)$$

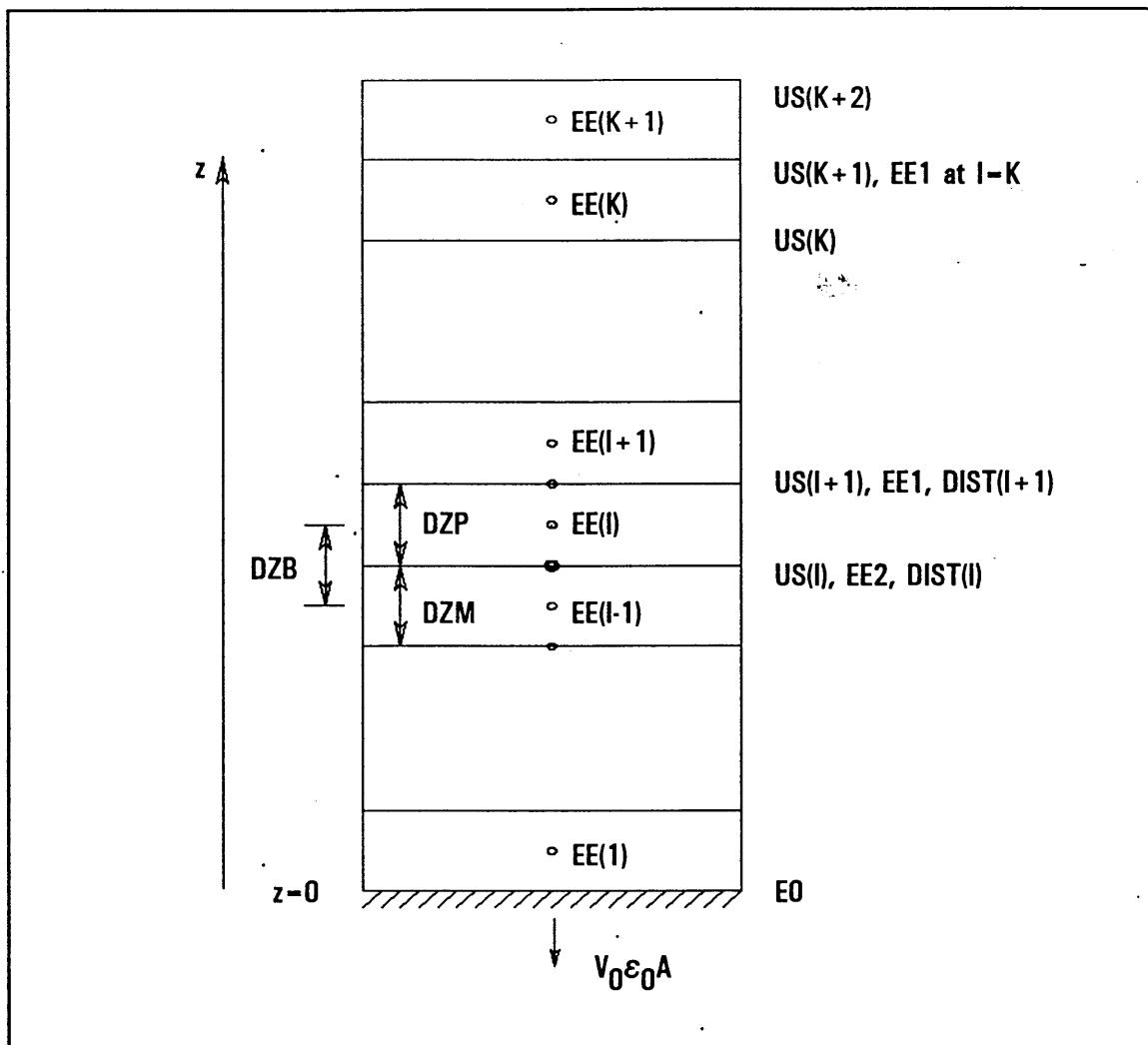


Figure 5. Grid layout used in the computer program with the porosity array (EE) evaluated at the control volume center and the solid velocity array (US) evaluated at the control volume edges. EE1 and EE2 represent porosity evaluated at $i \pm \frac{1}{2}$ (where i is at the control volume center).

Finite Difference Form of "Momentum" Equation

The "momentum" equation (Equation 3.9, representing total momentum with continuity) was put into a general explicit-implicit finite difference scheme, as shown in Table VII. The table shows Equation 3.9 with: (1) the V_s term prior to discretization, (2) the discretized or finite difference form of the V_s term (as either a function of time or in both its explicit and implicit formulation), and (3) the coefficient of the term. This table is discussed further below when comparing the explicit and implicit solution strategies, comparing the effect of using a central difference versus an upwind difference of the spatial derivative of the solid velocity, and describing the linearization of the non-linear terms.

Explicit vs Implicit Solution Strategy for "Momentum" Equation. The fully explicit formulation for the "momentum" equation required a very, very small Δt to remain stable, resulting in a very lengthy computational time. The implicit solution technique allowed larger time steps, while avoiding excessive buildup of round-off error (Farlow, 1982). In other words, relative to the discretization error, this round-off error was small (Carnahan, Luther, and Wilkes, 1969).

Figure 6 compares the explicit and implicit schemes. In the explicit scheme, the solid velocity at the next time step (V_s^{n+1}) is a function of the solid velocities at the initial time step n [i.e., $(V_s^n)_{i-1}$, $(V_s^n)_i$, and $(V_s^n)_{i+1}$]. Thus, the only grid point at the advanced time level is the one which is being solved for. This is contrasted to the implicit scheme where V_s^{n+1} is a function of the velocities at surrounding nodes at the advanced time level $n+1$, as well as the solid velocities at the initial time level n . Explicit methods solve for $(V_s^{n+1})_i$ explicitly in terms of earlier values (Farlow, 1982). Whereas with implicit methods, a system of algebraic equations is solved to find all three of the values (Farlow, 1982) of V_s^{n+1} simultaneously [i.e., $(V_s^{n+1})_{i-1}$, $(V_s^{n+1})_i$, and $(V_s^{n+1})_{i+1}$].

In general, explicit schemes are simpler to formulate, but have severe restrictions on the grid spacing and time increments. Although implicit methods are more complicated, they are also more versatile. They require greater computer storage capacity, but use less running time than explicit methods. More computation time is required per time step, but less steps are involved due

TABLE VII
DISCRETIZATION OF EQUATION 3.9

V _e term	Discretized Terms			Coefficient (all terms evaluated at timestep n)
	f(t) term	Explicit term: (V _e term) ⁿ	Fully implicit term: (V _e term) ⁿ⁺¹	
$\frac{\partial v_e}{\partial t}$	$\frac{(v_e)_i^{n+1} - (v_e)_i^n}{\Delta t}$			$A = (1-\epsilon) \rho_1 + \epsilon \rho_e$
$\frac{\partial v_e}{\partial z}$		Central difference: $\frac{(v_e)_{i+1}^n - (v_e)_{i-1}^n}{2\Delta z}$ Upwind: $\frac{(v_e)_i^n - (v_e)_{i-1}^n}{\Delta z}$	Central difference: $\frac{(v_e)_{i+1}^{n+1} - (v_e)_{i-1}^{n+1}}{2\Delta z}$ Upwind: $\frac{(v_e)_{i+1}^{n+1} - (v_e)_i^{n+1}}{\Delta z}$	$B_1 = \left(\frac{1-\epsilon}{\epsilon}\right) \rho_1 \epsilon_0 V_0$
$v_e \frac{\partial v_e}{\partial z}$ $\frac{\partial \left(\frac{v_e^2}{2}\right)}{\partial z}$		Central difference: $\frac{\left(\frac{v_e^2}{2}\right)_{i+1}^n - \left(\frac{v_e^2}{2}\right)_{i-1}^n}{2\Delta z}$ Upwind: $\frac{\left(\frac{v_e^2}{2}\right)_{i+1}^n - \left(\frac{v_e^2}{2}\right)_i^n}{\Delta z}$	Central difference: $\frac{[v_e^n v_e^{n+1} - \left(\frac{v_e^2}{2}\right)_{i+1}^n]_{i+1} - [v_e^n v_e^{n+1} - \left(\frac{v_e^2}{2}\right)_{i-1}^n]}{2\Delta z}$ Upwind: $\frac{[v_e^n v_e^{n+1} - \left(\frac{v_e^2}{2}\right)_{i+1}^n]_{i+1} - [v_e^n v_e^{n+1} - \left(\frac{v_e^2}{2}\right)_i^n]}{\Delta z}$	$B_2 = \frac{-\rho_1 (1-\epsilon)^2}{\epsilon} + \epsilon \rho_e$
v_e		$(v_e)_i^n$	$(v_e)_i^{n+1}$	$C = -\frac{\rho_1}{\epsilon} \frac{\partial \epsilon}{\partial t}$
				$D = \frac{-\rho_1 (\epsilon_0 V_0)}{\epsilon} \frac{\partial \epsilon}{\partial t}$
				$E = \frac{\rho_1}{\epsilon^2} (\epsilon_0 V_0)^2 \frac{\partial \epsilon}{\partial z}$
v_e		$(v_e)_i^n$	$(v_e)_i^{n+1}$	$F = \frac{\rho_1}{\epsilon^2} (\epsilon_0 V_0) \frac{\partial \epsilon}{\partial z}$
v_e		$(v_e)_i^n$	$(v_e)_i^{n+1}$	$G_1 = \frac{-\rho_1}{\epsilon^2} \epsilon_0 V_0 (1-\epsilon) \frac{\partial \epsilon}{\partial z}$
$(v_e)^2$		$[(v_e)^2]_i^n$	$[(v_e)^2]_i^{n+1} - 2(v_e)_i^n (v_e)_i^{n+1} - [(v_e)^2]_i^n$	$G_2 = \frac{-\rho_1}{\epsilon^2} (1-\epsilon) \frac{\partial \epsilon}{\partial z}$
				$H = -\rho_1 \frac{\partial (\epsilon_0 V_0)}{\partial t}$
				$I = \epsilon g (\rho_1 - \rho_e) *$
				$J = \frac{F}{(1-\epsilon)} \epsilon_0 V_0 *$
v_e		$(v_e)_i^n$	$(v_e)_i^{n+1}$	$K = -\frac{F}{(1-\epsilon)} *$
				$L = \frac{\epsilon}{(1-\epsilon) m_v} \frac{\partial \epsilon}{\partial z} *$

*Note these terms are on the right side of the equation.

Explicit vs Implicit Solution Strategy for "Momentum" Equation. The fully explicit formulation for the "momentum" equation required a very, very small Δt to remain stable, resulting in a very lengthy computational time. The implicit solution technique allowed larger time steps, while

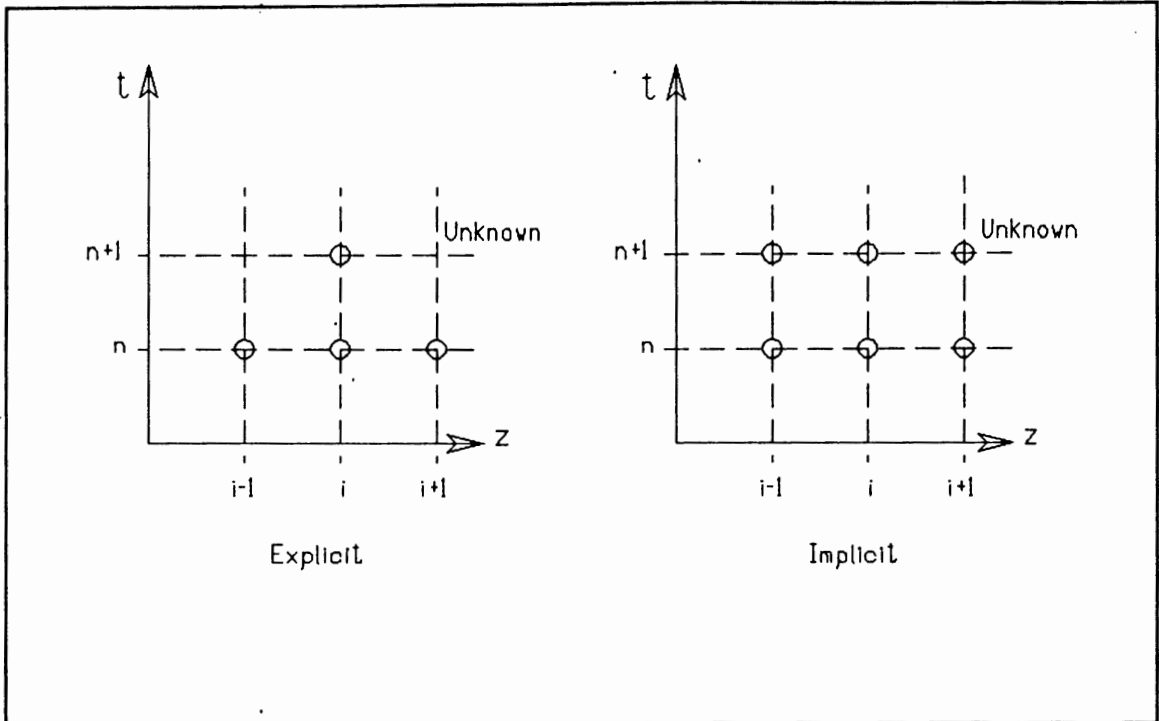


Figure 6. Comparison of explicit and implicit numerical strategies.

to the use of a larger time step; this is possible because they are usually unconditionally stable (Anderson, Tannehill, and Pletcher; 1984).

To use the implicit scheme, a system of simultaneous linear algebraic equations is written for the differential equation, and a Gaussian elimination procedure is used. The procedure is systematic, reducing the general matrix equation to a tridiagonal system. This system can be solved with the Thomas algorithm (Anderson, Tannehill, and Pletcher; 1984).

Central Difference vs Upwind with the Implicit Formulation. The "momentum" governing equation could be discretized with either a central difference or upwind formulation for those terms with the spatial derivative $\frac{\partial v_x}{\partial z}$, the terms with the B_1 and B_2 coefficients shown in Table VII. Figure

7, shown below, compares the central difference and upwind formulations.

To be as general as possible, both central and forward difference formulations were used in the computer code. The central difference term adds numerical dispersive error, while the upwind

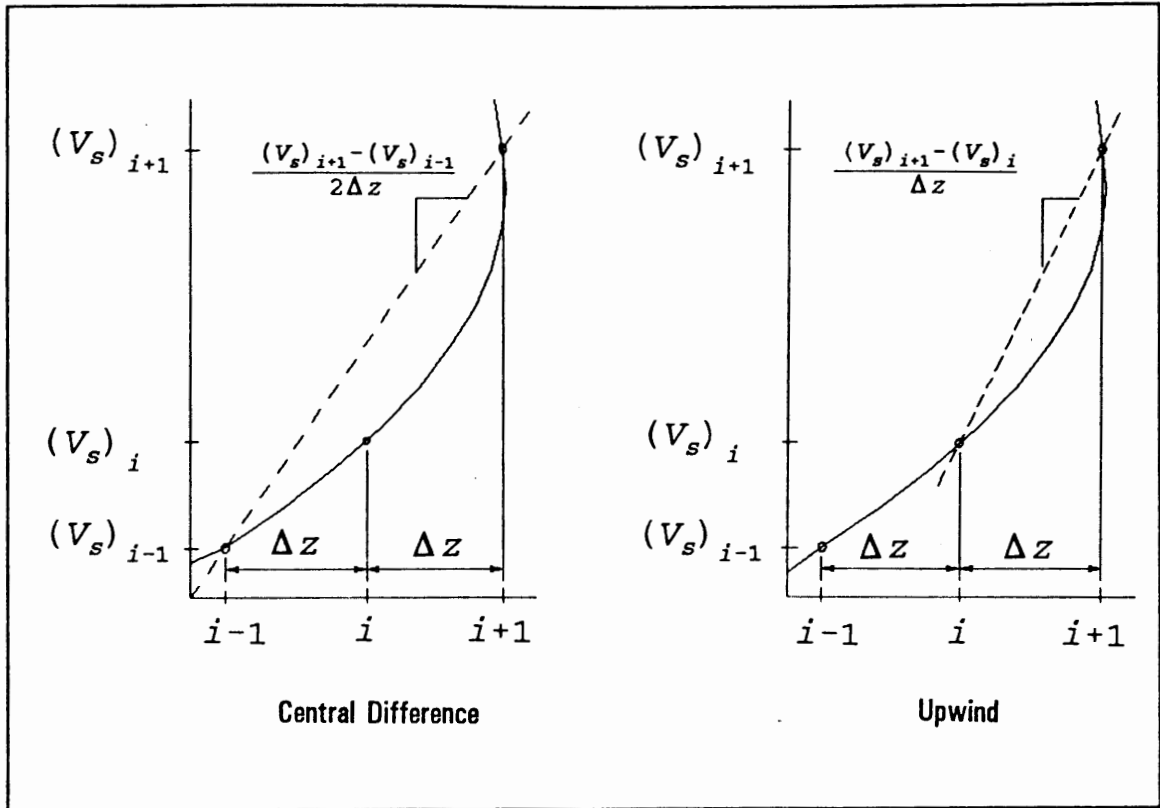


Figure 7. Comparison of central and upwinding differencing.

formulation adds numerical diffusive error. These effects are discussed in the section analyzing the modified equation.

Linearizing the "Momentum" Equation for the Implicit Solution Scheme. It was necessary to "linearize" the terms at the $n+1$ timestep, which had either a $(V_s)^2$ or $V_s \frac{\partial V_s}{\partial z}$ in them. All V_s 's at the n timestep were already known, and therefore did not require linearizing.

The terms requiring linearizing were the second and second-to-last terms of the right side of Equation 3.9, the "momentum" equation (shown as the terms with the " B_2 " and " G_2 " coefficients in Table VII). The general method for doing this involved defining the V_s term at timestep $n+1$, as follows (Anderson, Tannehill, and Pletcher, 1984):

$$(V_s \text{ term})^{n+1} = (V_s \text{ term})^n + \frac{\partial (V_s \text{ term})}{\partial V_s} (V_s^{n+1} - V_s^n) \quad (3.14)$$

The second term on the right side of Equation 3.9, the "momentum" equation (the term with the "B₂" coefficient in Table VII), was linearized as follows.

$$\text{From Table VII: } \left(V_s \frac{\partial V_s}{\partial z} \right)^{n+1} = \left(\frac{\partial \left(\frac{V_s^2}{2} \right)}{\partial z} \right)^{n+1} \rightarrow (V_s \text{ term})^{n+1} = \left(\frac{V_s^2}{2} \right)^{n+1} \quad (3.15)$$

$$\text{Linearizing: } \left(\frac{V_s^2}{2} \right)^{n+1} \approx \left(\frac{V_s^2}{2} \right)^n + \left(\frac{\partial \left(\frac{V_s^2}{2} \right)}{\partial V_s} \right)^n (V_s^{n+1} - V_s^n) \rightarrow \left(\frac{V_s^2}{2} \right)^{n+1} \approx \left(\frac{V_s^2}{2} \right)^n + V_s^n (V_s^{n+1} - V_s^n) \quad (3.16)$$

$$\text{Combining like terms: } \left(\frac{V_s^2}{2} \right)^{n+1} \approx V_s^n V_s^{n+1} - \left(\frac{V_s^2}{2} \right)^n \quad (3.17)$$

The resulting n+1 terms were no longer non-linear (i.e., they no longer had a squared term at the n+1 timestep).

Similarly, the second-to-last term on the right-hand side of Equation 3.9, the "momentum" equation (the term with the "G₂" coefficient in Table VII), was also linearized:

$$\text{From Table VII: } V_s \text{ term} = V_s^2 \quad (3.18)$$

$$\text{Linearizing: } (V_s^2)^{n+1} \approx (V_s^2)^n + \left(\frac{\partial (V_s^2)}{\partial V_s} \right)^n (V_s^{n+1} - V_s^n) \rightarrow (V_s^2)^{n+1} \approx (V_s^2)^n + 2 V_s^n (V_s^{n+1} - V_s^n) \quad (3.19)$$

$$\text{Combining like terms: } (V_s^2)^{n+1} \approx 2(V_s^n V_s^{n+1}) - (V_s^2)^n \quad (3.20)$$

Final Form of the "Momentum" Equation for the Tridiagonal Matrix. The finite difference equations were formulated as a general explicit-implicit scheme in Tables VIII and IX. This finite difference scheme weighted the V_s terms at timesteps n and n+1 (as shown in Table VII) by θ and (1-θ), respectively. When θ=0 the scheme was fully implicit, and when θ=1, the scheme was fully explicit.

The procedure for writing the "momentum" equations as a tridiagonal matrix, involved: (1) re-writing the weighted finite difference equation with like terms grouped together, (2) re-organizing the

equations, (3) incorporating appropriate boundary conditions, and (4) writing the equations in the tridiagonal matrix form. This procedure is shown in Tables VIII and IX.

Table VIII shows the use of a central difference of the spatial derivative term for V_s , and Table IX shows the upwind scheme of the spatial derivative term for V_s . A comparison of the two matrices for the central and upwind schemes are shown in Tables VIII and IX. The upwind and central difference schemes were identical in form, except x_1 and x_2 were equated to zero for the upwind case.

An Analysis of the Modified "Momentum" Equation

The modified equation was determined for the finite difference form of the "momentum" equation. The modified equation is the equation satisfied by the numerical approximation when the leading truncation errors were included. The leading truncation errors represent the difference between the partial differential equation and the finite difference equation in its discretized form.

To evaluate the modified equation, the governing partial differential equation must be linear in the V_s terms. This analysis is shown in Table X below and differs from the numerical model formulation in that the B and G coefficients include V_s as a constant. Thus, the modified equation is only an estimate of the truncation error of the finite difference equation used in the model.

The truncation error was derived in the following manner: (1) the finite difference approximation for the modified equation was determined by weighting the V_s terms at both time levels n and $n+1$ by θ and $(1-\theta)$, respectively; (2) the Taylor's series expansion for each derivative was substituted into the governing equation; and (3) the leading order term from the Taylor series expansions were retained and all higher-order terms neglected; and (4) the second derivative with respect to time, $\frac{\partial^2 V_s}{\partial t^2}$, was determined from the original partial differential equation, thus changing the time derivative in the truncation error to a spatial derivative. These steps are shown in Tables XI and XII, for the central difference and forward difference, respectively.

TABLE VIII

SUMMARY OF DEVELOPMENT OF EQUATION 3.9
(CENTRAL DIFFERENCE SCHEME)

A weighted average of the finite difference approximation is determined by weighting the V_i terms, which were defined above at both timesteps n and $n+1$, by θ and $(1-\theta)$.

$$\begin{aligned}
 & A \left[\frac{(V_i^{n+1} - V_i^n)}{\Delta t} \right] + B_1 \left[\theta \left(\frac{(V_i^n - V_i^{n-1}))}{2\Delta z} \right) + (1-\theta) \left(\frac{(V_i^{n+1} - V_i^{n-1}))}{2\Delta z} \right) \right] + \\
 & B_2 \left[\theta \left(\frac{(V_i^n - V_i^{n-1}))}{2\Delta z} \right) + (1-\theta) \left(\frac{(V_i^{n+1} - V_i^{n-1}))}{2\Delta z} \right) \right] + \\
 & C[\theta (V_i^n + (1-\theta) (V_i^{n+1})) + D + E + F[\theta (V_i^n + (1-\theta) (V_i^{n+1})) + \\
 & G_1[\theta (V_i^n + (1-\theta) (V_i^{n+1})) + G_2[\theta (V_i^n + (1-\theta) (2(V_i^n - V_i^{n-1} - (V_i^{n-1}))) + H - I + J + K[\theta (V_i^n + (1-\theta) (V_i^{n+1})) + L
 \end{aligned} \tag{3.21}$$

Re-writing and grouping like terms:

$$\begin{aligned}
 & \left[\frac{-(1-\theta)(B_1 + B_2(V_i^n))}{2\Delta z} \right] (V_i^{n+1}) + \left[\frac{A}{\Delta t} + (1-\theta)(C + F + G_1 + 2G_2(V_i^n - K)) \right] (V_i^n) + \left[\frac{(1-\theta)(B_1 + B_2(V_i^n))}{2\Delta z} \right] (V_i^{n-1}) \\
 & + \left[\frac{\theta B_1 - (1-2\theta)B_2(V_i^n)}{4\Delta z} \right] (V_i^n) + \left[\frac{A}{\Delta t} + \theta(-C - F - G_1 + K) + (1-2\theta)G_2(V_i^n) \right] (V_i^n) + \left[\frac{\theta B_1 - (1-2\theta)B_2(V_i^n)}{4\Delta z} \right] (V_i^{n-1}) + (-D - E - H + I + J + L)
 \end{aligned} \tag{3.22}$$

The terms can be re-named as follows, so as to set up the tridiagonal system.

$$X_0 = -D - E - H + I + J + L \tag{3.23}$$

$$\text{Explicit: } X_1 = \frac{\theta B_1}{2\Delta z} - \frac{(1-2\theta)B_2(V_i^n)}{4\Delta z}; \quad Y_1 = \frac{A}{\Delta t} + \theta(-C - F - G_1 + K) + (1-2\theta)G_2(V_i^n); \quad Z_1 = \frac{-\theta B_1 + (1-2\theta)B_2(V_i^n)}{2\Delta z} + \frac{(1-2\theta)B_2(V_i^n)}{4\Delta z} \tag{3.24}$$

$$\text{Implicit: } X_2 = \frac{-(1-\theta)(B_1 + B_2(V_i^n))}{2\Delta z}; \quad Y_2 = \frac{A}{\Delta t} + (1-\theta)(C + F + G_1 + 2G_2(V_i^n - K)); \quad Z_2 = \frac{(1-\theta)(B_1 + B_2(V_i^n))}{2\Delta z} \tag{3.25}$$

Substituting the terms for x_0 , x_1 , y_1 , z_1 , x_2 , y_2 , and z_2 into Equation 3.22:

$$x_2 (V_i^{n+1}) + y_2 (V_i^n) + z_2 (V_i^{n-1}) = x_1 (V_i^n) + y_1 (V_i^{n-1}) + z_1 (V_i^{n-2}) + X_0 \tag{3.26}$$

Boundary conditions:

Bottom: $(V_i)_1 = 0$

Top: $\frac{\partial V_i}{\partial z} = 0$ or $(V_i)_{k-2} = (V_i)_k$, $(V_i)_{k-2}^{n+1} = (V_i)_k^{n+1}$

TABLE IX
SUMMARY OF DEVELOPMENT OF EQUATION 3.9
(UPWIND SCHEME)

A weighted average of the finite difference approximation is determined by weighting the V_i terms, which were defined above at both timesteps n and $n+1$, by θ and $(1-\theta)$.

$$\begin{aligned}
 & A \left[\frac{(V_p)_{i+1}^{n+1} - (V_p)_i^n}{\Delta t} \right] + B_1 \left[\theta \left(\frac{(V_p)_{i+1}^n - (V_p)_i^n}{\Delta z} \right) + (1-\theta) \left(\frac{(V_p)_{i+1}^{n+1} - (V_p)_i^{n+1}}{\Delta z} \right) \right] + \\
 & B_2 \left[\theta \left(\frac{\left(\frac{V_p^2}{2} \right)_{i+1}^n - \left(\frac{V_p^2}{2} \right)_i^n}{\Delta z} \right) + (1-\theta) \left(\frac{\left[V_p^n V_p^{n+1} - \left(\frac{V_p^2}{2} \right)_{i+1}^n \right] - \left[V_p^n V_p^{n+1} - \left(\frac{V_p^2}{2} \right)_i^n \right]}{\Delta z} \right) \right] + \\
 & C[\theta (V_p)_i^n + (1-\theta) (V_p)_i^{n+1}] + D + E + F[\theta (V_p)_i^n + (1-\theta) (V_p)_i^{n+1}] + \\
 & G_1[\theta (V_p)_i^n + (1-\theta) (V_p)_i^{n+1}] + G_2[\theta (V_p)_i^n + (1-\theta) (2(V_p)_i^n (V_p)_{i+1}^{n+1} - (V_p^2)_i^n)] + H + I + J + K[\theta (V_p)_i^n + (1-\theta) (V_p)_i^{n+1}] + L
 \end{aligned} \tag{3.28}$$

Re-writing and grouping like terms:

$$\begin{aligned}
 & \left[\frac{A}{\Delta t} + (1-\theta) \left(\frac{-B_1 - B_2 (V_p)_i^n}{\Delta z} + C + F + G_1 + 2G_2 (V_p)_i^n - K \right) \right] (V_p)_{i+1}^{n+1} + \left[\frac{(1-\theta)(B_1 + B_2 (V_p)_{i+1}^n)}{\Delta z} \right] (V_p)_{i+1}^{n+1} \\
 & = \left[\frac{A}{\Delta t} + \theta \left(\frac{B_1}{\Delta z} - C - F - G_1 + K \right) + (1-2\theta) \left(\frac{-B_2}{2\Delta z} + G_2 \right) (V_p)_i^n \right] (V_p)_i^n + \left[\frac{\theta B_1}{\Delta z} - \frac{(1-2\theta) B_2 (V_p)_{i+1}^n}{2\Delta z} \right] (V_p)_{i+1}^n + (-D - E - H + I + J + L)
 \end{aligned} \tag{3.29}$$

The terms can be re-named as follows, so as to set up the tridiagonal system.

$$X_0 = -D - E - H + I + J + L \tag{3.30}$$

$$\text{Explicit: } x_1 = 0; \quad y_1 = \frac{A}{\Delta t} + \theta \left(\frac{B_1}{\Delta z} - C - F - G_1 + K \right) + (1-2\theta) \left(\frac{-B_2}{2\Delta z} + G_2 \right) (V_p)_i^n; \quad z_1 = \frac{-\theta B_1}{\Delta z} + \frac{(1-2\theta) B_2}{2\Delta z} (V_p)_{i+1}^n \tag{3.31}$$

$$\text{Implicit: } x_2 = 0; \quad y_2 = \frac{A}{\Delta t} + (1-\theta) \left[\frac{-B_1 - B_2 (V_p)_i^n}{\Delta z} + C + F + G_1 + 2G_2 (V_p)_i^n - K \right]; \quad z_2 = \frac{(1-\theta)(B_1 + B_2 (V_p)_{i+1}^n)}{\Delta z} \tag{3.32}$$

Substituting the terms for x_0 , x_1 , y_1 , z_1 , x_2 , y_2 , and z_2 into Equation 3.29:

$$x_2 (V_p)_{i-1}^{n+1} + y_2 (V_p)_i^{n+1} + z_2 (V_p)_{i+1}^{n+1} = x_1 (V_p)_{i-1}^n + y_1 (V_p)_i^n + z_1 (V_p)_{i+1}^n + x_0 \Rightarrow y_2 (V_p)_{i-1}^{n+1} + z_2 (V_p)_{i+1}^{n+1} = y_1 (V_p)_i^n + z_1 (V_p)_{i+1}^n + x_0 \tag{3.33}$$

Boundary conditions:

Bottom: $(V_p)_1 = 0$

Top: $\frac{\partial V_p}{\partial z} = 0$ or $(V_p)_{k-2}^n = (V_p)_k^n$, $(V_p)_{k-2}^{n+1} = (V_p)_k^{n+1}$

TABLE IX
 SUMMARY OF DEVELOPMENT OF EQUATION 3.9
 (UPWIND SCHEME)
 (continued)

Substituting $i=k+1$ into Equation 3.33: $x_2 (V_p)_k^{n+1} + y_2 (V_p)_{k+1}^{n+1} + z_2 (V_p)_{k+2}^{n+1} = x_1 (V_p)_k^n + y_1 (V_p)_{k+1}^n + z_1 (V_p)_{k+2}^n + x_0$
 Substituting top boundary condition $(V_p)_{k+2}^n = (V_p)_k^n$, $(V_p)_{k+2}^{n+1} = (V_p)_k^{n+1}$, $x_1=0$ and $x_2=0$ (Equations 31 and 32): $z_2 (V_p)_k^{n+1} + y_2 (V_p)_{k+1}^{n+1} = z_1 (V_p)_k^n + y_1 (V_p)_{k+1}^n + x_0$

The following is the matrix representing the system of equations to be solved:

$$\begin{bmatrix} 1 \\ 0 & 0 & y_2 & z_2 \\ 0 & 0 & 0 & y_2 & z_2 \\ \vdots & & \backslash & \backslash & \backslash \\ \vdots & & & \backslash & \backslash & \backslash \\ 0 & 0 & 0 & 0 & 0 & 0 & y_2 & z_2 \\ 0 & 0 & 0 & 0 & 0 & 0 & 0 & z_2 & y_2 \end{bmatrix} \begin{bmatrix} (V_p)_1^{n+1} \\ (V_p)_2^{n+1} \\ (V_p)_3^{n+1} \\ \vdots \\ (V_p)_k^{n+1} \\ (V_p)_{k+1}^{n+1} \end{bmatrix} = \begin{bmatrix} 0 \\ y_1 (V_p)_2 + z_1 (V_p)_3 + x_0 \\ y_1 (V_p)_3 + z_1 (V_p)_4 + x_0 \\ \vdots \\ y_1 (V_p)_k + z_1 (V_p)_{k+1} + x_0 \\ z_1 (V_p)_k + y_1 (V_p)_{k+1} + x_0 \end{bmatrix} \quad (3.34)$$

Accuracy. Accuracy was determined by the order of errors in the leading truncation error. The lowest order term in the truncation error gives the order of the method. In this case, the forward time centered space method is $O[\Delta t, \Delta z^2]$ (i.e., second order in space), and the upwind method is $O[\Delta t, \Delta z]$ (i.e., first order in space). Higher order indicates greater accuracy. Thus, the central difference scheme was more accurate.

Consistency. Consistency was an indication of the extent the finite difference equation approximated the governing partial differential equation. Consistency was determined by taking the limit of the truncation error as Δz and Δt go to zero, and showing that the result equates to zero. In both the central difference and the upwind, the solution was unconditionally consistent.

Analysis of the Truncation Error of the Modified Equation. The coefficients for each of the derivative terms in the truncation error were compared. The magnitude of the numerical diffusive and dispersive errors were analyzed for $\theta=1$ (an explicit scheme). This provided a simplistic comparison of these errors.

Terms with even derivatives led to numerical diffusion, and terms with odd derivatives led to numerical dispersion. Whereas the even derivative diffusive error was dissipative, the odd derivative dispersive error caused phase relations between various waves to be distorted (Anderson, Tannehill, and Pletcher, 1984). The magnitudes of these terms for both the central difference and upwind schemes are shown in Equations 3.46 and 3.54, respectively.

For both the central difference and upwind, the magnitude of the diffusive and dispersive terms were compared. Because the coefficient C_1 ($C_1 = C + F + G - K$, as shown in Tables XI and XII), included the drag force (the term with the K coefficient) which was always significant, the dispersive term was usually much larger than the diffusive term(s).

For both the central difference and upwind schemes, Δt and Δz could be decreased to improve numerical accuracy. Although reducing Δt changed the absolute magnitudes of the first two terms in Equations 3.46 and 3.54, the magnitude of the dispersive error remained significantly greater. On the

TABLE X
FORMULATION OF MODIFIED EQUATION

V_e term	f(t) term	$(V_e \text{ term})^n$	$(V_e \text{ term})^{n+1}$	Coefficient (all terms evaluated at timestep n)
$\frac{\partial v_e}{\partial t}$	$\frac{(v_e)_i^{n+1} - (v_e)_i^n}{\Delta t}$			$A = (1-\epsilon) \rho_1 + \epsilon \rho_e$
$\frac{\partial v_e}{\partial z}$		Central difference: $\frac{(v_e)_{i+1}^n - (v_e)_{i-1}^n}{2\Delta z}$ Upwind: $\frac{(v_e)_{i+1}^n - (v_e)_i^n}{\Delta z}$	Central difference: $\frac{(v_e)_{i+1}^{n+1} - (v_e)_{i-1}^{n+1}}{2\Delta z}$ Upwind: $\frac{(v_e)_{i+1}^{n+1} - (v_e)_i^{n+1}}{\Delta z}$	$B = \rho_1 (\epsilon_0 V_0 - (1-\epsilon) v_e) \left(\frac{1-\epsilon}{z} \right) + \epsilon \rho_e v_e$
v_e		$(v_e)_i^n$	$(v_e)_i^{n+1}$	$C = -\frac{\rho_1}{z} \frac{\partial \epsilon}{\partial t}$
				$D = \frac{-\rho_1 (\epsilon_0 V_0)}{z} \frac{\partial \epsilon}{\partial t}$
				$E = \frac{\rho_1}{z^2} (\epsilon_0 V_0)^2 \frac{\partial \epsilon}{\partial z}$
v_e		$(v_e)_i^n$	$(v_e)_i^{n+1}$	$F = \frac{\rho_1}{z^2} (\epsilon_0 V_0) \frac{\partial \epsilon}{\partial z}$
v_e		$(v_e)_i^n$	$(v_e)_i^{n+1}$	$G = \frac{-\rho_1}{z^2} (\epsilon_0 V_0 - v_e) (1-\epsilon) \frac{\partial \epsilon}{\partial z}$
				$H = -\rho_1 \frac{\partial (\epsilon_0 V_0)}{\partial t}$
				$I = \epsilon \sigma (\rho_1 - \rho_e) *$
				$J = \frac{F}{(1-\epsilon)} \epsilon_0 V_0 *$
v_e		$(v_e)_i^n$	$(v_e)_i^{n+1}$	$K = -\frac{F}{(1-\epsilon)} *$
				$L = \frac{\epsilon}{(1-\epsilon) m_e} \frac{\partial \epsilon}{\partial z} *$

*Note these terms are on the right side of the equation.

TABLE XI

**THE MODIFIED EQUATION
(CENTRAL DIFFERENCE)**

A weighted average of the finite difference approximation is determined by weighting the V_i terms, which were defined above at both timesteps n and $n+1$, respectively by θ (i.e., explicit) and $1-\theta$ (i.e., implicit).

$$A \left[\frac{(V_i)^{n+1} - (V_i)^n}{\Delta t} \right] + \left(\theta B \left[\frac{(V_i)^n - (V_i)^{n-1}}{\Delta z} \right] + (1-\theta) B \left[\frac{(V_i)^{n+1} - (V_i)^n}{\Delta z} \right] \right) +$$

$$[\theta C (V_i)^n + (1-\theta) C (V_i)^{n+1}] + D + E + [\theta F (V_i)^n + (1-\theta) F (V_i)^{n+1}] +$$

$$[\theta G (V_i)^n + (1-\theta) G (V_i)^{n+1}] + H + I + J + [\theta K (V_i)^n + (1-\theta) K (V_i)^{n+1}] + L \quad (3.35)$$

Based on Taylor series, the following terms can be substituted back into the finite difference equation:

Forward time:
$$\frac{\partial V_i}{\partial t} = \frac{(V_i)^{n+1} - (V_i)^n}{\Delta t} - \frac{\Delta t}{2} \frac{\partial^2 V_i}{\partial t^2} \Big|_n + \dots \quad (3.36)$$

Central difference at n :
$$\frac{\partial V_i}{\partial z} \Big|_n = \frac{(V_i)^n_{i+1} - (V_i)^n_{i-1}}{2\Delta z} + \frac{\Delta z^2}{3!} \frac{\partial^3 (V_i)^n}{\partial z^3} \Big|_n + \dots \quad (3.37)$$

Central difference at $n+1$:
$$\frac{\partial V_i}{\partial z} \Big|_{n+1} = \frac{(V_i)^{n+1}_{i+1} - (V_i)^{n+1}_{i-1}}{2\Delta z} + \frac{\Delta z^2}{3!} \frac{\partial^3 (V_i)^{n+1}}{\partial z^3} \Big|_{i+1} + \dots \quad (3.38)$$

The first two terms of the weighted average finite difference equation can then be rewritten, including the truncation error:

$$A \left[\left(\frac{(V_i)^{n+1} - (V_i)^n}{\Delta t} - \frac{\Delta t}{2} \frac{\partial^2 (V_i)}{\partial t^2} \Big|_n + \dots \right) + \theta B \left[\left(\frac{(V_i)^n_{i+1} - (V_i)^n_{i-1}}{2\Delta z} + \frac{\Delta z^2}{3!} \frac{\partial^3 (V_i)^n}{\partial z^3} + \dots \right) \right] + (1-\theta) B \left[\left(\frac{(V_i)^{n+1}_{i+1} - (V_i)^{n+1}_{i-1}}{2\Delta z} + \frac{\Delta z^2}{3!} \frac{\partial^3 (V_i)^{n+1}}{\partial z^3} + \dots \right) \right] \right] \quad (3.39)$$

The truncation error is:

$$A \left[-\frac{\Delta t}{2} \frac{\partial^2 (V_i)}{\partial t^2} \Big|_n + \dots \right] + \theta B \left[+\frac{\Delta z^2}{3!} \frac{\partial^3 (V_i)^n}{\partial z^3} + \dots \right] + (1-\theta) B \left[+\frac{\Delta z^2}{3!} \frac{\partial^3 (V_i)^{n+1}}{\partial z^3} + \dots \right] \quad (3.40)$$

The original partial differential equation can be written as follows (with the coefficients as defined for the formulation of the modified equation):

$$A \frac{\partial V_i}{\partial t} + B \frac{\partial V_i}{\partial z} + (C + F + G - K) V_i + (-D - E - H + I + J + L) =$$

More simply:

$$A \frac{\partial V_i}{\partial t} + B \frac{\partial V_i}{\partial z} + C_1 V_i = D_1, \text{ where } C_1 = C + F + G + K \text{ and } D_1 = -D - E - H + I + J + L$$

And, finally:

$$\frac{\partial V_i}{\partial t} = -\frac{B}{A} \frac{\partial V_i}{\partial z} - \frac{C_1}{A} V_i + \frac{D_1}{A} \quad (3.41)$$

TABLE XI

THE MODIFIED EQUATION
(CENTRAL DIFFERENCE)
(continued)

<p>Taking another derivative with respect to time (of the original partial differential equation again) in order to change the time derivative in the truncation error to a spatial derivative:</p> $\frac{\partial^2 V_s}{\partial t^2} - \frac{B}{A} \frac{\partial}{\partial z} \left(\frac{\partial V_s}{\partial t} \right) - \frac{C_1}{A} \frac{\partial V_s}{\partial t} \quad (3.42)$
<p>Substituting $\frac{\partial V_s}{\partial t}$ from the original partial differential equation into $\frac{\partial^2 V_s}{\partial t^2}$ above:</p> $\frac{\partial^2 V_s}{\partial t^2} - \frac{B}{A} \frac{\partial}{\partial z} \left(-\frac{B}{A} \frac{\partial V_s}{\partial z} - \frac{C_1}{A} V_s + \frac{D_1}{A} \right) - \frac{C_1}{A} \left(-\frac{B}{A} \frac{\partial V_s}{\partial z} - \frac{C_1}{A} V_s + \frac{D_1}{A} \right) \quad (3.43)$
<p>Re-writing and grouping like terms:</p> $\frac{\partial^2 V_s}{\partial t^2} \left(\frac{B^2}{A^2} \right) \frac{\partial^2 V_s}{\partial z^2} + \left(\frac{2BC_1}{A^2} \right) \frac{\partial V_s}{\partial z} + \left(\frac{C_1^2}{A^2} \right) V_s - \left(\frac{C_1 D_1}{A^2} \right) \quad (3.44)$
<p>Substituting $\frac{\partial^2 V_s}{\partial t^2}$ (Equation 3.8) into the first term of the truncation error for the central difference scheme (Equation 3.39):</p> $-A \frac{\Delta t}{2} \left[\left(\frac{B^2}{A^2} \right) \frac{\partial^2 V_s}{\partial z^2} + \left(\frac{2BC_1}{A^2} \right) \frac{\partial V_s}{\partial z} + \left(\frac{C_1^2}{A^2} \right) V_s - \left(\frac{C_1 D_1}{A^2} \right) + \dots \right] + \theta B \left[+ \frac{\Delta z^2}{3!} \frac{\partial^3 (V_s)^n}{\partial z^3} + \dots \right] + (1-\theta) B \left[+ \frac{\Delta z^2}{3!} \frac{\partial^3 (V_s)^{n+1}}{\partial z^3} + \dots \right]$ <p>Simplifying:</p> $\left(\frac{B^2 \Delta t}{2A} \right) \frac{\partial^2 V_s}{\partial z^2} + \left(\frac{BC_1 \Delta t}{A} \right) \frac{\partial V_s}{\partial z} + \left(\frac{C_1^2 \Delta t}{2A} \right) V_s - \left(\frac{C_1 D_1 \Delta t}{2A} \right) + \theta B \left[+ \frac{\Delta z^2}{3!} \frac{\partial^3 (V_s)^n}{\partial z^3} + \dots \right] + (1-\theta) B \left[+ \frac{\Delta z^2}{3!} \frac{\partial^3 (V_s)^{n+1}}{\partial z^3} + \dots \right] \quad (3.45)$
<p>Accuracy is determined by the order of errors in the leading truncation error. (Note: this can be seen in the truncation error both before and after substituting for $\frac{\partial^2 V_s}{\partial t^2}$.) The order of errors are Δt and Δz^2.</p>
<p>Consistency is determined by taking the limit of the difference between the partial differential equation and the finite difference equation (this difference is the truncation error) as the grid spacing Δz and Δt go to zero.</p> $\lim_{\Delta z, \Delta t \rightarrow 0} \left[\left(\frac{B^2 \Delta t}{2A} \right) \frac{\partial^2 V_s}{\partial z^2} + \left(\frac{BC_1 \Delta t}{A} \right) \frac{\partial V_s}{\partial z} + \left(\frac{C_1^2 \Delta t}{2A} \right) V_s - \left(\frac{C_1 D_1 \Delta t}{2A} \right) + \theta B \left[+ \frac{\Delta z^2}{3!} \frac{\partial^3 (V_s)^n}{\partial z^3} + \dots \right] + (1-\theta) B \left[+ \frac{\Delta z^2}{3!} \frac{\partial^3 (V_s)^{n+1}}{\partial z^3} + \dots \right] \right] = 0$ <p>This solution is unconditionally consistent.</p>

TABLE XI

THE MODIFIED EQUATION
(CENTRAL DIFFERENCE)
(continued)

An analysis of the coefficients (of the derivative terms) for an explicit scheme ($\theta=1$) are:

$$\left[\frac{B^2 \Delta t}{2A} \frac{\Delta V_e}{\Delta z^2} \right] \left[\frac{BC_1 \Delta t}{A} \frac{\Delta V_e}{\Delta z} \right] \left[\frac{6B \Delta z^2}{3!} \frac{\Delta V_e}{\Delta z^3} |_{n+\dots} \right]$$

Multiplying each term by $\frac{\Delta z^2}{\Delta V_e B}$, leads to:

$$\left[\frac{B \Delta t}{2A} \right] \quad \left[\frac{C_1 \Delta t \Delta z}{A} \right] \quad \left[\frac{\Delta z}{3!} \right]$$

Diffusive Dispersive Dispersive

(3.46)

Each term can be evaluated by substituting approximate values for A, B, C₁, Δt, and Δz, as follows:

$$A \approx 1$$

$$B \approx 0, \text{ where } B = B_1 + B_2 V_e \text{ (see Tables VI and IX)}$$

$$C_1 \approx 10^8, \text{ where } C_1 = C + F + G + K, \text{ and } G = G_1 + G_2 V_e \text{ (see Tables VI and IX)}$$

$$\Delta t \approx 1$$

$$\Delta z \approx 1$$

Evaluating the relative magnitude of the three terms:

$$[-0] \quad \quad [-10^8] \quad \quad [-10^{-1}]$$

Diffusive Dispersive Dispersive

*Based on using constitutive properties for kaolin suspensions (Wells and Dick, 1993)

TABLE XII
THE MODIFIED EQUATION
(UPWIND)

A weighted average of the finite difference approximation is determined by weighting the V_i terms, which were defined above at both timesteps n and $n+1$, respectively by θ (i.e., explicit) and $1-\theta$ (i.e., implicit).

$$A \left[\frac{(V_i)^{n+1} - (V_i)^n}{\Delta t} \right] + \left(\theta B \left[\frac{(V_i)^n - (V_i)^{n-1}}{2\Delta z} \right] + (1-\theta) B \left[\frac{(V_i)^{n+1} - (V_i)^{n-1}}{2\Delta z} \right] \right) +$$

$$[\theta C (V_i)^n + (1-\theta) C (V_i)^{n+1}] + D + E + [\theta F (V_i)^n + (1-\theta) F (V_i)^{n+1}] +$$

$$[\theta G (V_i)^n + (1-\theta) G (V_i)^{n+1}] + H - I + J + [\theta K V_i^n + (1-\theta) K (V_i)^{n+1}] + L \quad (3.47)$$

Based on Taylor series, the following terms can be substituted back into the finite difference equation:

$$\text{Forward time: } \frac{\partial V_i}{\partial t} = \frac{(V_i)^{n+1} - (V_i)^n}{\Delta t} - \frac{\Delta t}{2} \frac{\partial^2 V_i}{\partial t^2} \Big|_n + \dots \quad (3.48)$$

$$\text{Upwind at } n: \quad \frac{\partial V_i}{\partial z} \Big|_n = \frac{(V_i)^n - (V_i)^{n-1}}{\Delta z} - \frac{\Delta z}{2!} \frac{\partial^2 (V_i)^n}{\partial z^2} \Big|_n + \dots \quad (3.49)$$

$$\text{Upwind at } n+1: \quad \frac{\partial V_i}{\partial z} \Big|_{n+1} = \frac{(V_i)^{n+1} - (V_i)^n}{\Delta z} + \frac{\Delta z}{2!} \frac{\partial^2 (V_i)^{n+1}}{\partial z^2} \Big|_n + \dots \quad (3.50)$$

The first two terms of the weighted average finite difference equation can then be rewritten, including the truncation error:

$$A \left[\left(\frac{(V_i)^{n+1} - (V_i)^n}{\Delta t} \right) - \frac{\Delta t}{2} \frac{\partial^2 (V_i)}{\partial t^2} \Big|_n + \dots \right] + \theta B \left[\left(\frac{(V_i)^n - (V_i)^{n-1}}{\Delta z} \right) + \frac{\Delta z}{2!} \frac{\partial^2 (V_i)^n}{\partial z^2} + \dots \right] + (1-\theta) B \left[\left(\frac{(V_i)^{n+1} - (V_i)^{n-1}}{\Delta z} \right) + \frac{\Delta z}{2!} \frac{\partial^2 (V_i)^{n+1}}{\partial z^2} + \dots \right] \quad (3.51)$$

The truncation error is:

$$A \left[-\frac{\Delta t}{2} \frac{\partial^2 (V_i)}{\partial t^2} \Big|_n + \dots \right] + \theta B \left[+\frac{\Delta z}{2!} \frac{\partial^2 (V_i)^n}{\partial z^2} + \dots \right] + (1-\theta) B \left[+\frac{\Delta z}{2!} \frac{\partial^2 (V_i)^{n+1}}{\partial z^2} + \dots \right] \quad (3.52)$$

The second derivative with respect to time (of the original partial differential equation) can be derived, using Equations 3.40-3.43 in the previous table. (Note they are the same as for the central difference scheme.) The final equation (3.43) is re-stated here:

$$\frac{\partial^2 V_i}{\partial t^2} = \left(\frac{B^2}{A^2} \right) \frac{\partial^2 V_i}{\partial z^2} + \left(\frac{2BC_1}{A^2} \right) \frac{\partial V_i}{\partial z} + \left(\frac{C_1^2}{A^2} \right) V_i - \left(\frac{C_1 D_1}{A^2} \right)$$

Substituting $\frac{\partial^2 V_i}{\partial t^2}$ (Equation 3.43) into the first term of the truncation error for the upwind scheme (Equation 3.51):

$$-A \frac{\Delta t}{2} \left[\left(\frac{B^2}{A^2} \right) \frac{\partial^2 V_i}{\partial z^2} + \left(\frac{2BC_1}{A^2} \right) \frac{\partial V_i}{\partial z} + \left(\frac{C_1^2}{A^2} \right) V_i - \left(\frac{C_1 D_1}{A^2} \right) + \dots \right] + \theta B \left[+\frac{\Delta z}{2!} \frac{\partial^2 (V_i)^n}{\partial z^2} + \dots \right] + (1-\theta) B \left[+\frac{\Delta z}{2!} \frac{\partial^2 (V_i)^{n+1}}{\partial z^2} + \dots \right]$$

Simplifying:

$$\left(\frac{B^2 \Delta t}{2A} \right) \frac{\partial^2 V_i}{\partial z^2} + \left(\frac{BC_1 \Delta t}{A} \right) \frac{\partial V_i}{\partial z} + \left(\frac{C_1^2 \Delta t}{2A} \right) V_i - \left(\frac{C_1 D_1 \Delta t}{2A} \right) + \theta B \left[+\frac{\Delta z}{2!} \frac{\partial^2 (V_i)^n}{\partial z^2} + \dots \right] + (1-\theta) B \left[+\frac{\Delta z}{2!} \frac{\partial^2 (V_i)^{n+1}}{\partial z^2} + \dots \right] \quad (3.53)$$

TABLE XII
THE MODIFIED EQUATION
(UPWIND)
(continued)

<p>Accuracy is determined by the order of errors in the leading truncation error. The order of errors are Δt and Δz.</p>
<p>Consistency is determined by taking the limit of the difference between the partial differential equation and the finite difference equation (this difference is the truncation error) as the grid spacing Δz and Δt go to zero.</p> $\lim_{\Delta z, \Delta t \rightarrow 0} \left[\left(\frac{B^2 \Delta t}{2A} \right) \frac{\partial^2 V_s}{\partial z^2} + \left(\frac{BC_1 \Delta t}{A} \right) \frac{\partial V_s}{\partial z} + \left(\frac{C_1^2 \Delta t}{2A} \right) V_s - \left(\frac{C_1 D_1 \Delta t}{2} \right) + \theta B \left[+ \frac{\Delta z}{2!} \frac{\partial^2 (V_s)_s}{\partial z^2} + \dots \right] + (1-\theta) B \left[+ \frac{\Delta z}{2!} \frac{\partial^2 (V_s)_{s+1}}{\partial z^2} + \dots \right] \right] = 0$
<p>This solution is unconditionally consistent.</p>
<p>An analysis of the coefficients (of the derivative terms) for an explicit scheme ($\theta=1$) are:</p> $\left[\frac{B^2 \Delta t}{2A} \frac{\Delta V_s}{\Delta z^2} \right] \left[\frac{BC_1 \Delta t}{A} \frac{\Delta V_s}{\Delta z} \right] \left[\theta B \frac{\Delta z}{2!} \frac{\Delta V_s}{\Delta z^2} + \dots \right]$ <p>Multiplying each term by $\frac{\Delta z^2}{\Delta V_s B}$ leads to:</p> $\left[\frac{B \Delta t}{2A} \right] \quad \left[\frac{C_1 \Delta t \Delta z}{A} \right] \quad \left[\frac{\Delta z}{2!} \right]$ <p style="text-align: center;"><i>Diffusive Dispersive Diffusive</i></p> <p style="text-align: right;">(3.54)</p>
<p>Each term can be evaluated by substituting approximate values for A, B, C₁, Δt, and Δz, as follows:</p> <p>A \approx 1 B \approx 0, where B = B₁ + B₂V_s (see Tables VI and IX) C₁ \approx 10^{8*}, where C₁ = C + F + G + K, and G = G₁ + G₂V_s (see Tables VI and IX) $\Delta t \approx$ 1 $\Delta z \approx$ 1</p> <p>Evaluating the relative magnitude of the three terms:</p> $\begin{matrix} [-0] & [-10^8] & [-1] \\ \text{Diffusive} & \text{Dispersive} & \text{Diffusive} \end{matrix}$

*Based on using constitutive properties for kaolin suspensions (Wells and Dick, 1993)

other hand, if Δz was decreased, the relative dispersive error decreased, and the relative diffusive error remained constant or decreased. Decreasing Δt and Δz sufficiently to eliminate significant diffusive and dispersive errors was not practical because of the increased computational time required.

Artificial Diffusion (or Artificial Viscosity)

An artificial viscosity or diffusive term can be introduced to counteract the mathematical effects of the dispersive error introduced by the numerical scheme (Von Neumann and Richtmeyer, as cited by Plaskett, 1992). This artificial viscosity term would result in smoothing the shock front in the numerical solution. The term will be of the form of the diffusive term, i.e., a second derivative using central finite differences, such as:

$$\omega' \rho_s \frac{\partial^2 V_s}{\partial Z^2} = \omega' \rho_s \left(\frac{V_{s_{i+1}} - 2V_{s_i} + V_{s_{i-1}}}{\Delta Z^2} \right) \quad \text{where, } \omega = \frac{\omega' \rho_s}{\Delta Z^2} \quad (3.55)$$

and ω' is the artificial diffusion coefficient [L^2/T].

$$\omega' \rho_s \frac{\partial^2 V_s}{\partial Z^2} = \omega (V_{s_{i-1}} - 2V_{s_i} + V_{s_{i+1}}) \quad (3.56)$$

Weighting the V_s terms by θ and $(1-\theta)$ respectively for the general explicit and implicit schemes:

$$\omega' \frac{\partial^2 V_s}{\partial Z^2} = \theta \omega (V_{s_{i-1}} - 2V_{s_i} + V_{s_{i+1}}) + (1-\theta) \omega (V_{s_{i-1}} - 2V_{s_i} + V_{s_{i+1}}) \quad (3.57)$$

Adding the artificial viscosity, defined in Equation 3.57, to Equation 3.26 (or Equation 3.33):

$$\begin{aligned} & (x_2 - (1-\theta) \omega) (V_s)_{i-1}^{n+1} + (y_2 + (1-\theta) (2\omega)) (V_s)_i^{n+1} + (z_2 - (1-\theta) \omega) (V_s)_{i+1}^{n+1} \\ & = (x_1 + \theta \omega) (V_s)_{i-1}^n + (y_1 - \theta (2\omega)) (V_s)_i^n + (z_1 + \theta \omega) (V_s)_{i+1}^n + x_0 \end{aligned} \quad (3.58)$$

And, finally, redefining the x_1 , y_1 , z_1 , and x_2 , y_2 , and z_2 terms used in Equations 3.24 and 3.25 (and 3.31 and 3.32):

$$\begin{aligned} X_2 &= x_2 - (1-\theta) \omega; \quad Y_2 = y_2 + (1-\theta) (2\omega); \quad Z_2 = z_2 - (1-\theta) \omega; \\ X_1 &= x_1 + \theta \omega; \quad Y_1 = y_1 - \theta (2\omega); \quad Z_1 = z_1 + \theta \omega \end{aligned} \quad (3.59)$$

These re-defined terms were substituted into the tridiagonal matrix. solution form in Equations 3.27 and 3.34.

Comparing the Numerical Model to an Analytical Solution by Soo

The numerical gravity sedimentation model, with the implicit formulation, was compared to Soo's (1989) analytical solution for "the simplest nontrivial situation". Soo (1989) made the following simplifying assumptions: (1) no liquid flow out the bottom ($V_l=0$ at $z=0$) and (2) solid density much larger than liquid density ($\rho_s \gg \rho_l$). Soo's (1989) equations also do not consider the effect of effective strength, σ' . Therefore, to simulate Soo's simplified case, σ' was set equal to 0 within the numerical model.

Soo's (1989) analytical solution for settling velocity, V_s , and fluid velocity, V_l , was:

$$\frac{-V_s F'}{g} = (1 - e^{-F't}) = \frac{V_l F' (1 - \alpha_o)}{\alpha_o g} \quad (3.60)$$

where:

$$F' = \frac{F_{Soo}}{\varepsilon^2} = 10 \text{ sec}^{-1}$$

$$\alpha_o = 1 - \varepsilon_o \text{ (volume fraction solid)}$$

The boundary conditions in the numerical model at both the top and the bottom were:

$$V_s^n = 0 \text{ and } V_s^{n+1} = 0$$

The numerical model was simplified by dividing both sides of Equation 3.9 by ρ_s and then equating $\frac{\rho_l}{\rho_s} = 0$ (based on the assumption that $\rho_s \gg \rho_l$). The initial condition of $V_s = 0$ at $t=0$ was

assumed. The following coefficients, shown in Table X, were used to simulate Soo's simplified case:

$$A = \varepsilon$$

$$B = \varepsilon V_s = 0$$

$$C = D = E = F = G = H = 0$$

$$I = -\varepsilon g$$

$$J=0$$

$$K = -\frac{F_{Wells}}{(1-\varepsilon)\rho_s} = -F_{SoC} = -F' \text{ (see Table II)}$$

A comparison of the analytical solution to the numerical solution is shown in Figure 8.

Constitutive Relationships

Constitutive relationships were required to model gravity sedimentation. These relationships, the coefficient of volume compressibility, m_v , and intrinsic permeability, k , are both functions of porosity, ε .

Coefficient of Volume Compressibility. The coefficient of volume compressibility, m_v , describes the empirical relationship between porosity, ε , and effective stress, σ' , where:

$$m_v = -\frac{\partial \varepsilon}{\partial \sigma'} \quad (3.61)$$

Plaskett (1992) determined and used the following constitutive equation, which fit the experimental data for cake filtration from Wells (1990).

$$\varepsilon = \nu \sigma' \frac{\zeta}{\sigma' - \sigma'_1} - \varepsilon_1 \quad (3.62)$$

- ε = porosity [-]
- ν = coefficient for dimensional consistency [L-T²/M]
- σ' = effective stress, kPa [M/L-T²]
- ζ = empirical constant, = 0.54 kPa [M/L-T²]
- σ'_1 = empirical constant corresponding to limiting effective stress [M/L-T²]
- ε_1 = empirical constant corresponding to limiting porosity [-]

A plot of the equation (3.62) compared to the experimental data is shown in Figure 9.

As seen in Equations 3.61 and 3.62, the coefficient of volume compressibility, m_v , was a function of ε and σ' . Knowing ε , a root finding technique was required to determine σ' . Knowing σ' , as well as ε , allowed m_v to be determined.

A bi-section technique was used for the root finding algorithm. An initial guess for σ' was required for this technique. After calculating the corresponding ε , σ' was either doubled or halved until its corresponding porosity and the porosity corresponding to the previous guess were on either

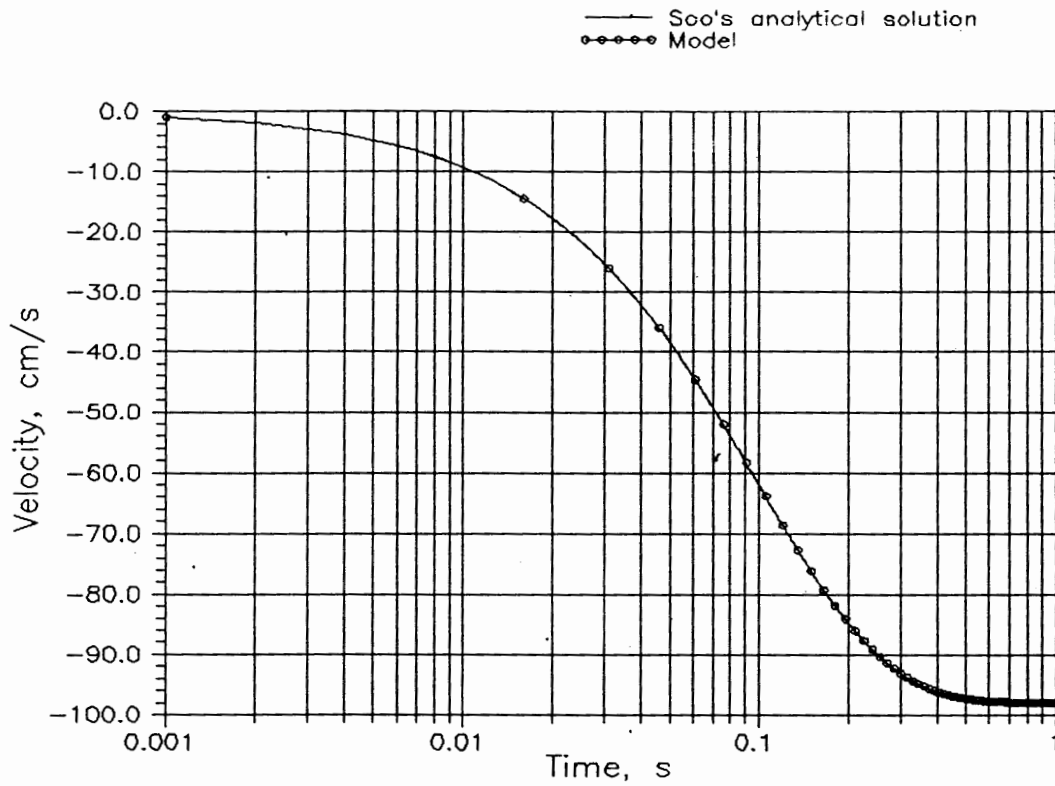


Figure 8. Comparison of Soo's (1989) analytical solution to the numerical model results.

side of the known porosity value for which the root was being sought. This technique was repeated until the two values for porosity were very close (within $\pm 1.0 \times 10^{-6}$).

The coefficient of volume compressibility, m_v , as given by Equation 3.61, was determined by taking the natural log of both sides of Equation 3.62,

$$\ln \varepsilon = \left(\frac{\zeta}{\sigma' - \sigma'_1} \ln(v\sigma') - \ln \varepsilon_1 \right)$$

and differentiating by parts.

$$\frac{1}{\varepsilon} \partial \varepsilon = \left(\frac{\zeta}{\sigma' - \sigma'_1} \frac{1}{(v\sigma')} - \frac{\zeta}{(\sigma' - \sigma'_1)^2} \ln(v\sigma') \right) \partial \sigma'$$

After multiplying both sides by $-\varepsilon$, and substituting Equation 3.62 for ε :

$$m_v = -\frac{\partial \varepsilon}{\partial \sigma'} = -\left((v \sigma') \frac{\zeta}{\sigma' - \sigma'_1} - \varepsilon_1 \right) \left(\frac{\zeta}{\sigma' - \sigma'_1} \frac{1}{(v \sigma')} - \frac{\zeta}{(\sigma' - \sigma'_1)^2} \ln (v \sigma') \right) \quad (3.63)$$

A plot of the relationship between porosity, ε , and the coefficient of volume compressibility, m_v , is shown in Figure 10.

Another technique by Wells (1990) used the following constitutive equation, which fit experimental data for gravity sedimentation and cake filtration.

$$\sigma' (kPa) = 1.69 \times 10^9 \exp(-28.9 \varepsilon) \quad (3.64)$$

where:

$$m_v (kPa^{-1}) = 2.04 \times 10^{-11} \exp(28.9 \varepsilon) \quad (3.65)$$

Figures 9 and 10 show a graphical presentation of Equations 3.64 and 3.65.

Intrinsic Permeability. Experimental data for kaolin clay suspensions collected at the Cornell High Energy Synchrotron Source (CHESS) showed that the intrinsic permeability is an exponential function of the following general form (Wells, 1990).

$$k = \alpha \exp(\beta \varepsilon) \quad (3.66)$$

Wells and Dick (1993) determined the spatial and temporal distribution of permeability within the filter cake, and a best-fit equation for $\varepsilon < .65$, as shown in Figure 11, was:

$$k_1 (cm^2) = 2.7 \times 10^{-16} \exp(20 \varepsilon) \quad (3.67)$$

For $\varepsilon < .65$, the scatter appears to be in the limits of the experimental technique. However, in the higher porosity regions where the cake was growing ($\varepsilon \geq 0.65$), the data scatter appeared to be greater than the limits of the experimental technique, and an equation with a different set of coefficients was determined. Another exponential equation was used in the upper range ($\varepsilon \geq 0.65$), such as:

$$k_2 = \alpha_2 \exp(\beta_2 \varepsilon) \quad (3.68)$$

The coefficient β_2 was input to the model, and the coefficient α_2 was determined by setting Equation 3.67 equal to Equation 3.68 at $\varepsilon = 0.65$, i.e.,

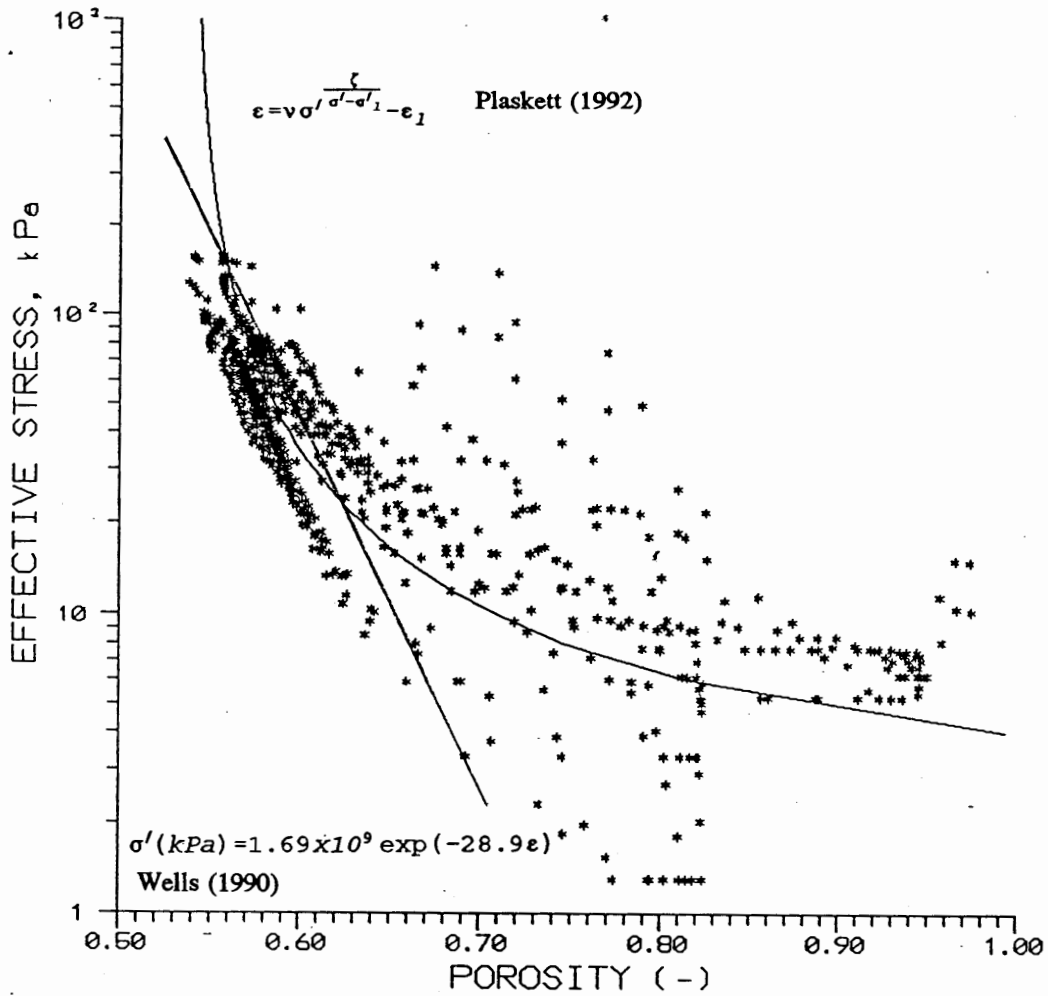


Figure 9. Plot of data obtained from Wells (1990) and constitutive relationships for porosity, ϵ , vs. the effective stress, σ' , from Plaskett (1992) and Wells (1990).

$$2.7 \times 10^{-16} \exp(20 \times 0.65) = \alpha_2 \exp(\beta_2 \times 0.65) \quad (3.69)$$

$$\alpha_2 = 2.7 \times 10^{-16} \exp((20 - \beta_2) 0.65) \quad (3.70)$$

β_2 was determined by calibrating porosity model predictions to data.

In the computer code, the permeability was constrained to be a function of the initial porosity if $\epsilon > \epsilon_{initial}$. This occurred in the upper range, and Equations 67 and 68 became:

$$k_1 (cm^2) = 2.7 \times 10^{-16} \exp(20 \epsilon_{initial}) \quad (3.71)$$

$$k_2 = \alpha_2 \exp(\beta_2 \epsilon_{initial}) \quad (3.72)$$

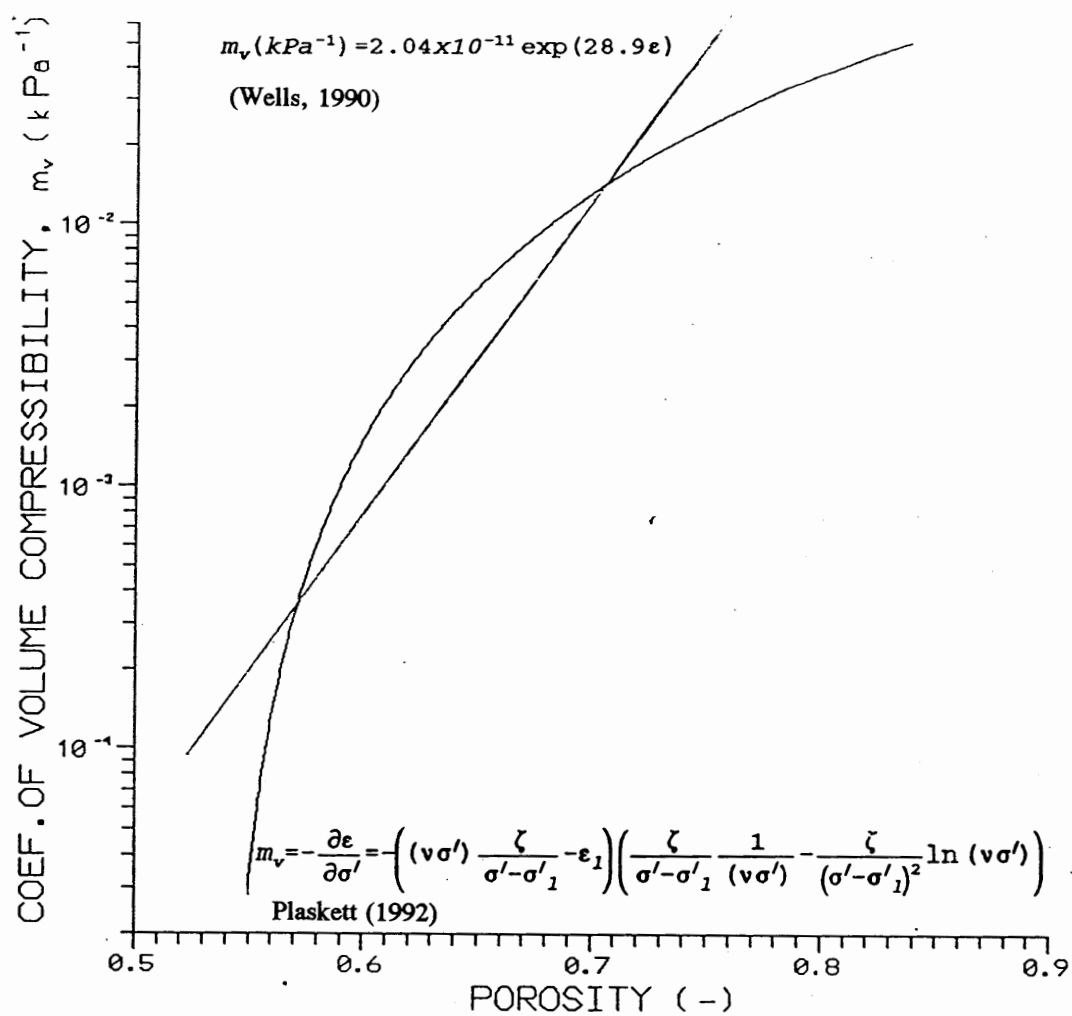


Figure 10. Plaskett's (1992) and Wells' (1990) relationships between porosity, ε , and the coefficient of volume compressibility, m_v .

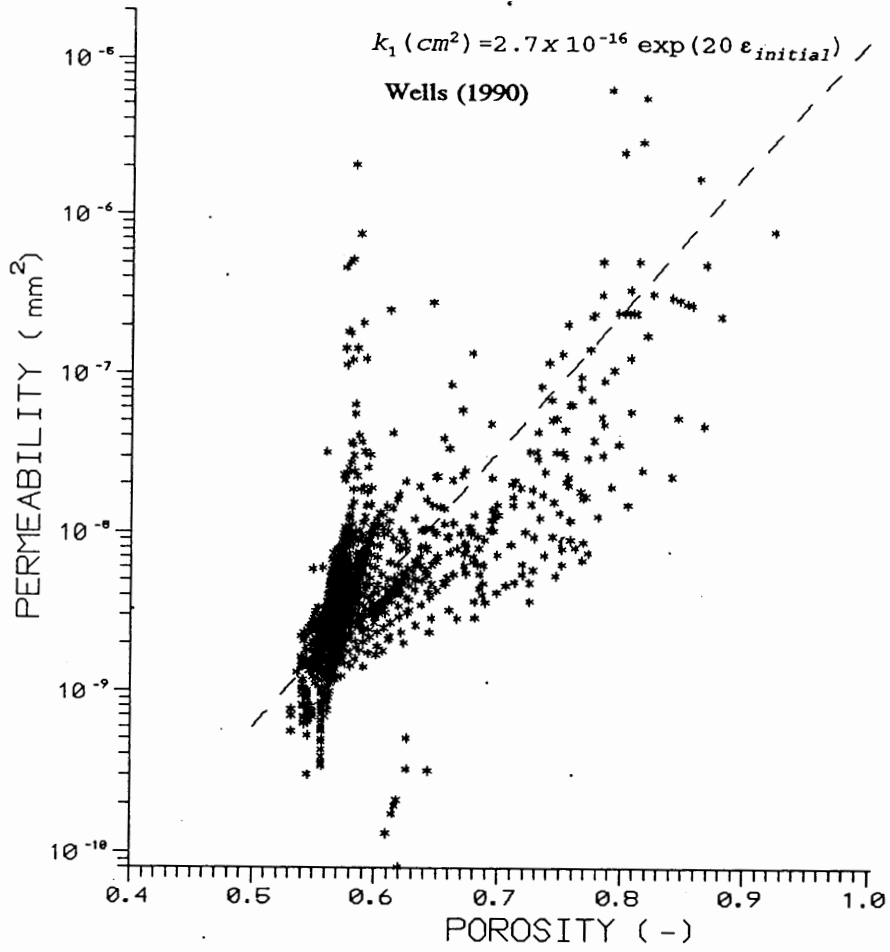


Figure 11. Plot of porosity vs. permeability from cake filtration data for kaolin clay suspensions (Wells, 1990)

CHAPTER IV

MODEL RESULTS

CALIBRATION TO GRAVITY SEDIMENTATION DATA

The model was calibrated by varying model parameters until model predictions of suspended solids compared well with gravity sedimentation suspended solids data obtained by Wells (1990) at the Cornell High Energy Synchrotron Source (CHESS). The data was real-time suspended solids concentration measurements at 0.5 mm vertical separation and interpolated to 1 minute intervals. Experimental error in suspended solids concentrations between replicate experiments was on the order of $\pm 8\%$ (Wells, 1990).

The model parameters included: the Δt , the scheme (central difference or upwind), and the ω factor (a multiplier after calculating the artificial viscosity from the initial porosity (ϵ_i), m_v (the coefficient of volume compressibility) and the permeability in the upper range.

Wells (1990) obtained six different gravity sedimentation data sets for kaolin clay suspensions. The six data sets each had a different initial suspended solids concentration (low, medium, and high), cell size (small, medium, and large), temperature (24°C, 26°C, and 27°C), and time period of experiment (ranging from 10-29 minutes). The appropriate initial porosity, cell size, temperature, and time length were input into the model. Initial porosity could be calculated knowing initial suspended solids concentration and solid density (assumed to be 2.616 gm/cm³ for kaolin clay), $C_i = \rho_s(1-\epsilon)$.

The model was calibrated to the data set SEDM1K (D2), which was based on a medium initial concentration (0.31 g/cm³), medium cell size (8.1 cm x 1.905 cm), 24°C temperature, and an 18 minute duration. The calibrated model used: a time step Δt of 1 second, the central difference scheme, an ω factor of 0 (i.e., no artificial diffusion), constitutive relationship for m_v as shown in Equation 3.65

from Wells (1990), and the constitutive relationship for permeability with $\beta_2=24$ such that the equation for k_2 in Equation 3.68 is as follows.

$$k_2 (\text{cm}^2) = 2.0 \times 10^{-17} \exp(24\varepsilon) \quad (4.1)$$

A plot comparing the relationships of k_1 and k_2 is shown in the model sensitivity section.

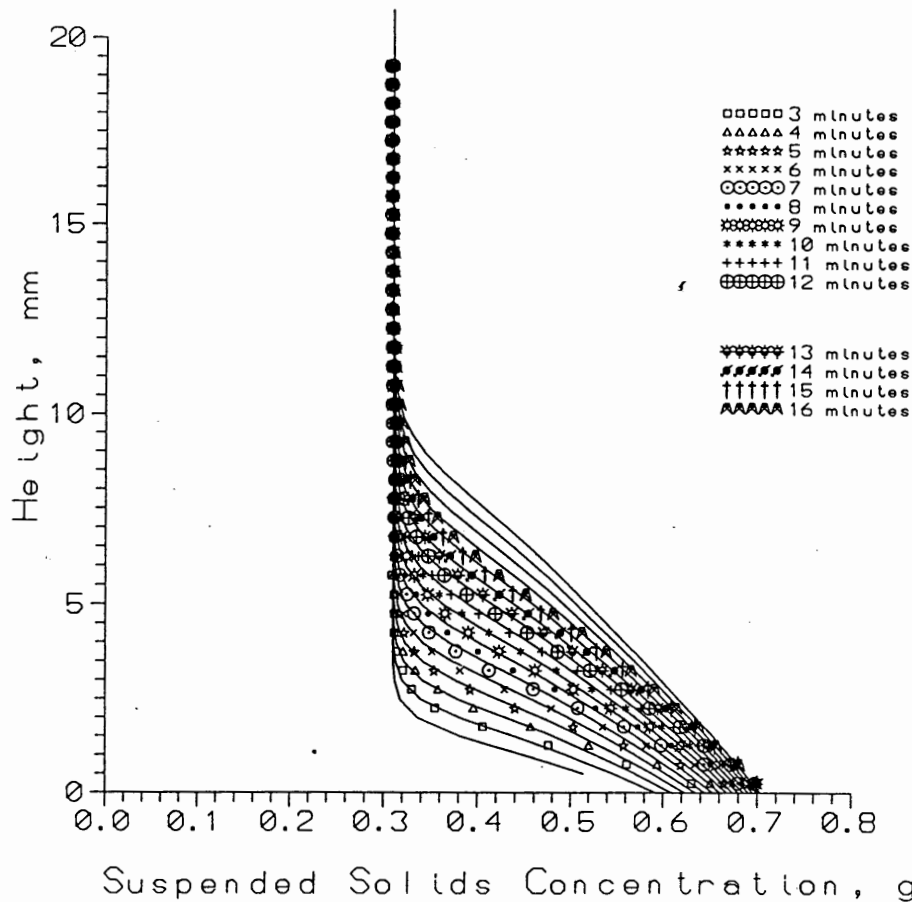


Figure 12. Comparison of model predictions for suspended solids (solid lines) to data set SEDM1K (D2). Data set (symbols) with initial concentration=0.31 g/cm³, cell size 26.325 cm², and temperature=24°C.

Figure 12 shows the calibrated model predictions of suspended solids concentration to suspended solids data set SEDM1K (D2). Even though the model domain included prediction of the clarification at the top of the model domain, CHES data was limited to the thickening region. The mean error and root

mean square (RMS) errors, defined as $\frac{\sum (C_{data} - C_{model})}{n}$ and $\sqrt{\frac{\sum (C_{data} - C_{model})^2}{n}}$ where C is

the suspended solids concentration and n is the number of observations, are shown in Table XIII.

Solid velocity predictions from the same model simulation, with the calibrated model parameters are compared to calculations of solid velocity from suspended solids data in Figure 13. The solid velocity from the CHESSE prorsity data was calculated using Equation 3.10. The mean and root mean square (RMS) errors are shown in Table XIII.

The simulation took approximately 80 seconds using a 486 25 mHz PC to approximate 15 minutes of real time.

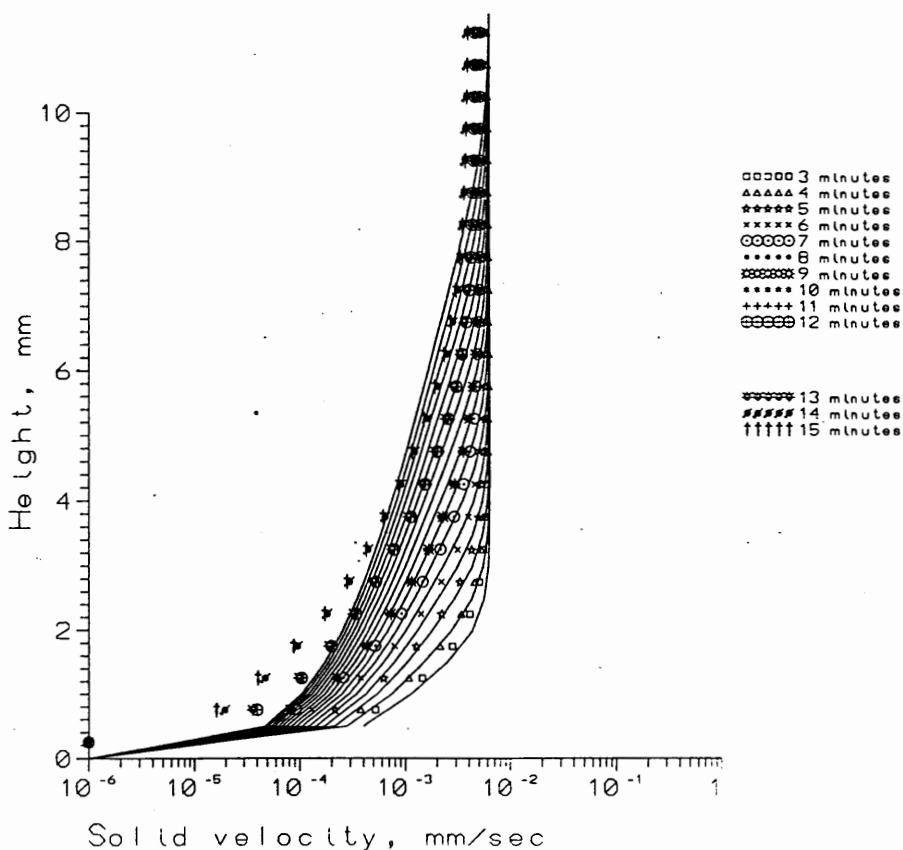


Figure 13. Comparison of model predictions for solid velocity (solid lines) to data set SEDM1K (D2). Data set (symbols) with initial concentration=0.31 g/cm³, cell size=26.325 cm², and temperature=24°C. (Note: 10⁻⁶ mm/second is a default value for any solid velocity <10⁻⁶.)

The mass vs. time was plotted in Figure 14 for the model simulation which was calibrated to the SEDM1K (D2) data set. Figure 14 shows that mass is, in general, conserved during the model simulation. It can be noted that at the onset mass is lost rather rapidly, but by the end of the simulation approximately half this mass has been regained. In the case of the low initial porosity simulations, far less mass is regained by the end of the simulation.

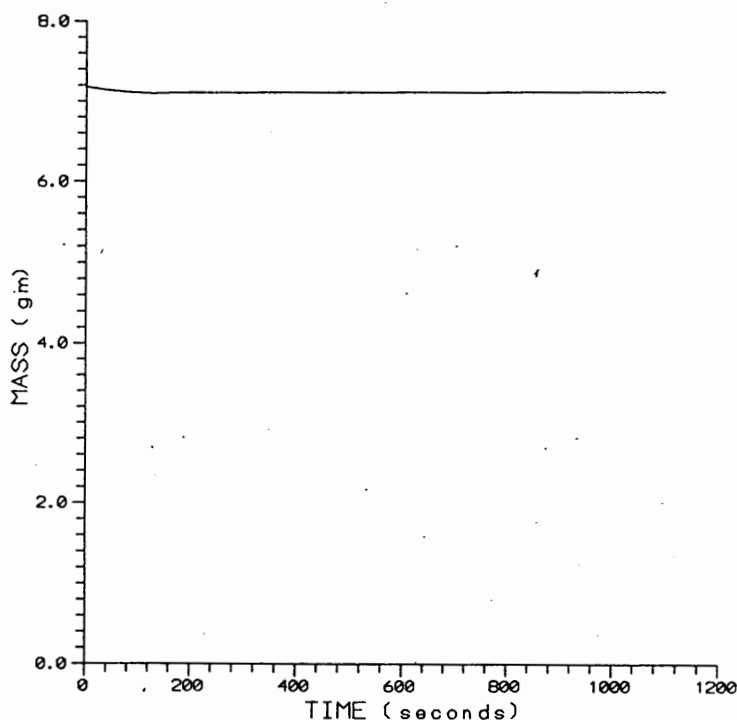


Figure 14. Plot of mass vs. time for the model simulation which was calibrated to the SEDM1K (D2) data set.

MODEL VERIFICATION

Without changing the model coefficients for the constitutive relationships from those used during the calibration, other simulations were run in order to verify the validity of the model predictions. As during the calibration, the time step $\Delta t=1$ and the central difference scheme was used during the simulations. The ω factor was 0 for the medium and high initial concentrations. In the case of the two data sets with low initial concentration, SEDL3K (D7) and DPK6 (D11), the model simulation became numerically unstable without artificial viscosity.

Table XIII shows a summary of comparisons between the model predictions of suspended solids and solid velocity profiles and the CHES data with their respective mean and RMS errors. Figures 15-19 show the model results graphically compared to the data for both suspended solids concentrations and solid velocities.

TABLE XIII

STATISTICS FROM MODEL RESULTS FOR SUSPENDED SOLIDS CONCENTRATION COMPARED TO GRAVITY SEDIMENTATION DATA FOR KAOLIN CLAY SUSPENSIONS

CHES Data	Initial Concentration (g/cm ³)	Cell Size (cm ²)	Temp (°C)	No. of comparisons **	Mean Error**	RMS Error**	Conservation of Mass***
SEDM1K (D2)	0.31	15.4305	24°C	531 267	.004988 -.000667	.016376 .001758	99.5%
SEDL2K (D7)	0.48	26.3250	24°C	832 400	.029761 -.000389	.046786 .000590	99.6%
SEDL3K (D10)	0.14	26.3250	24°C	335 191	.097291 -.003050	.130913 .005939	98.0%
DPK6 (D11)	0.15	8.0190	27°C	216 115	.041247 -.007026	.086124 .007767	98.2%
KDM10 (D13)	0.31	15.4305	26°C	274 115	.013180 -.000610	.041873 .001483	99.2%
LKD4 (D14)*	0.31	26.33	26°C	335 267	-.080199 -.000721	.102047 .001769	99.4%

*After 20 minutes Δp of 15 psi applied

**First number is for suspended solids (g/cm³), and second number is for solid velocity (mm/sec)

***Based on final mass divided by initial mass

Correlations of the calibrated model to data with a low initial concentration indicated that the constitutive parameters in the low suspended solids region may need to be readjusted. Simulations with low initial concentration required the addition of artificial diffusion. The ω factor of 10^8 was used, and still some instability was apparent.

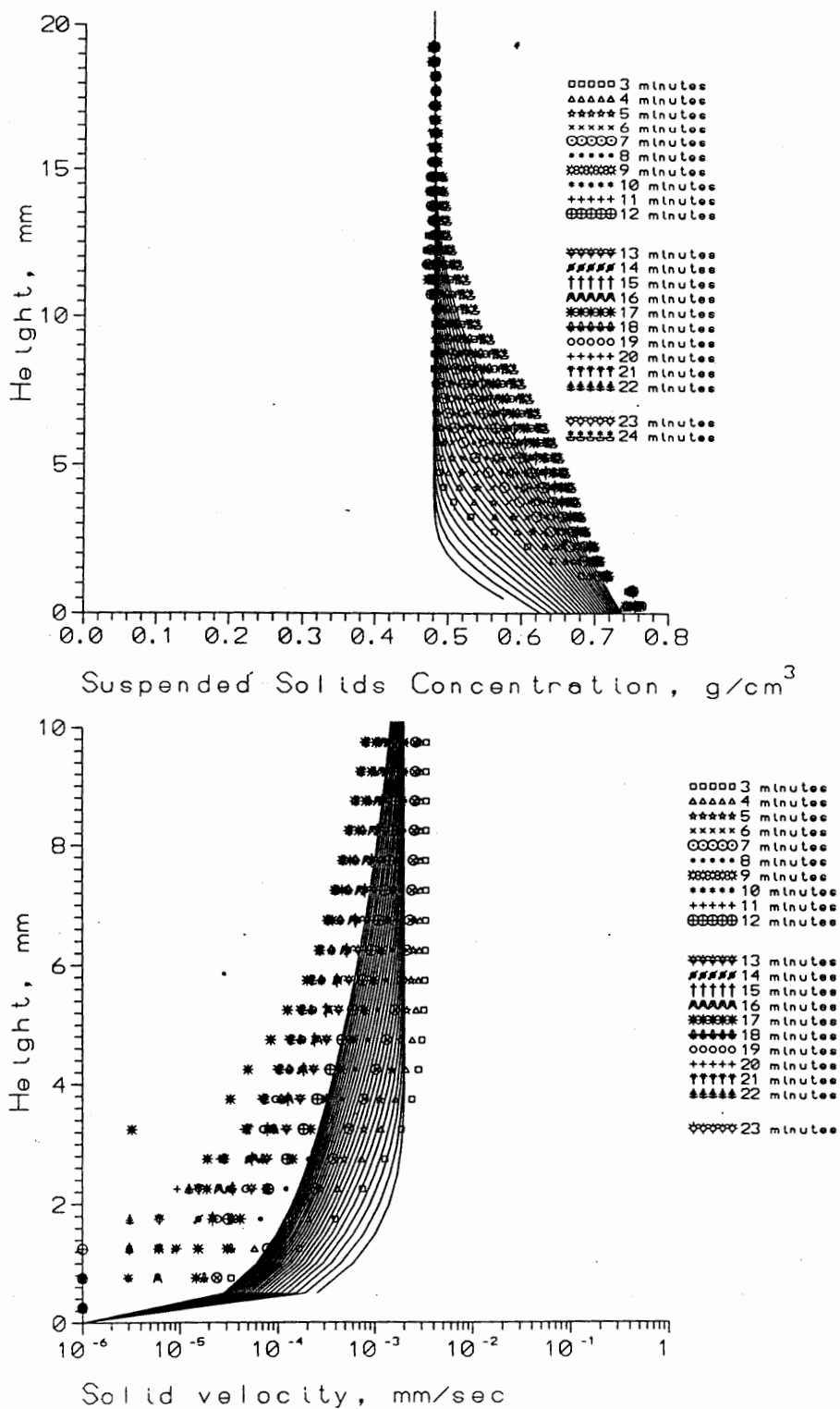


Figure 15. Comparison of model predictions to data set SEDL2K (D7). Model verification (solid lines) to data (symbols) with initial concentration= $0.48 \text{ g}/\text{cm}^3$, cell size= 26.325 cm^2 , and temperature= 24°C . (Note: $10^{-6} \text{ mm}/\text{second}$ is a default value for any solid velocity $< 10^{-6}$.)

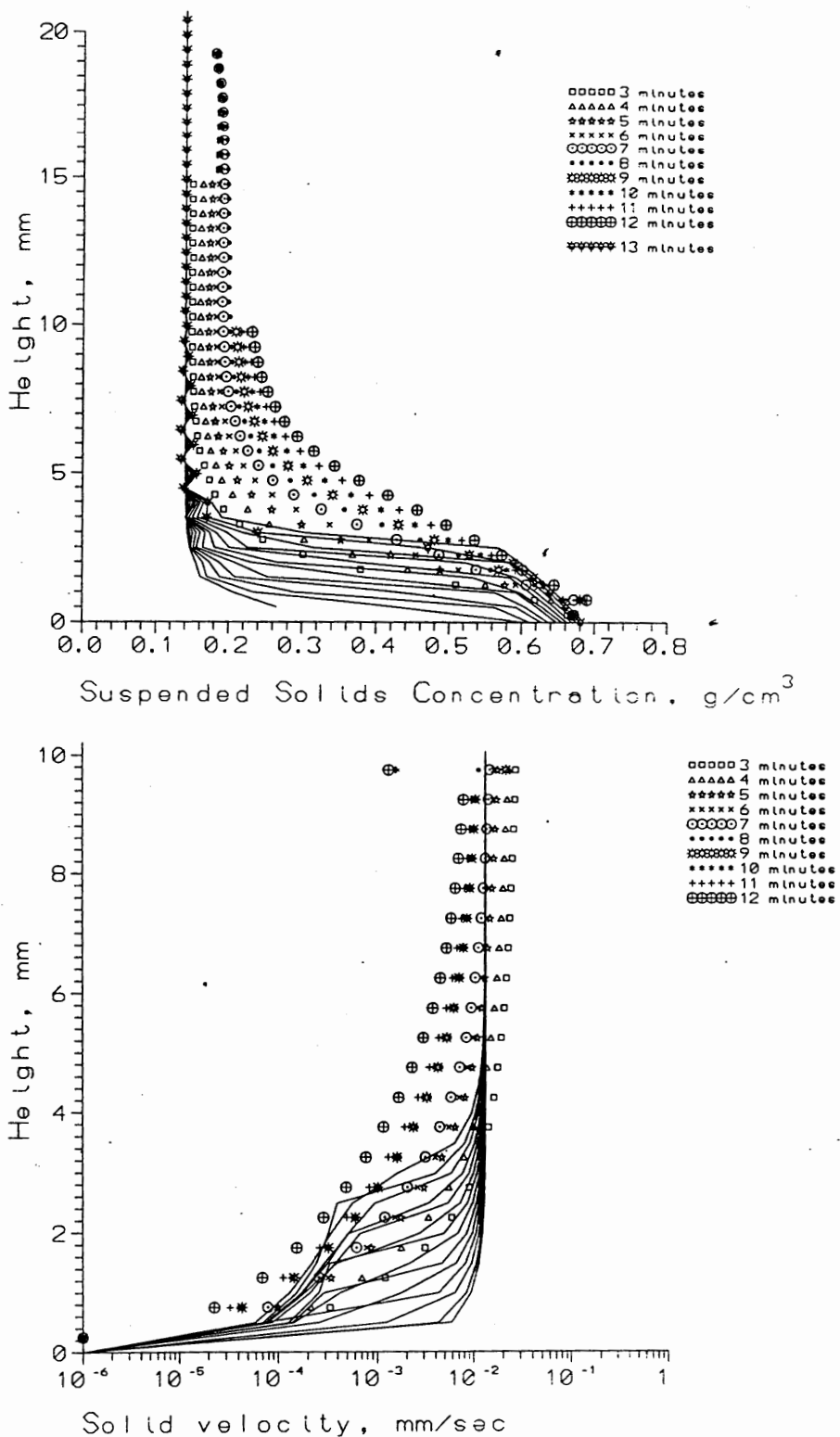


Figure 16. Comparison of model predictions to data set SEDL3K (D10). Model verification (solid lines) to data (symbols) with initial concentration= $0.14 \text{ g}/\text{cm}^3$, cell size= 26.325 cm^2 , and temperature= 24°C . (Note: $10^{-6} \text{ mm}/\text{second}$ is a default value for any solid velocity $< 10^{-6}$.)

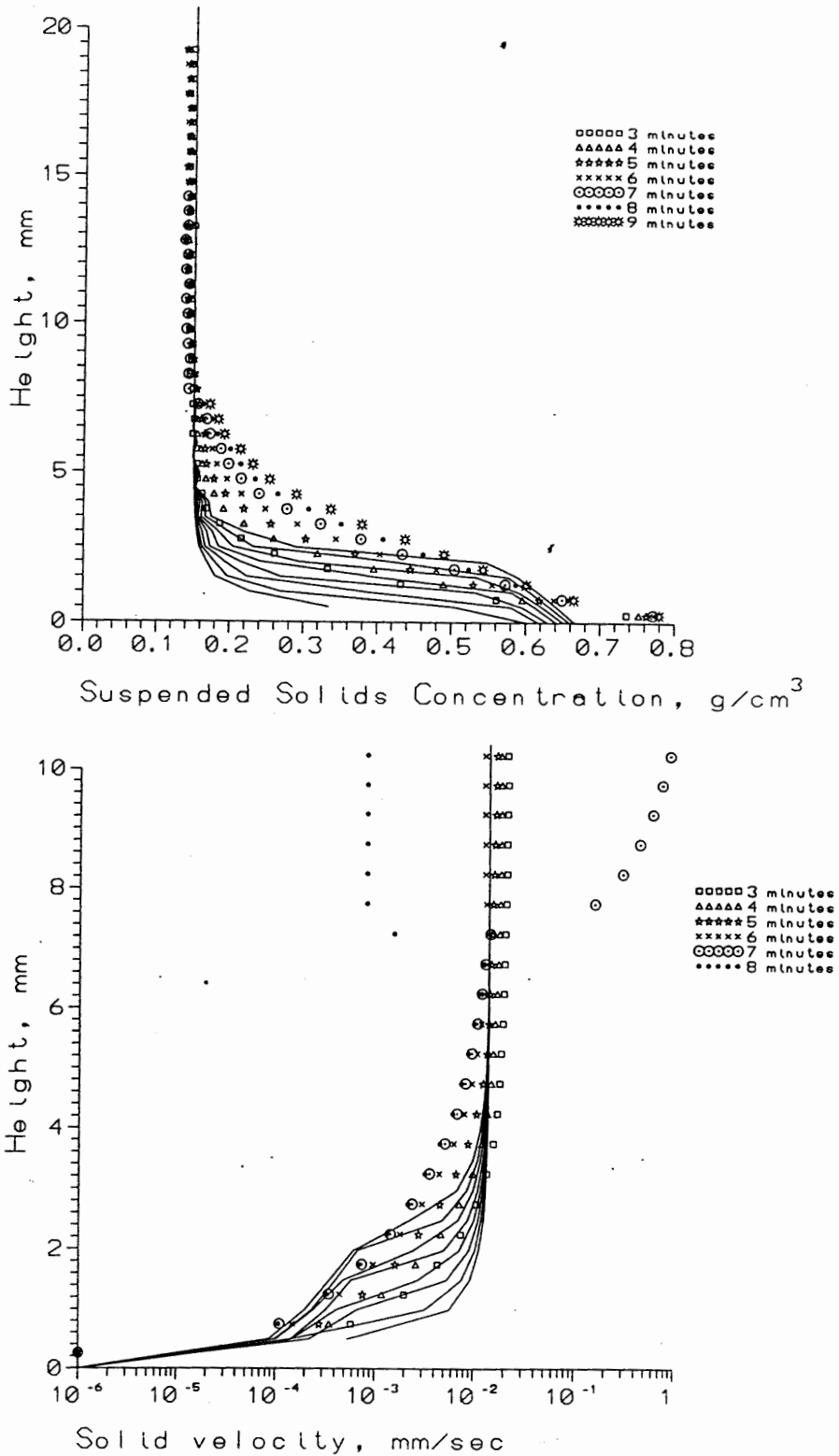


Figure 17. Comparison of model predictions to data set DPK6 (D11). Model verification (solid lines) to data (symbols) with initial concentration=0.15 g/cm³, cell size=8.019 cm², and temperature=27°C. (Note: 10⁻⁶ mm/second is a default value for any solid velocity < 10⁻⁶.)

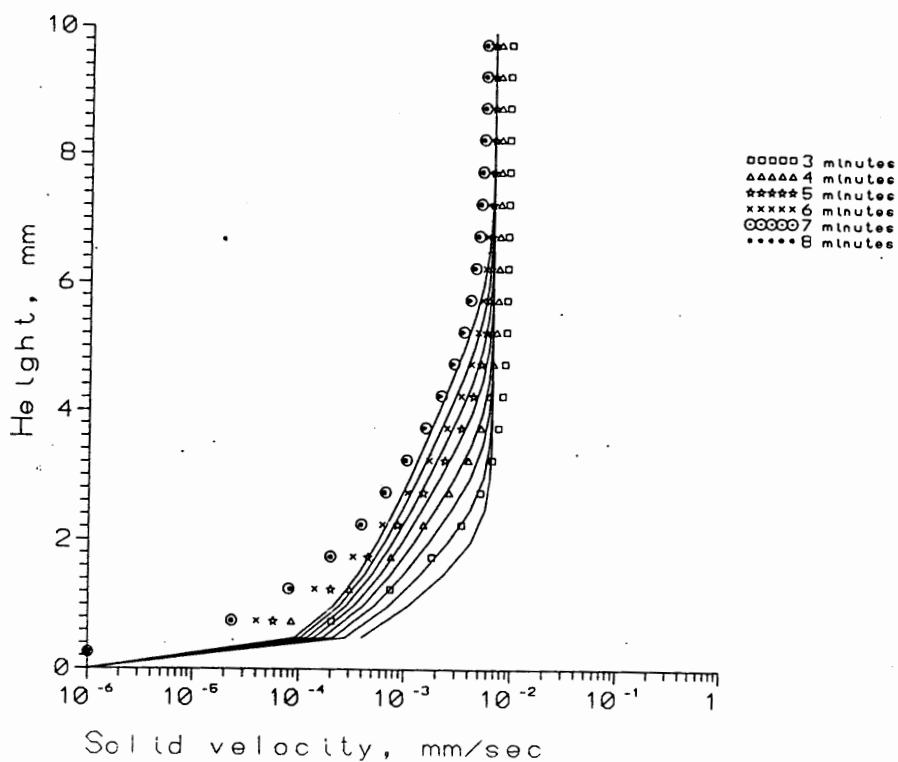
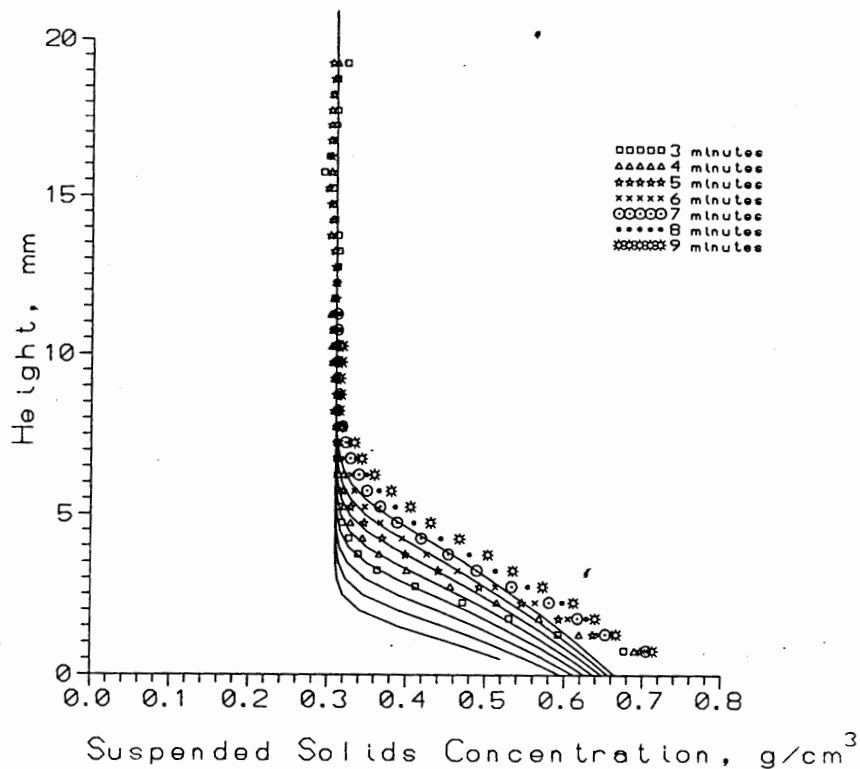


Figure 18. Comparison of model predictions to data set KDM10 (D13). Model verification (solid lines) to data (symbols) with initial concentration= $0.31 \text{ g}/\text{cm}^3$, cell size 15.4305 cm^2 , and temperature= 26°C . (Note: $10^{-6} \text{ mm}/\text{second}$ is a default value for any solid velocity $< 10^{-6}$.)

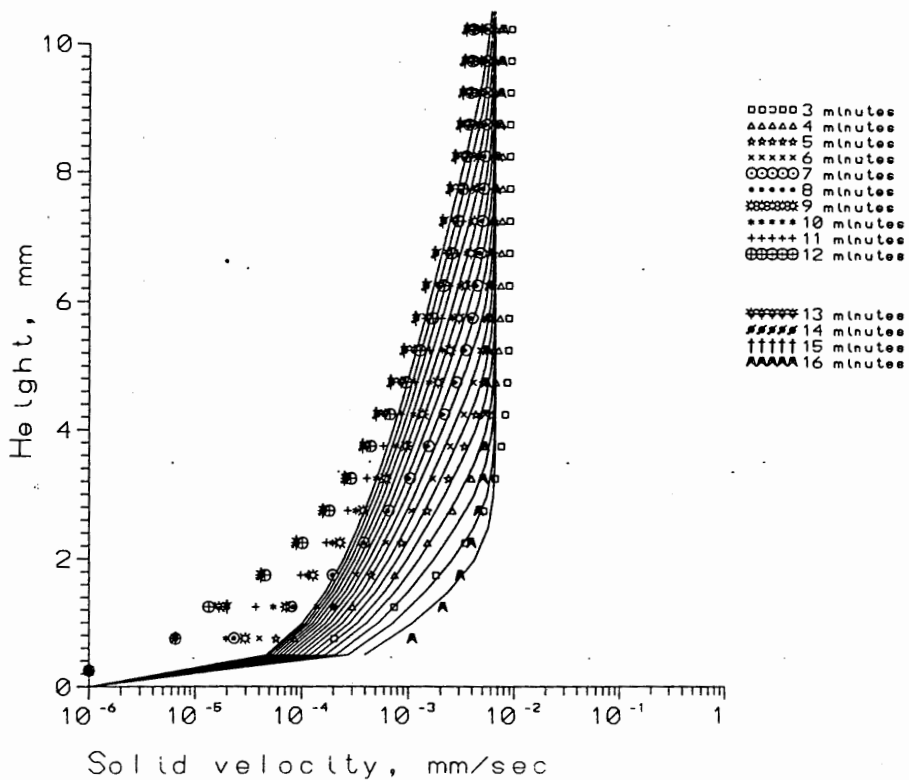
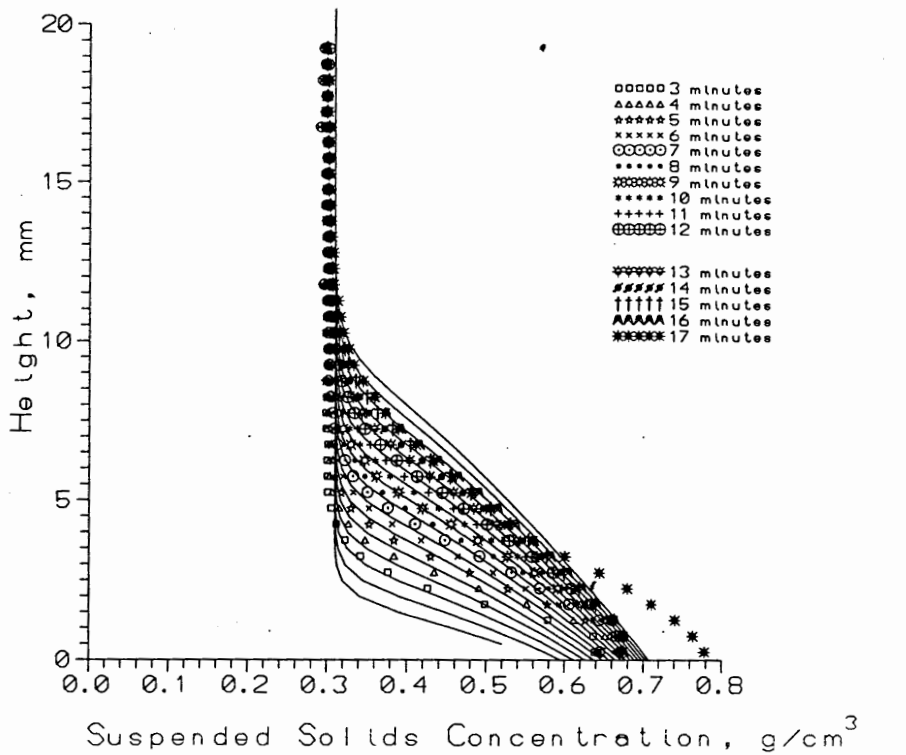


Figure 19. Comparison of model predictions to data set LKD4 (D14). Model verification (solid lines) to data (symbols) with initial concentration= $0.31 \text{ g}/\text{cm}^3$, cell size 26.325 cm^2 , and temperature= 26°C . (Note: 10^{-6} mm/second is a default value for any solid velocity $< 10^{-6}$.)

MODEL SENSITIVITY

Model sensitivity to the following parameters were considered: coefficient of volume compressibility (m_v), permeability (k), artificial viscosity (ω factor), central difference vs. upwind, time step (Δt), and degree of explicitness/implicitness (θ). Predicted suspended solids profiles at 3 minutes and 5 minutes were compared between simulations with two different sets of parameter values.

Constitutive Relationships

Permeability. Figure 20 is a graphical presentation of k_1 (Equation 3.67) and k_2 (Equation 4.1) superimposed over the plotted permeability data obtained from Wells (1990). The permeability was compared between the calibrated coefficient value for the upper range ($\varepsilon \geq 0.65$), $\beta_2=24$, and $\beta_2=21$. This difference had a significant effect, as shown in Figure 20a. Both the 3 minute and 5 minute model predictions for $\beta_2=21$ predicted less concentration at the bottom and more concentration at the top.

Coefficient of Volume Compressibility. The constitutive relationship for m_v by Wells (1990) was compared to the relationship by Plaskett (1992), as shown in Figure 21b. Model simulations with Plaskett's (1992) relationship predicted an almost constant concentration at the bottom, because of the use of a limiting porosity (ε_L): at which m_v was turned on. If the porosity was greater than ε_L , m_v was set to a very large number, thus making the effective stress term approximately 0. The rationale for this approach was that there would be no effective stress above a limiting porosity value, ε_L .

Central Difference vs. Upwind

The central difference and upwind formulations were compared for the parameters of the data set SEDM1K (D2), with medium initial concentration, as shown in Figure 22a. The model predictions appeared the same for the two formulations, indicating that the convective acceleration term (where the two schemes were applied) was very small. This is shown in a later section which compares the orders of magnitude of the different terms of the equation.

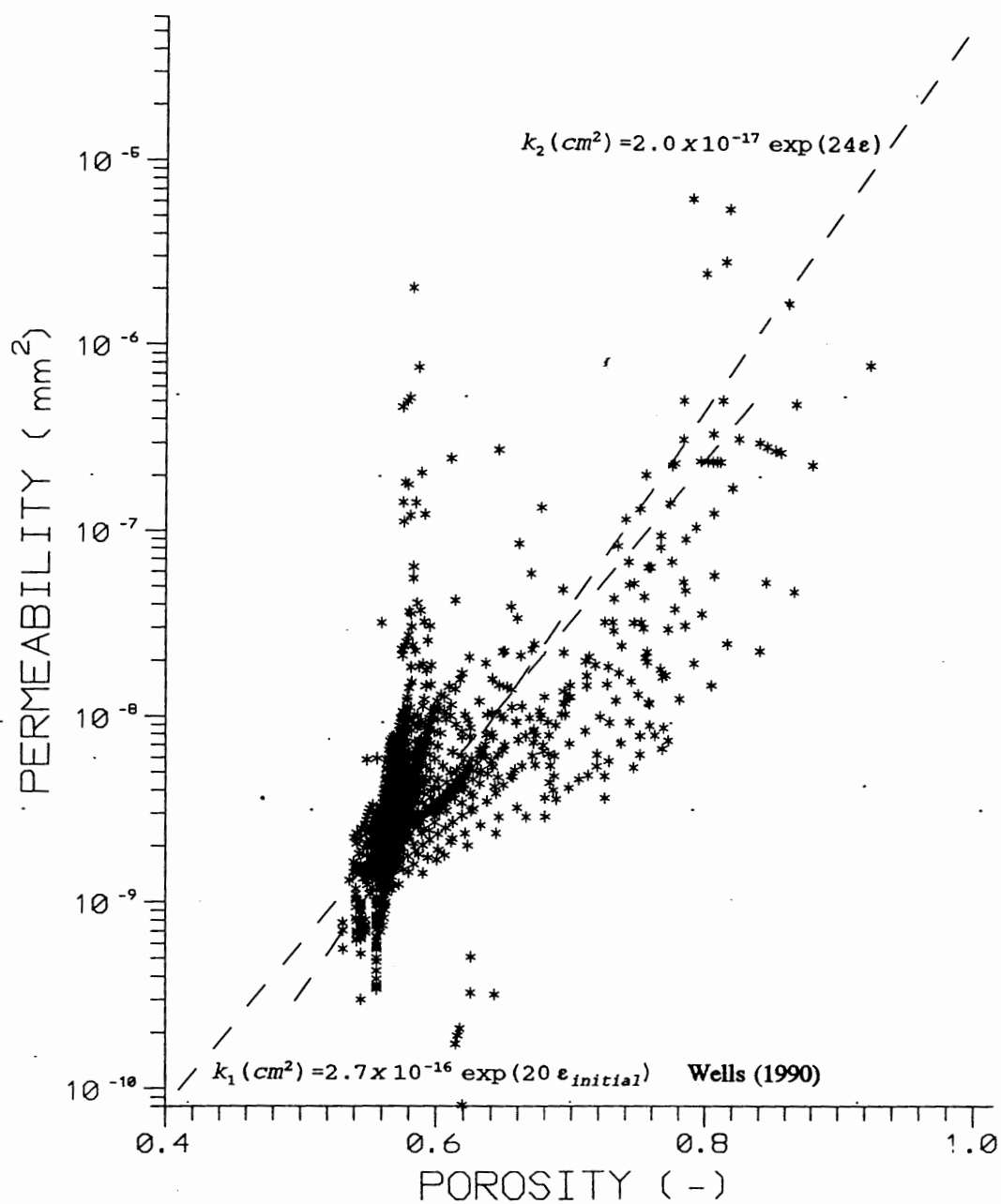


Figure 20. Comparison of constitutive relationships for permeability. K_1 (Equation 3.67) and k_2 (Equation 4.1) superimposed over the plotted permeability data obtained from Wells (1990).

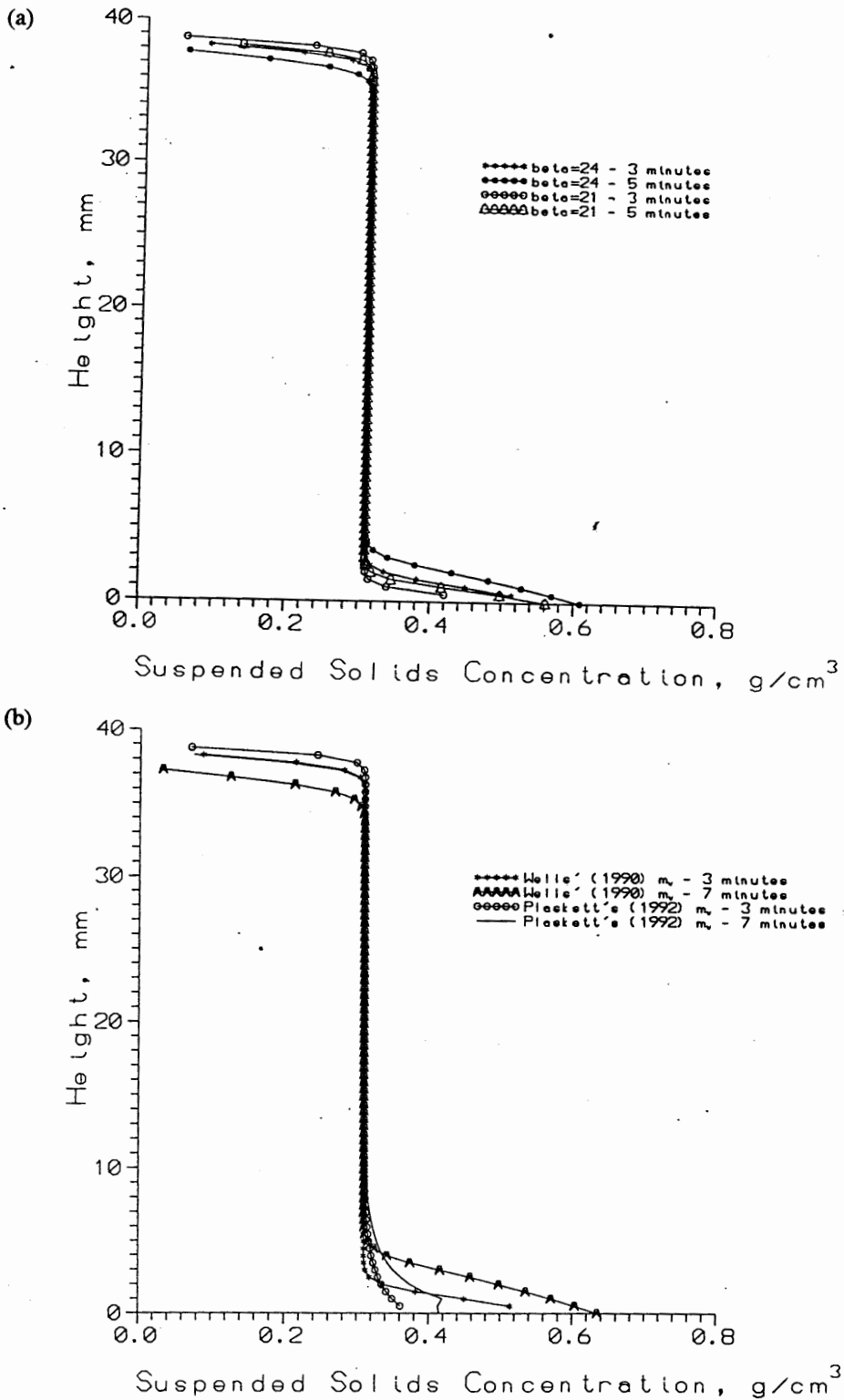


Figure 21. Sensitivity of constitutive relationships. (a) Permeability relationships with $\beta_2=21$ compared to $\beta_2=24$ (calibrated coefficient). (b) Coefficient of volume compressibility with m_v by Plaskett (1992) compared to m_v by Wells (1990), which the model was calibrated with.

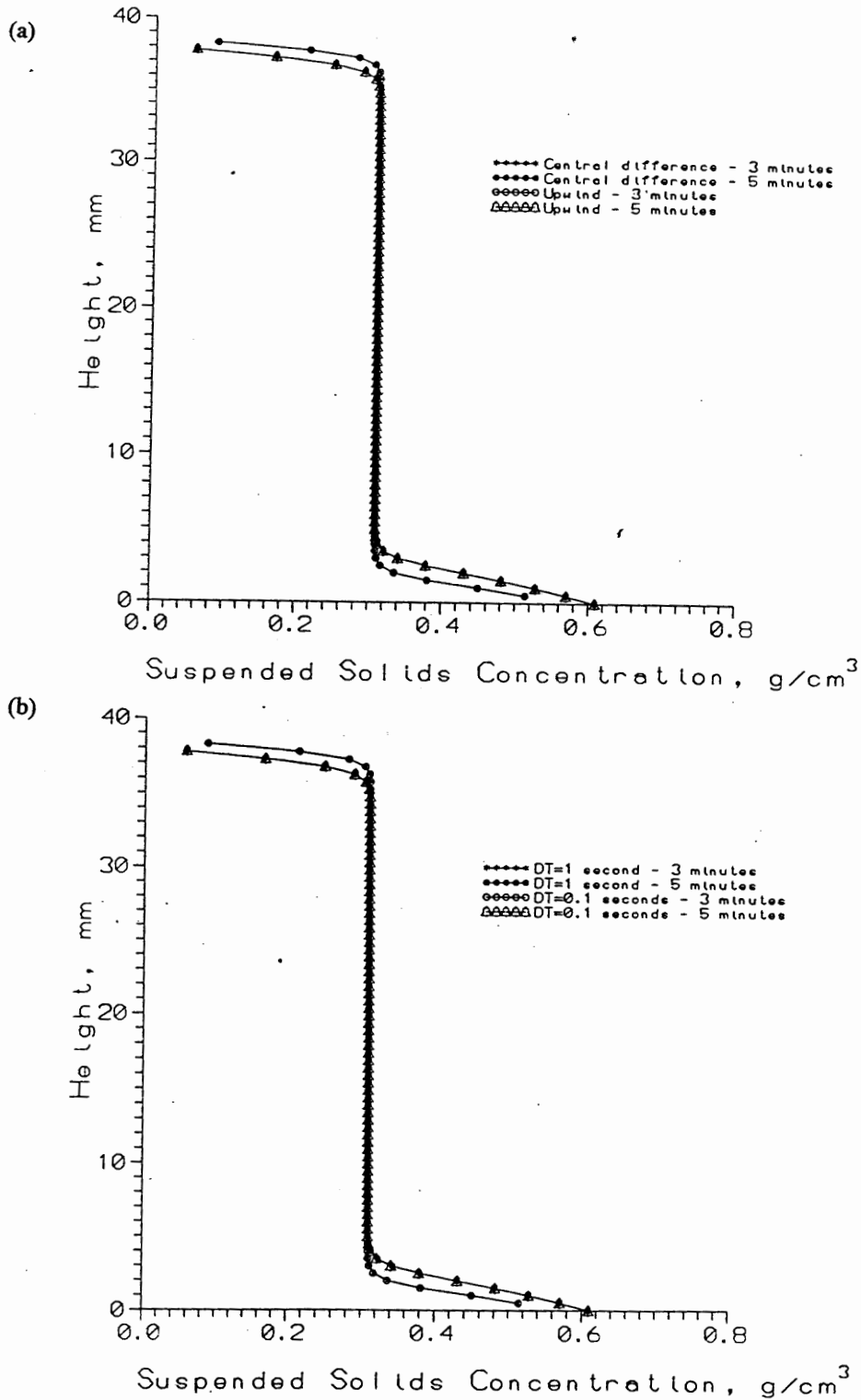


Figure 22. Sensitivities of central difference vs. upwind and time step. (a) Upwind formulation compared to the central difference formulation with the data set SEDM1K (D2) used to calibrate the model. (b) Time step, $\Delta t=0.1$ seconds compared to $\Delta t=1$ second with the data set SEDM1K (D2) used to calibrate the model.

Comparisons of two simulations with low initial concentrations also produced similar results.

These two simulations were based on the parameters of data set DPK6 (D11), and included an ω factor of 10^8 .

Time Step, Δt

The effect of changing the time step, Δt , from 1 second to 0.1 seconds is shown in Figure 21b for the calibration model simulation. The model predictions appeared the same.

Effect of Artificial Diffusion

Changes in the ω factor between simulations had a significant effect at the bottom of the domain near $z=0$. Figure 23a compares ω factor= 10^{10} to 10^8 (used in the verification runs for the low initial concentration). Whereas with a $\Delta t=1$, the simulations with low initial concentration would not run, lowering the Δt to .01 with an ω factor= 1 caused the simulation to run for an elapsed time of 143 seconds. This suggests that a small enough time step could compensate for the ω . This is discussed in the section, Analysis of the Modified "Momentum" Equation, which shows that the numerical dispersive error decreases as Δt decreases.

Degree of Explicitness/Implicitness

Setting θ at 0.6 or greater (model is fully explicit at $\theta=1$) caused numerical instabilities in the model for the calibration simulation with $\omega=0$ and a time step of $\Delta t=1$. As the degree of explicitness increases, the Δt must decrease or the model will become unstable. A comparison of θ at 0.0 and 0.5, shown in Figure 23b, appeared to result in the same predictions.

MAGNITUDE OF TERMS

Figures 24-26 show the magnitude of terms given by the model for low, medium, and high initial concentrations. The process was gravity-driven. Therefore, the gravity term was always significant,

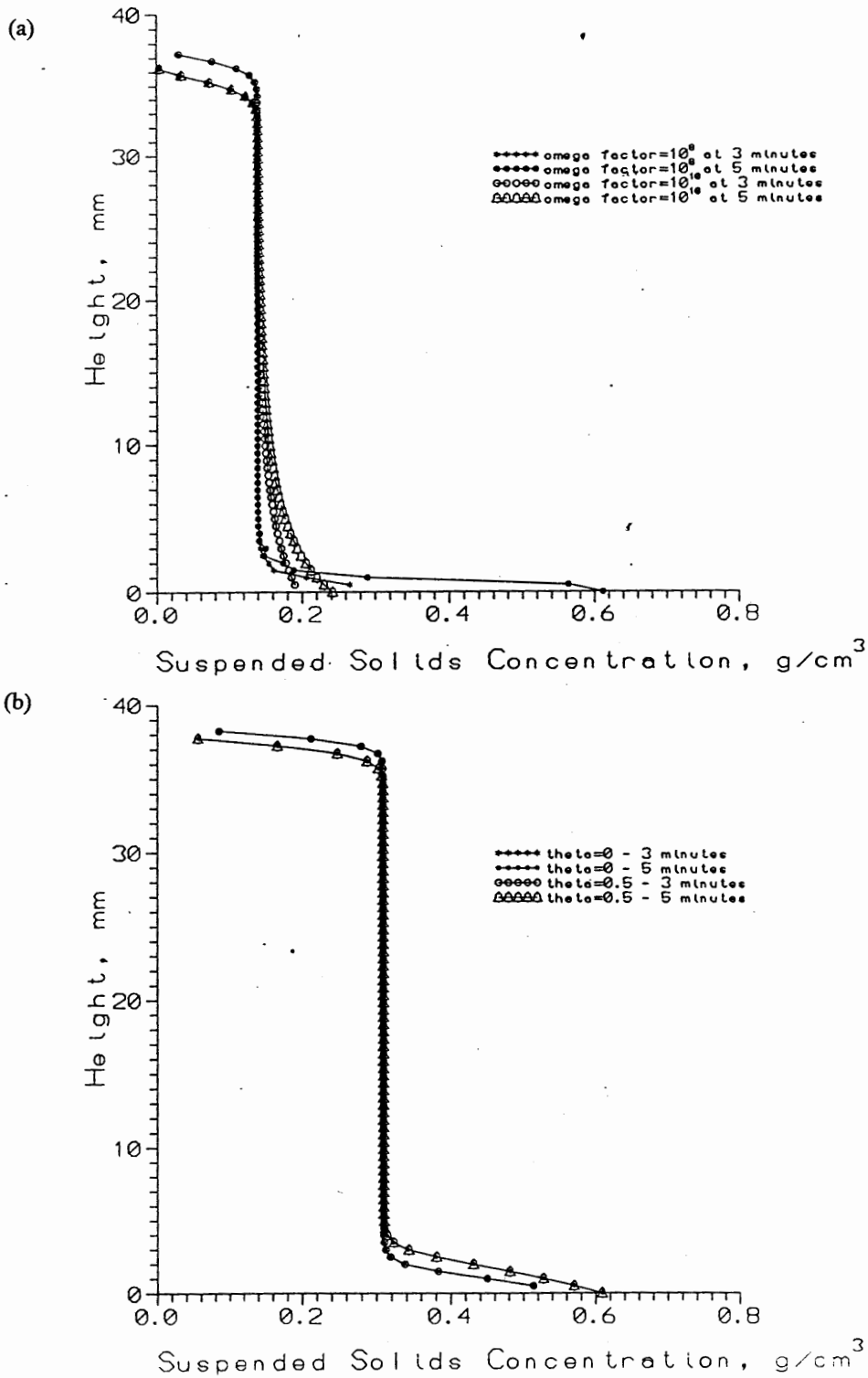


Figure 23. Sensitivities of artificial diffusion and degree of explicitness/implicitness. (a) ω factor of 10^{10} compared to ω factor of 10^8 with the data set SEDL3K (D10) with low initial concentration. (b) Degree of explicitness/implicitness $\theta=0.0$ compared to $\theta=0.5$ with the data set SEDM1K (D2) used to calibrate the model.

whereas the inertial terms were many orders of magnitude less than gravity. However, the lower the initial concentration, the larger the inertial terms.

The effective stress was largest at the bottom of the domain, and decreased with height.

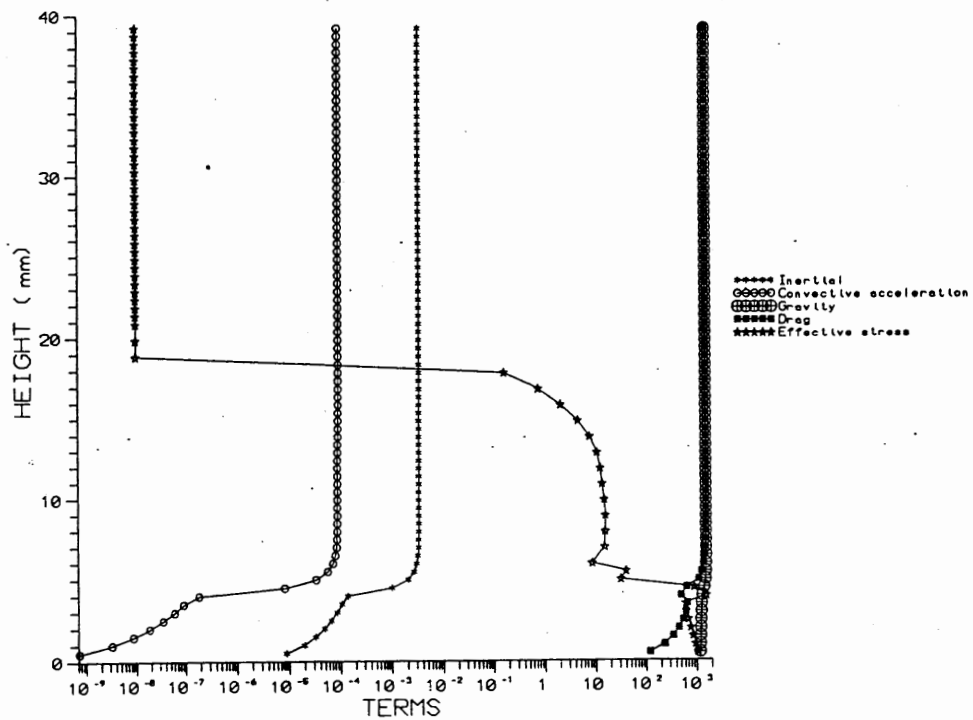
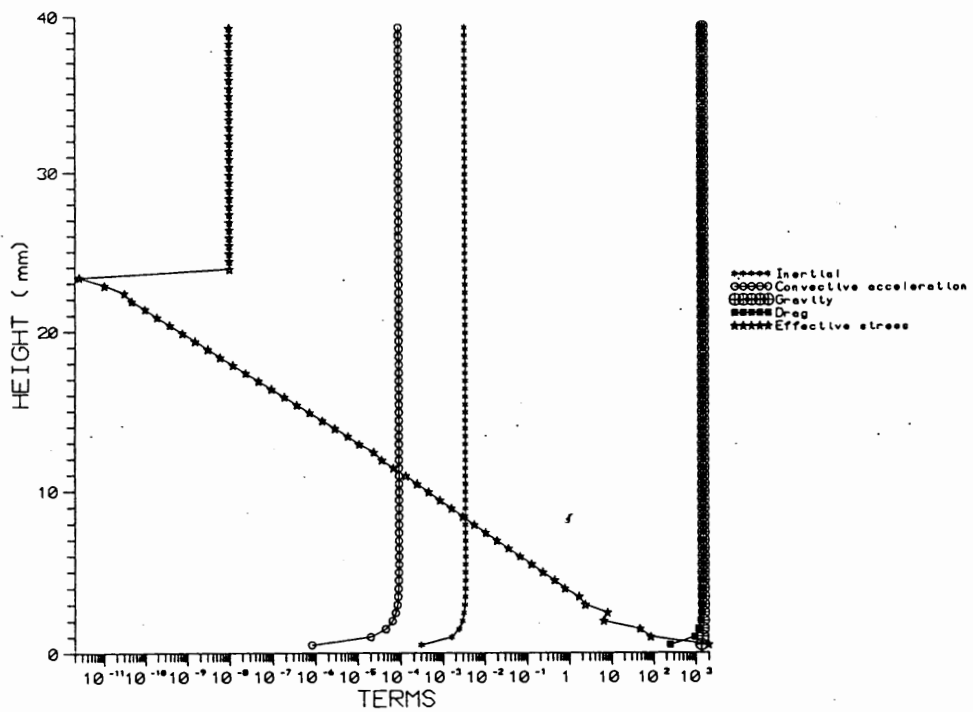


Figure 24. Order of magnitude of terms of Equation 3.9 at low initial concentrations at 3 minutes and 20 minutes. (Note: 10^{-8} is a default value for any solid velocity $< 10^{-6}$.)

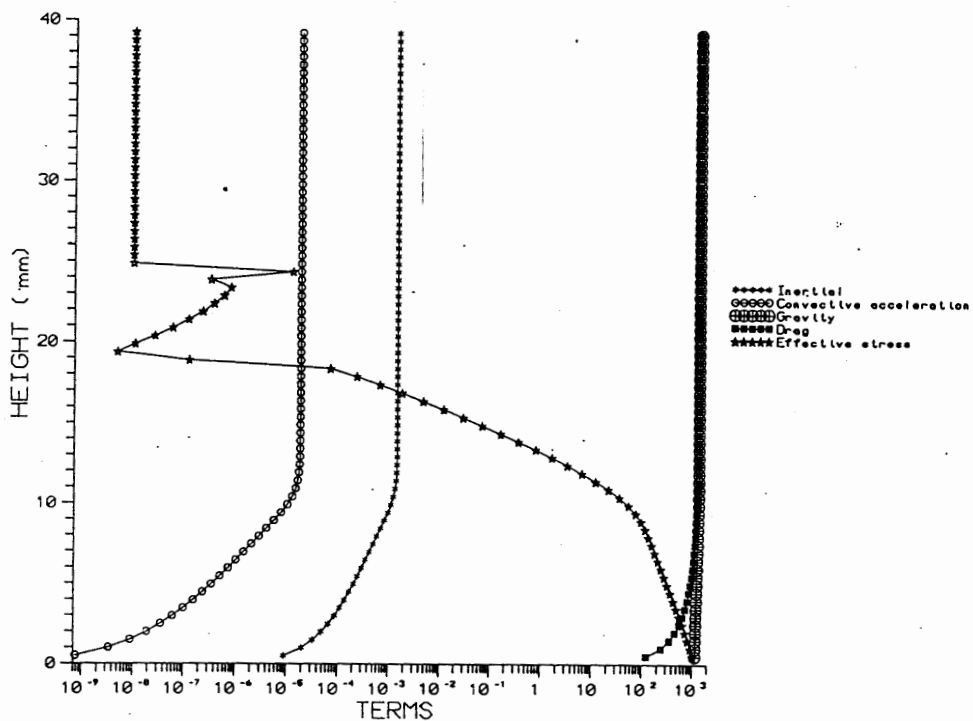
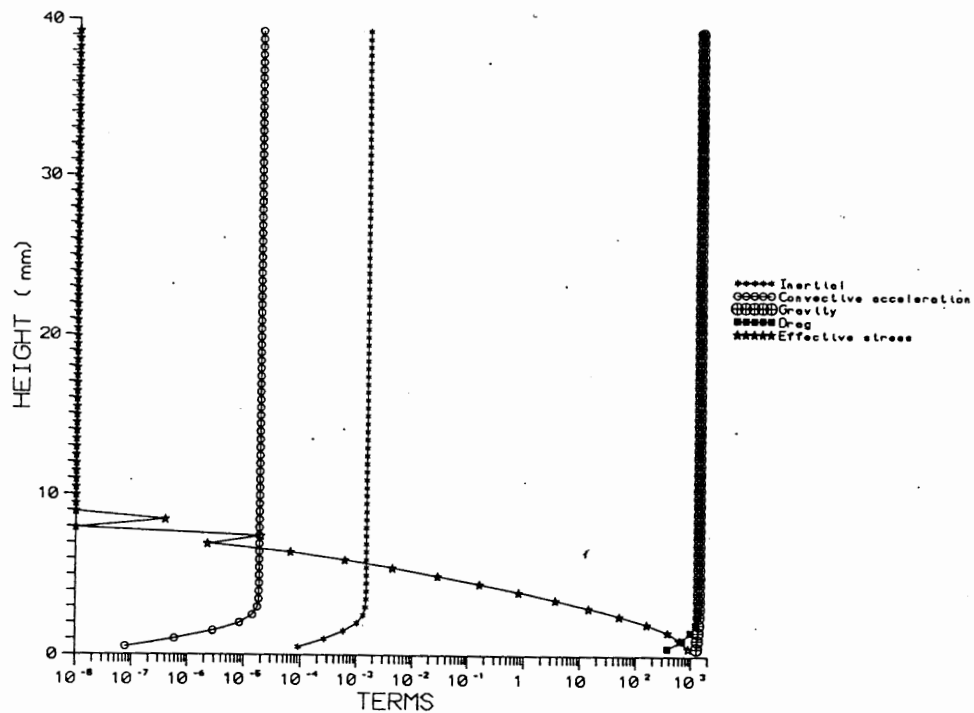


Figure 25. Order of magnitude of terms of Equation 3.9 at medium initial concentrations at 3 minutes and 20 minutes. (Note: 10^{-8} is a default value for any solid velocity $< 10^{-6}$.)

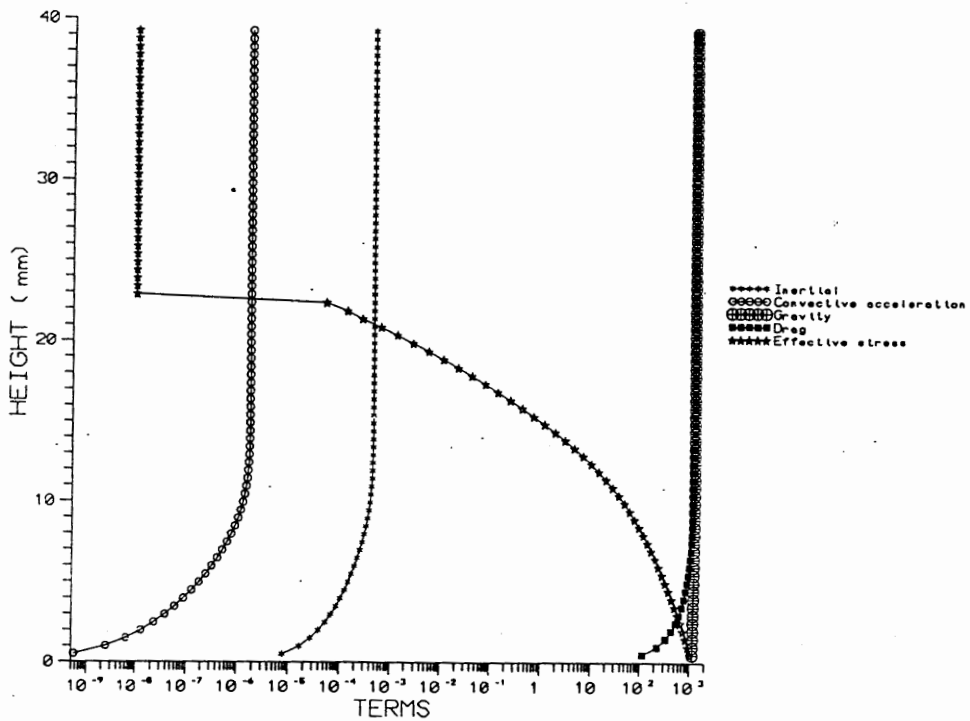
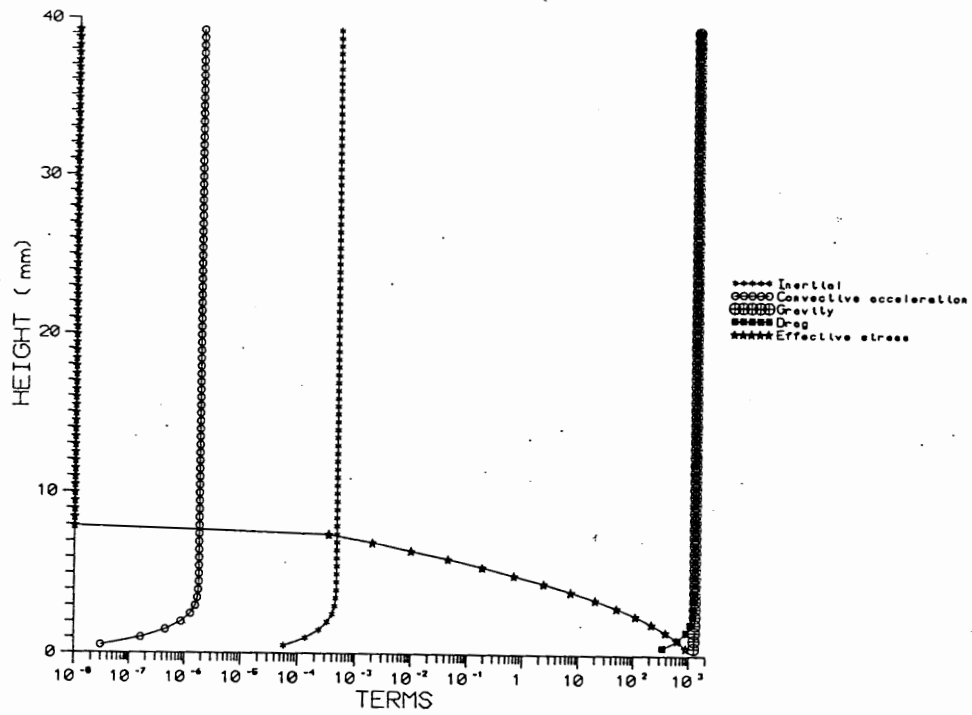


Figure 26. Order of magnitude of terms of Equation 3.9 at high initial concentrations at 3 minutes and 20 minutes. (Note: 10^{-8} is a default value for any solid velocity $< 10^{-6}$.)

CHAPTER V

CONCLUSIONS AND RECOMMENDATIONS FOR FURTHER RESEARCH

This research developed, calibrated, and verified a numerical computer model of the physics of gravity sedimentation. This is an important step towards a more comprehensive model simulating the gravity section of a dewatering process, such as the gravity drainage section of the belt filter press.

The gravity sedimentation model was developed from a physically-based numerical model of cake filtration by Wells (1990). Both the cake filtration and gravity sedimentation models were based on the liquid and solid continuity and liquid and solid momentum equations. However, as opposed to the cake filtration model, the inertial and gravity terms were retained in the gravity sedimentation model.

Two final governing equations were developed - solid continuity and total momentum with continuity ("momentum"). The finite difference equations used a "space-staggered" mesh. The solid continuity equation was solved using an explicit formulation, with a forward difference in time and central difference in space. The "momentum" equation used a fully implicit formulation with a forward difference in time. The modeler could choose either a central difference or forward difference in space for the convective acceleration terms. Non-linear terms were linearized. Boundary conditions and constitutive relationships were determined. Numerical errors in the numerical model were analyzed.

The calibrated model was extremely sensitive to the constitutive relationships used, but relatively unaffected by the use of central difference or forward difference for the spatial derivative term in the "momentum" equation. The model was stable when $\theta=0.5$ or less, and unstable as it became more explicit with no artificial viscosity. Correlation of model predictions of suspended solids concentration and solid velocity to data taken at CHESS by Wells (1990) show excellent agreement at initial suspension concentrations of 0.31 g/cm^3 . Agreement was still good, but not excellent, at initial suspension concentrations of 0.14 g/cm^3 and 0.47 g/cm^3 using calibrated constitutive properties from an

initial suspended solids concentration of 0.31 g/cm^3 . Model runs with low initial concentration required the addition of artificial viscosity to remain stable. The mass, in general, was conserved during the model simulations.

The gravity term was always significant, whereas the inertial terms were many orders of magnitude less than gravity. However, the lower the initial concentration, the larger the inertial terms. The relatively unimportant inertial terms are a result of the small particle size and choice of constitutive model.

As shown by the model's sensitivity to the constitutive relationships, they could be improved with further research. Suspensions with larger particle sizes could be studied to determine under what conditions the inertial terms are important.

In addition to the belt filter press, the model can be applied to cake filtration and the design of gravity sedimentation tanks.

REFERENCES

- Anderson, D.A., J.C. Tannehill, and R.H. Pletcher, 1984. Computational Fluid Mechanics and Heat Transfer, Hemisphere Publishing Corporation, Washington.
- Atsumi, K. and T. Akiyama. 1975. "A Study of Cake Filtration - Formulation as a Stefan Problem," Journal Chemical Engineering Japan, 8, 487-492.
- Azbel, D.S. and N.P. Cheremisinoff. 1983. Fluid Mechanics and Unit Operations, Ann Arbor Science, Ann Arbor, MI.
- Batchelor, G.K. 1967. An Introduction to Fluid Dynamics, Cambridge University Press, Cambridge.
- Been, K., 1980. "Stress Strain Behaviour of a Cohesive Soil Deposited Under Water," Ph.D. Dissertation, University of Oxford, Oxford, United Kingdom.
- Been, K., and G.C. Sills. 1981. "Self-Weight Consolidation of Soft Soils: An Experimental and Theoretical Study," Geotechnique, 31, 519-535.
- Benson, R.E., Jr. 1987. "A Consolidation Model for Sludge Dewatering", in Environmental Engineering Specialty Conference, ed. by J.D. Dietz, American Society of Civil Engineers, New York, 276-284.
- Bierck, B.R., S.A. Wells, and R.I. Dick. 1988, "Compressible Cake Filtration: Monitoring Cake Formation and Shrinkage Using Synchrotron X-Rays," Journal Water Pollution Control Federation, 60 (5), 645-649.
- Biot, M.A. 1941. "General Theory of Three-Dimensional Consolidation," Journal of Applied Physics, 12, 155-164.
- Biot, M.A. 1972. "Theory of Finite Deformations of Porous Solids," Indiana University of Mathematics Journal, 21, 597-620.
- Bloomquist, D.G. and F.C. Townsend. 1984. "Centrifugal Modeling of Phosphatic Clay Consolidation," in Sedimentation Consolidation Models: Predictions and Validation, ed. by R.N. Yong and F.C. Townsend, American Society of Civil Engineers, New York, 565-580.
- Carnahan, B., H.A. Luther, and J.O. Wilkes. 1969. Applied Numerical Methods, John Wiley & Sons, New York.
- Carter, J.P., J.C. Small, and J.R. Booker. 1977. "A Theory of Finite Elastic Consolidation," International Journal of Solids and Structures, 13, 467-478.
- Coe, H.S. and G.H. Clevenger. 1916. "Methods for Determining the Capacities of Slime-Settling Tanks," Transactions of the American Institution of Mining Engineers, 55, 356.

- Cole, J.A., L.B. Polkowski, and J.A. Hoopes. 1973. "Thickening of Compressible Sludges," in Proceedings of the 28th Industrial Waste Conference, Purdue University, Lafayette, Indiana, 293-308.
- Comings, E.W. 1940. "Thickening Calcium Carbonate Slurries," Industrial and Engineering Chemistry, 32(5), 663-667.
- Concha, F. and M.C. Bustos. 1985. "Theory of Sedimentation of Flocculated Fine Particles," in Flocculation, Sedimentation and Consolidation, ed. by B.M. Moudgil and P. Somasundaran, Proceedings Engineering Foundation Conference, Sea Island, GA, 39-55.
- Croce, P., V. Pane, D. Znidarcic, H.Y. Ko, H.W. Olsen, and R.L. Schiffman. 1984. "Evaluation of Consolidated Theories by Centrifugal Modeling," Proceedings of the Conference on Applications of Centrifuge Modeling to Geotechnical Design, Manchester University, United Kingdom, 380-401.
- Darcy, H.P.G. 1856. Les Fontaines Publiques de la Ville de Dijon, Dalmont, Paris, France.
- Dick, R.I. 1970a. "Thickening Characteristics of Activated Sludge," in Advances in Water Pollution Research, Proceedings of the 4th International Conference of Water Pollution Res., Prague, 1969, ed. by S.H. Jenkins, Pergamon Press, New York, 625.
- Dick, R.I. 1970b. "Role of Activated Sludge Final Settling Tanks," Journal of the Sanitary Engineering Division, ASCE, 36(SA2), 423-436.
- Dick, R.I. and K.W. Young. 1972. "Analysis of Thickening Performance of Final Settling Tanks," in Proceedings of the 27th Industrial Waste Conference, Purdue University, Lafayette, Indiana, 33-54.
- Dick, R.I. and R.O. Ball. 1980. "Sludge Dewatering," Critical Reviews in Environmental Control, 10, 269-337.
- Dick, R.I. and B.B. Ewing. 1967. "Evaluation of Activated Sludge Thickening Theories," Journal of the Sanitary Engineering Division, ASCE, 93(SA4), 9-29.
- Dixon, D.C., P. Souter, and J.E. Buchanan. 1976. Chem. Eng. Sci., 31, 737.
- Dixon, D.C. 1979. "Theory of Gravity Thickening," in Progress in Filtration and Separation, ed. by R.J. Wakeman, Elsevier, The Netherlands.
- Dixon, D.C., P. Souter, and J.E. Buchanan. 1985. "Argument Not Invalidated," Filtration & Separation, 22(3), 183.
- Eckenfelder, W.W., Jr., T.F. Rooney, T.B. Burger, and J.T. Gruspier, 1958. "Studies on Dissolved Air Flotation of Biological Sludges," in Biological Treatment of Sewage and Industrial Wastes-Volume 2, Anaerobic Digestion and Solids-Liquid Separation, ed. by J. McCabe and W.W. Eckenfelder, Jr., Reinhold Publishing Corporation, New York, New York, 251-258.
- Edde, H.J. and W.W. Eckenfelder, Jr. 1968. "Theoretical Concept of Gravity Sludge Thickening; Scaling-up Laboratory Units to Prototype Design," Journal Water Pollution Control Federation, 40(8), 1486-1498.

- Evans, B. and D. Filman. 1988. "Solids Handling Costs at Large Sewage Treatment Plants," Specialty Conference Proceedings - Joint CSCE-ASCE National Conference on Environmental Engineering, Vancouver, BC, 590-598.
- Farlow, S.J. 1982. Partial Differential Equations for Scientists and Engineers, John Wiley & Sons, New York.
- Fitch, E.B. 1958. in Biological Treatment of Sewage and Industrial Wastes - Volume 2: Anaerobic Digestion and Solids-Liquid Separation, ed. by J. McCabe and W.W. Eckenfelder, Jr., Reinhold Publishing Corp., New York, 159-170.
- Fitch, B. 1979. "Sedimentation of Flocculent Suspensions: State of the Art," AICHE Journal, Vol. 25, No. 6, 913-930.
- Fitch, B. 1983. "Kynch Theory and Compression Zones," AICHE Journal, Vol. 29, No. 6, 940-947.
- Gersevanov, N.M. 1934. "Dinamika Mekhaniki Grunkov" Foundations of Soil Mechanics, 2, Gosstroisdat, USSR.
- Gibson, R.E., G.L. England, and M.J.L. Hussey. 1967. "The Theory of One-Dimensional Consolidation of Saturated Clays, I. Finite Non-Linear Consolidation of Thin Homogeneous Layers," Geotechnique, 17, 261-273.
- Gibson, R.E., R.L. Schiffman, and K.W. Cargill. 1981. "The Theory of One-Dimensional Consolidation of Saturated Clays. II. Finite Non-Linear Consolidation of Thick Homogeneous Layers," Canadian Geotechnical Journal, 18, (2), 280-293.
- Gidaspow, D. and B. Ettehadleh. 1983. "Fluidization in Two-Dimensional Beds with a Jet, Part II. Hydrodynamic Modeling," I&EC Fundamentals, 22, 193-201.
- Giadspow, D., Y.C. Seo, and B. Ettehadieh. 1983. "Hydrodynamics of Fluidization: Experimental and Theoretical Bubble Sizes in a Two Dimensional Bed with a Jet," Chem. Eng. Communications, 22, 253-272.
- Halde, R.E. 1980. "Filterbelt Pressing of Sludge - A Laboratory Simulation," Journal Water Pollution Control Federation, 52, 310-316.
- Halde, R.E., 1980. "Filterbelt Pressing of Sludge - A Laboratory Simulation," Journal Water Pollution Control, Vol. 52, No. 2, 31-316.
- Hammer, M.J. 1986. Water and Wastewater Technology, John Wiley & Sons, New York.
- Harris, C.C., P. Somasundaran, and R.R. Jensen. 1975. "Sedimentation of Compressive Materials: Analysis of Batch Seimentation Curve," Powder Technology, 11, 75-84.
- Hawksley, P.G.W. "Some Aspects of Fluid Flow," Symposium, Edward Arnold & Co., London.
- Howe, R.H.L. 1958. "A Mathematical Interpretation of Flotation for Solids-Liquid Separation," in Biological Treatment of Sewage and Industrial Wastes-Volume 2, Anaerobic Digestion and Solids-Liquid Separation, ed. by J. McCabe and W.W. Eckenfelder, Jr., Reinhold Publishing Corporation, New York, New York, 241-250.

- Kammermeyer, K. 1941. "Settling and Thickening of Aqueous Suspensions," Industrial and Engineering Chemistry, 33(12), 1484-1491.
- Kehoe, P. 1972. "A Moving Boundary Problem with Variable Diffusivity," Chemical Engineering Science, 27, 1184-1185.
- Kos, P. and D.D. Adrian. 1975. "Transport Phenomena Applied to Sludge Dewatering," Journal of the Environmental Engineering Division, ASCE, 101, 947-965.
- Kos, P. 1977. "Fundamentals of Gravity Thickening," Chemical Engineering Progress, 73, (11), 99-105.
- Kos, P. 1985. "Sedimentation and Thickening - General Overview", in Flocculation, Sedimentation, and Consolidation, ed. by B.M. Moudgil and P. Somasundaran, Sea Island, GA, 39-55.
- Kreyszig, E. 1983. Advanced Engineering Mathematics, John Wiley & Sons, New York.
- Kynch, G.J. 1952, "A Theory of Sedimentation," Transactions of the Faraday Society, 48, 166-176.
- Lamb, H. 1932. Hydrodynamics (Sixth edition), Dover Publications, New York, New York.
- Leclerc, D. and S. Rebouillat. 1985. "Dewatering by Compression," in Mathematical Models & Design Methods in Solid-Liquid Separation, ed. by A. Rushton, Martinus-Nijhoff, 356-391.
- Leung, P.K., R.L. Schiffman, H.Y. Ko, and V. Pane. 1984. "Centrifuge Modeling of Shallow Foundations on Soft Soil," Proceedings, Sixteenth Annual Offshore Technology Conference, 4308, 3, 275-282.
- McCormack, P.D. and L. Crane. 1973. Physical Fluid Dynamics, Academic Press, New York.
- Michaels, A.S. and J.C. Bolger. 1962. "Settling Rates and Sediment Volumes of Flocculated Kaolin Suspensions," Industrial and Engineering Chemistry, 1, (1), 24-33.
- Mikasa, M. 1963. The Consolidation of Soft Clay - A New Consolidation Theory and its Application, Kajima Institution Publishing Co., Ltd. (in Japanese).
- Mikasa, M. and N. Takada. 1984. "Self-Weight Consolidation of Very Soft Clay by Centrifuge," in Sedimentation Consolidation Models: Predictions and Validation, ed. by R.N. Yong and F.C. Townsend, ASCE, 121-140.
- Mishler, R.T. 1912. "Settling Slimes at the Tigre Mill," The Engineering and Mining Journal, 94(14), 643-646.
- Mohlman, F.W. 1934. "The Sludge Index," Sewage Work Journal, 6, 119-122.
- Morse, D. 1989. "Sludge in the Nineties," Civil Engineering, 59, No. 8, 47-50.
- Mulbarger, M.C. and D.D. Huffman. 1970. "Mixed Liquor Solids Separation by Flotation," Journal of the Sanitary Engineering Division, ASCE, 96(SA4), 861-871.
- Okey, R.W. 1989. "The Evolution of Sludge Thickening Practice," in Environmental Engineering, ed. by J.F. Malina, Jr., Proceedings of the 1989 Specialty Conference, Austin, 507-522.

- Olson, R.E. and C.C. Ladd. 1979. "One-Dimensional Consolidation Problems," Journal of Geotechnical Engineering Division, ASCE, 105, (1), 1979.
- Pane, V. 1981. "One-Dimensional Finite Strain Consolidation," M.S. Thesis, Department of Civil Engineering, University of Colorado, Boulder, Colorado.
- Pane, V. and R.L. Schiffman. 1985, "A Note on Sedimentation and Consolidation." Geotechnique, 35, 69-72.
- Pane, V. 1985. "Sedimentation and Consolidation of Clays," Ph.D. Thesis, Department of Civil Engineering, University of Colorado, Boulder, Colorado.
- Plaskett, J. 1992. Parameter Uncertainty and Modeling of Sludge Dewatering in One-Dimension, Masters Thesis, School of Engineering and Applied Science, Portland State University, Portland, OR.
- Ravenscroft, G.A. 1992. "Managing a Special Waste: Sewage Sludge," Solid Waste & Power.
- Richardson, J.F. and W.N. Zaki. 1954. "Sedimentation and Fluidisation: Part I" Trans. Instn Chem. Engrs.
- Robinson, C.S. 1926. Industrial Engineering Chemistry, 18, 869.
- Schiffman, R.L., V. Pane, and R.E. Gibson. 1984. "The Theory of One-Dimensional Consolidation of Saturated Clays, IV. An Overview of Nonlinear Finite Strain Sedimentation and Consolidation," in Sedimentation Consolidation Models: Predictions and Validation, ed. by R.N. Yong and F.C. Townsend, American Society of Civil Engineers, New York, 1-29.
- Schiffman, R.L., V. Pane, and V. Sunara. 1985. "Sedimentation and Consolidation," Flocculation, Sedimentation and Consolidation, ed. B.M. Moudgil & P. Somasundaran, Sea Island, Georgia, 57-121.
- Scully, R.W., R.L. Schiffman, H.W. Olsen, and H.Y. Ko. 1984. "Validation of Consolidation Properties of Phosphatic Clay at Very High Void Ratios," in Sedimentation Consolidation Models: Predictions and Validation, ed. by R.N. Yong and F.C. Townsend, American Society of Civil Engineers, New York, 158-181.
- Searle, T.G. and M.C. Bennett, III. 1987. "Belt Filter Press Dewatering of Alum Sludge", in Environmental Engineering, ed. Unknown, 269-275.
- Shin, B.S. and Dick, R.I. 1980. "Applicability of Kynch Theory to Flocculent Suspensions," Journal of the Environmental Engineering Division, ASCE.
- Shirato, M., Kato, H, Kobayashi, K., and Sakazaki, H. 1970. "Analysis of Settling of Thick Slurries due to Consolidation," Journal of Chemical Engineering, (Japan), 3, 94-104.
- Smiles, D. 1970. "A Theory of Constant Pressure Filtration," Chemical Engineering Science, 25, 985-996.
- Smith, J.E. and J.A. Semon. 1989. "Dewatering Municipal Sewage Sludges - Selecting a Process", in Environmental Engineering, ed. by J.F. Malina, Jr., Austin, 515-522.

- Somasundaran, P. 1981. "Thickening or Dewatering of Slow-Settling Mineral Suspensions," Mineral Processing, Proceedings, Thirteenth International Mineral Processing Congress, ed. by J. Laskowski, Elsevier, Amsterdam, The Netherlands, 2 (A), 233-261.
- Somogyi, F. 1980. "Large Strain Consolidation of Fine-Grained Slurries," presented at Canadian Society for Civil Engineers, Annual Conference, Winnipeg, Manitoba, 1980.
- Somogyi, F., B. Keshian, Jr., and L.G. Bromwell. 1981. "Consolidation Behavior of Impounded Slurries," Presented at ASCE Spring Convention, New York, New York.
- Soo, S.L. 1989. Particulates and Continuum Multiphase Fluid Dynamics, Hemisphere Publishing Corporation, New York.
- Steinoir, H.H. 1944. Industrial Engineering Chemistry, 36, 618.
- Stokes, G.G. 1901. Mathematical and physical papers.
- Task Committee on Belt Filter Presses. 1988. "Belt Filter Press Dewatering of Wastewater Sludge," Journal of Environmental Engineering, 114, (5), 991-1006.
- Terzaghi, K. 1923. "Die Berechnung der Durchlassigkeitsziffer des Tones aus dem Verlauf der Hydrodynamischen Spannungserscheinungen," Akademie der Wissenschaften in Wien, Sitzungsberichte, 132, (3/4), 125-138.
- Terzaghi, K. 1942. Theoretical Soil Mechanics, John Wiley and Sons, Inc., New York, New York.
- Tiller, F.M. and T.C. Green, 1973. "Role of Porosity in Filtration IX Skin Effect with Highly Compressible Materials," AIChE Journal, 19(6), 1266-1269.
- Tiller, F.M. 1981. "Revision of Kynch Sedimentation Theory," AIChE Journal, 27, No. 5, 823-829.
- Torpey, W.N. 1954. "Concentration of Combined Primary and Activated Sludges in Separate Thickening Tanks," Journal of Sanitary Engineering Division, ASCE, 80, 443.
- Torpey, W.N. and N.R. Melbinger. 1967. "Reduction of Digested Sludge Volume by Controlled Recirculation," Journal of Water Pollution Control Federation, 39(9), 1464-1474.
- Tosun, I. 1986. "Formulation of Cake Filtration," Chemical Engineering Science, 41, 2563-2568.
- Townsend, F.C. and J. Hernandez. 1985. "Predictions of Phosphatic Clay Consolidation by Numerical & Centrifugal Models," in Floc., Sed. & Consolidation, ed. B.M. Moudgil & P. Somasundaran, Sea Island, GA, 449-455.
- U.S. Environmental Protection Agency. 1982. "Dewatering Municipal Wastewater Sludges," Municipal Environmental Research Laboratory, Cincinnati, OH.
- U.S. Environmental Protection Agency. 1986. Design Information Report: Belt Filter Presses, Water Engineering Research Laboratory, Cincinnati, OH.
- U.S. Environmental Protection Agency. 1987. Dewatering Municipal Wastewater Sludges, Municipal Environmental Research Laboratory, Cincinnati, OH.

- U.S. Environmental Protection Agency. 1990. National Sludge Survey.
- Verruijt, A. 1969. "Elastic Storage of Aquifers," in Flow Through Porous Media, ed. by R.J.M. DeWiest, Academic Press, New York, New York, 331-376.
- Vesilind, P.A. 1968. "Theoretical Considerations: the Design of Prototype Thickeners from Batch Settling Tests," Water and Sewage Works, 115, 302-307.
- Vesilind, P.A. 1979. "Sludge Dewatering," Treatment and Disposal of Wastewater Sludges, Ann Arbor Science, Ann Arbor, 135-205.
- Vesilind, P.A., G.C. Hartman, and E.T. Skene. 1986. "Sludge Dewatering," Sludge Management & Disposal for the Practicing Engineer, Lewis Publishers, Inc., Chelsea, Michigan, 40-62.
- Viessman, W., Jr. and M.J. Hammer. 1985. Water Supply and Pollution Control, Harper & Row, New York.
- Villiers, R.V. and J.B. Farrell. 1977. "A Look at Newer Methods for Dewatering Sewage Sludges," Civil Engineering, 47, No. 12, 66-71.
- Wahl, A.J., C.C. Larson, J.B. Neighbor, T.W. Cooper, W.J. Katz, J.J. Wirts, S.J. Sebesta, and J.B. Hanlon. 1964. "1963 Operators' Forum," Journal Water Pollution Control Federation, 36(4), 401-433.
- Wakeman, R.J. 1978. "A Numerical Integration of the Differential Equations Describing the Formation and Flow in Compressible Cakes," Transactions Institute Chemical Engineering, 56, 258-265.
- Wakeman, R.J. and Holdich, R.G. 1982. "Theoretical and Experimental Modeling of Solids and Liquid Pressures in Batch Sedimentation," Proceedings of the Filtration Society.
- Wakeman, R.J. and R.G. Holdrich. 1984. "Theoretical and Experimental Modeling of Solids and Liquid Pressures in Batch Sedimentation," Filtration and Separation, 21, 420-422.
- Weber, W.J., Jr. 1972. Physicochemical Processes for Water Quality Control, John Wiley & Sons, Inc., New York.
- Wells, S.A. 1988. National Science Foundation proposal.
- Wells, S.A. and R.I. Dick. 1988. "Synchrotron Radiation Evaluation of Gravity Sedimentation Effects Prior to Dewatering," Proceedings ASCE-CSCE National Conference on Environmental Engineering, Vancouver, B.C.
- Wells, S.A. and R.I. Dick, 1989. "Mathematical Modeling of Compressible Cake Filtration," in ASCE-CSCE National Conference on Environmental Engineering Proceedings, ed. by J. Malina, Austin, Texas, 788-795.

- Wells, S.A. 1990. Compressible Cake Filtration Modeling and Analysis, Ph.D. Dissertation, School of Civil and Environmental Engineering, Cornell University, Ithaca, N.Y.
- Wells, S.A. and R.I. Dick, 1993, "Permeability, Liquid and Solid Velocity, and Effective Stress Variations in Compressible Cake Filtration," Chicago American Filtration Society Conference, Chicago, IL.
- Willis, M.S. 1983. "A Multiphase Theory of Filtration," in Progress in Filtration and Separation, ed. by R.J. Wakeman, Elsevier Scientific, New York, 1-56.
- Yong, R.N. and C.A. Ludwig. 1984. "Large Strain Consolidation Modelling of Land Subsidence," Symposium on Geotechnical Aspects of Mass and Materials Transportation, Bangkok, Thailand.
- Znidarcic, D., and R.L. Schiffman. 1982. "On Terzaghi's Concept of Consolidation," Geotechnique, 32, 387-389, Discussions and Reply in Geotechnique, 34, 130-134.

APPENDIX A

GRAVITY SEDIMENTATION - FORTRAN COMPUTER CODE

```

C*****
C GRAVCU13.FOR (5/93)
C*****
C NUMERICAL SCHEME IS EXPLICIT FOR SOLID CONTINUITY WITH FTCS
C SCHEME IS EXPLICIT/IMPLICIT FOR "MOMENTUM" EQUATION WITH
C FORWARD DIFFERENCE IN TIME.  MODELER CAN CHOOSE BETWEEN
C UPWIND OR CENTRAL DIFFERENCE FOR SPATIAL DERIVATIVES
C*****
C
      IMPLICIT DOUBLE PRECISION(A-H,O-Z)
      real inert2, inert3, icoef, jcoef, kcoef, lcoef
      COMMON/OUT/ TIML,NPR,NITL,INPOR
      COMMON/POR/ V0,E0
      COMMON/POR/ DT,DZ,AREA,DVIS,K,EE(100),S0,TIM,TEMP,
1      EI,PAPP,RM,DL,NFIL,NSOL,FACT,EYLD
      COMMON/PRIM/ U(100),US(100),P(100),SIGMA(100),
1      AA(100),BB(100),CC(100),DD(100)
      COMMON/DIAG/ IDIAG(8),IPLOT,IDT
      COMMON/DOWN/ DIST(100),EET(100),UST(100)
      COMMON/PERMC/ PERMZ(100)
      COMMON/AVCAL/AVA,AVB,EL
      COMMON/PERMCAL/PKA1,PKB1,NKC,PKA2,PKB2,EKP,A
C
C READ IN INPUT FILE:
      CALL INIT(E0,THETA)
      WRITE(*,333)
333      FORMAT(1X,'ENTER DT IN S IN F10.0')
      READ(*,*)DT
      TIM=0.0
C -The following will determine whether to use an upwind or
C central difference scheme for the spatial derivative of
C solid velocity, DUDZ.
C -SCHEME=0 (Central Difference); SCHEME=1 (Upwind)
      WRITE(*,444)
444      FORMAT(1X,'ENTER SCHEME: 0=Central Difference (numerical',
      ' smoothing); 1=Upwind')
      READ(*,*)SCHEME
C
      SUMQ=0.0
      NSTOP=0
      VOLCUM=0.0
      DLL=DL
      DL2=DL
      NIT=0
      N30=1
      NP30=1
      DIST(1)=0.0
      NHOLD=0
      NFILT=1
C
C ESTABLISH DZ AND DIST (PRINTED AS J=2,K+1):
      IF(INPOR.NE.1)GO TO 65
      DZ=DIST(K+1)-DIST(K)
      DIST(K+2)=DIST(K+1)+DZ
      DIST(K+3)=DIST(K+2)+DZ
C REDO DOMAIN IF NO SOLIDS IN CELLS DUE TO SEDIMENTATION
      DO 64 J=1,K+1
64      IF(EE(J).EQ.1.0)GO TO 63
C
C DVOL IS TOTAL WATER VOL ABOVE CAKE AFTER FORMATION PERIOD
63      DVOL=AREA*(K-J+2)*DZ
      K=J-2
      DL=DIST(K+1)
      DLL=DL
      DL2=DL
      GO TO 1
C
65      DZ=DL/REAL(K)
C
      DO 4381 J=1,K+2
4381      DIST(J)=REAL(J-1)*DZ

```

```

do 457 j=1,k+1
  if(j.eq.1)write(12,507)dist(j),ee(j),tim
  if(j.eq.1)write(18,507)dist(j),us(j),tim
  if(j.ne.1)write(12,508)dist(j),ee(j)
457  if(j.ne.1)write(18,508)dist(j),us(j)
ngo=0
C
1  AV=AVV(EE(1))
C
C*****
C This solution technique involves two equations: (1) solid continuity;
C and (2) total momentum with continuity ("momentum"). The solid
C continuity is used to solve for porosity at the next timestep, and the
C the "momentum" - using the newly solved for porosity - is used to
C solve for the solid velocity at the next timestep.
C*****
C
C BOUNDARY CONDITIONS
  US(1)=0.0
  US(K+2)=us(k)

700  CONTINUE
C -Time: Compute max. allowable time step based on stability
C restrictions:
C
  ee(k+1)=ee(k)
  DO 4431 J=1,K+1
4431  PERMZ(J)=PERM(EE(J))
      PERMZ(K+2)=PERM(EE(K+1))
C
21  CONTINUE
  IF((TIM+DT).GT.TIML)DT=TIML-TIM
  NIT=NIT+1
  TIM=TIM+DT
C -Density parameters for kaolin slurry:
  DENL=1.0
  DENS=2.62
C -Other Parameters/Definitions:
  G=980.
C CALCULATE V0
  U(1)=V0
  V0=0.0
C
C THE FOLLOWING DO-LOOP BEGINS THE SOLUTION PROCESS:
  DO 10 I=1,K
    if(ee(i).eq.1.0)go to 10
C
C DEFINITIONS FOR DISCRETIZATION:
C -Distance:
  IF(I.GE.2)THEN
    DZM=DIST(I)-DIST(I-1)
  ELSE
    DZM=DZ
  DZP=DIST(I+1)-DIST(I)
  END IF
  DZB=0.5*(DZM+DZP)
C -Porosity:
  IF(I.GE.2)THEN
    EE1=(EE(I+1)+EE(I))/2.
    EE2=(EE(I-1)+EE(I))/2.
C UPPER BC *****
  IF(I.EQ.K)EE1=1.0
C *****
  ELSE
    EE1=(EE(I+1)+EE(I))/2.
    EE2=E0
  END IF
C

```

```

C SOLID CONTINUITY EQUATION:
  EET(I)=EE(I)+(((1.0-EE1)*US(i+1))-((1.0-EE2)*US(i)))
  *DT/DZP
  if(eet(i).gt.1.0)eet(i)=1.0
10 continue
C CALCULATE EOT AND VOT -NEW VARIABLES
  EOT=EET(1)
  VOT=0.0

C
C COMBINED MOMENTUM EQUATION:
C -Due to the repetition of these, the following variables are created:
C -Boundary conditions:
  US(1)=0.0
  US(K+2)=us(k)
  UST(K+2)=ust(k)
  UST(1)=0.0
  do 11 i=2,K+1
  DZP=DIST(I+1)-DIST(I)
  DZM=DIST(I)-DIST(I-1)
  DZB=0.5*(DZM+DZP)
C -Porosity:
  EE1=(EE(I+1)+EE(I))/2.
c Note that these terms should apply only in a thickening region,
c not in a region where the solid mass is declining...why don't these
c equations deal with that??? so a quick fix below....
  EE2=(EE(I-1)+EE(I))/2.
  if(i.eq.k+1)ee2=ee(k)
  if(ee2.gt.ei)ee2=ei
  EE2T=(EET(I-1)+EET(I))/2.
  if(i.eq.k+1)ee2t=eet(k)
C -Intrinsic Permeability:
  PERMZ2=(PERMZ(I)+PERMZ(I-1))/2.
C -Upwind or central diff. can be used for the spatial derivative of
C solid velocity, DUDZ. The "I" for solid velocity is defined
C differently than the "I" for porosity. All variables are evaluated
C around the "I" for solid velocity (which is the same as "I-1/2" for
C porosity).
c -Due to the repetition of these, the following variables are created:
C -Central difference:
  DEDT=(EE2T-EE2)/DT
  DEDZ=(EE(I)-EE(I-1))/DZB
  if(ee(i).ge.ei)dedt=0.0
  if(ee(i).ge.ei)dedz=0.0
  if(i.eq.k+1)dedz=0.0
  F=(EE2)*DVIS/PERMZ2
  POR=1.0-EE2
C -The solution is implicit, and uses the Thomas algorithm.
C Each term is divided into both a coefficient and solid velocity
C component (if it exists). The following are the coefficients,
C after linearizing.
  ACOEF=POR*DENL + EE2*DENS
  B1COEF=(DENL/EE2)*DENL*E0*V0
  B2COEF=-DENL*(POR**2)/EE2+EE2*DENS
  CCOEF=-(DENL/EE2)*DEDT
  DCOEF=-(DENL*E0*V0/EE2)*DEDT
  ECOEF=(DENL/EE2**2)*((E0*V0)**2)*DEDZ
  FCOEF=-(DENL/EE2**2)*E0*V0*DEDZ
  G1COEF=-(DENL/EE2**2)*E0*V0*POR*DEDZ
  G2COEF=-(DENL/EE2**2)*POR*DEDZ
  HCOEF=-DENL*(EOT*VOT-E0*V0)/DT
  ICOEF=EE2*G*(DENL-DENS)
  JCOEF=(F/POR)*(E0*V0)
  KCOEF=-(F/POR)
  LCOEF=EE2/(POR*AVV(EE2))*DEDZ
  term1=abs(acoef*us(i)/dt)
  convac=abs(b2coef*((us(i))**2)/dz)+abs(ccoef*us(i))+
1   abs(g2coef*((us(i))**2))
  gravit=abs(icoef)
  drag=abs(kcoef*us(i))
  es=abs(lcoef)
  if(es.eq.0.0)es=1.e-8

```

```

    if(TIM.EQ.180.AND.I.EQ.2)WRITE(13,515)(10*DIST(I)),
1      TERM1,CONVAC,TIM
    if(TIM.EQ.180.AND.I.EQ.2)WRITE(14,516)(10*DIST(I)),
1      GRAVIT,DRAG,ES,TIM
    if(TIM.EQ.180.AND.I.NE.2)WRITE(13,517)(10*DIST(I)),
1      TERM1,CONVAC
    if(TIM.EQ.180.AND.I.NE.2)WRITE(14,518)(10*DIST(I)),
1      GRAVIT,DRAG,ES
    if(TIM.EQ.1200.AND.I.EQ.2)WRITE(15,515)(10*DIST(I)),
1      TERM1,CONVAC,TIM
    if(TIM.EQ.1200.AND.I.EQ.2)WRITE(17,516)(10*DIST(I)),
1      GRAVIT,DRAG,ES,TIM
    if(TIM.EQ.1200.AND.I.NE.2)WRITE(15,517)(10*DIST(I)),
1      TERM1,CONVAC
    if(TIM.EQ.1200.AND.I.NE.2)WRITE(17,518)(10*DIST(I)),
1      GRAVIT,DRAG,ES
C -OMEGA CALCULATION
C Omega is the additional numerical diffusion coefficient
C Modeler can change omega at the screen by applying
C a multiplying factor. Omega is calculated at I=2.
    if(OMEGA.NE.0.0)GO TO 447
C To calculate omega at I=k:
C -Note: altho omega was derived from the "modified
C equation which has a single coefficient (G), here
C it uses G1 and G2. See thesis.
    OMEGA=(CCOEF+FCOEF+G1COEF+G2COEF-KCOEF)*DT*DZ/ACOEF
    WRITE(*,445)
    READ(*,446)FACTOR
445  FORMAT(1X,'ENTER OMEGA MULTIPLYING FACTOR in f15.6')
446  FORMAT(F15.6)
    OMEGA=OMEGA*FACTOR
C
C -SCHEME=0 (Central Difference); SCHEME=1 (Upwind)
447  IF (SCHEME.EQ.0) GO TO 6997
    IF (SCHEME.EQ.1) GO TO 6998
C -The following are for a central difference formulation:
6997 X0=-(DCOEF+ECOEF+HCOEF)+(ICOEF+JCOEF+LCOEF)
    X1=(THETA*B1COEF)/(2.0*DZB)-((1-2*THETA)*B2COEF)
1    /(4.0*DZB)+OMEGA*THETA
    Y1=(ACOEF/DT)+THETA*(-2.*OMEGA-CCOEF-FCOEF-G1COEF+KCOEF)+
1    (1.0-2.0*THETA)*G2COEF*US(I)
    Z1=-(THETA*B1COEF)/(2.0*DZB)+((1-2*THETA)*B2COEF*US(I+1))
1    /(4.0*DZB)+THETA*OMEGA
    X2=-(1.0-THETA)*((B1COEF+B2COEF*US(I-1))/(2.0*DZB)+OMEGA)
    Y2=(ACOEF/DT)+(1.0-THETA)*(2.*OMEGA+CCOEF+FCOEF+G1COEF+
1    (2.0*G2COEF*US(I))-KCOEF)
    Z2=((1.0-THETA)/(2.0*dzb))*(B1COEF+B2COEF*US(I+1))-
    (1.0-THETA)*OMEGA
C -The following defines variables within the tridiagonal
C system of equations for central difference:
    BB(I)=X2
    IF(I.EQ.K+1)BB(I)=BB(I)+Z2
    DD(I)=Y2
    AA(I)=Z2
    CC(I)=X1*US(I-1)+Y1*US(I)+Z1*US(I+1)+X0
    GO TO 11
C -The coefficients are simplified as follows, for upwind:
6998 X0=-(DCOEF+ECOEF+HCOEF)+(ICOEF+JCOEF+LCOEF)
    X1=OMEGA*THETA
    Y1=(ACOEF/DT)+THETA*((B1COEF/DZB)-CCOEF-FCOEF-G1COEF+KCOEF)+
1    (1.0-2.0*THETA)*((-B2COEF/2*dzb)+G2COEF*US(I))-2.*
1    OMEGA*THETA
    Z1=-((THETA*B1COEF)/(dzb))+((1.0-2.0*THETA)*
1    B2COEF/2*dzb)*US(I+1)+OMEGA*THETA
    X2=-OMEGA*(1.-THETA)
    Y2=(ACOEF/DT)+(1.0-THETA)*(((B1COEF+B2COEF*US(I))/dzb)+
1    CCOEF+FCOEF+G1COEF+(2.0*G2COEF*US(I))-KCOEF)+
1    2.*OMEGA*(1.-THETA)
    Z2=((1.0-THETA)/dzb)*(B1COEF+B2COEF*US(I+1))-
1    (1.-THETA)*OMEGA

```

```

C -The following defines variables within the tridiagonal
C system of equations for the upwind formulation:
  BB(I)=X2
  if(i.eq.k+1)bb(i)=bb(i)+z2
  DD(I)=Y2
  AA(I)=Z2
  CC(I)=X1*US(I-1)+Y1*US(I)+Z1*US(I+1)+X0
11  continue
C -SOLVE WITH THE THOMAS ALGORITHM
  IL=2
  IU=K+1
  CALL THOMAS (IL,IU)
c
  do 111 i=1,k+2
    if(i.eq.1)go to 110
    if(i.eq.k+2)go to 110
    UST(I)=CC(I)
C
C -THIS PRINTS DATA FOR PLOTTING AT SPECIFIED TIMES
110  ntim=tim
     min=60
     ntim60=ntim/min
     if((ntim60*min).ne.ntim.or.ngo.EQ.0) go to 111
     if(i.eq.1)write(12,507)dist(i),eet(i),tim
     if(i.eq.1)write(18,507)dist(i),ust(i),tim
     if(i.ne.1)write(12,508)dist(i),eet(i)
     if(i.ne.1)write(18,508)dist(i),ust(i)
C
111  CONTINUE
     if(ntim60*min.eq.ntim)ngo=0
     if(ntim60*min.ne.ntim)ngo=1
507  format(1x,F12.7,4X,E10.4,4X,F8.3)
508  format(1x,F12.7,4X,E10.4)
509  format(14(1X,E8.2),1X,F8.3)
515  format(1X,F8.3,2(1X,E10.4),1X,F8.3)
516  format(1X,F8.3,3(1X,E10.4),1X,F8.3)
517  format(1X,F8.3,2(1X,E10.4))
518  format(1X,F8.3,3(1X,E10.4))
500  FORMAT (1X,F10.5,1X,E10.4,1X,E10.4,1X,E10.4,1X,F10.8,1X,F14.8,
1    1X,E10.4,1X,F10.8,1X,F10.8)
C
  DO 701 I=1,k+1
    if(i.eq.k+1)go to 702
    EE(I)=EET(I)
702  continue
701  US(I)=UST(I)
     CALL SMASS(XX)
     WRITE(*,956)XX
     WRITE(11,957)tim,xx
956  FORMAT(1X,'MASS=',1X,E14.5)
957  FORMAT(1X,F8.3,1X,E14.5)
     IF(NITL.GT.NIT.and.TIML.GT.TIM)GO TO 700
C
  CLOSE(UNIT=10)
  CLOSE(UNIT=11)
  CLOSE(UNIT=12)
  CLOSE(UNIT=13)
  CLOSE(UNIT=14)
  CLOSE(UNIT=15)
  CLOSE(UNIT=16)
  CLOSE(UNIT=17)
  CLOSE(UNIT=18)
  CLOSE(UNIT=19)
  CLOSE(UNIT=20)
  CLOSE(UNIT=21)
C
C COMPUTE NEW DOMAIN
c  CALL SOLV2(NIT,NHOLD)
C  END
C

```

```

C*****
SUBROUTINE SOLV2(NIT,NHOLD)
C*****
C COMPUTES NEW DOMAIN AND
C SOLV2 SOLVES FOR LIQUID VELOCITY(CM/SEC)-U,
C SOLID VELOCITY(CM/SEC)-US,PORE WATER PRESSURE(GM/CM/SEC/SEC)-P,
C AND SOLID STRESS(GM/CM/SEC/SEC)-SIGMA,AND PERMEABILITY(CM*CM)
C
  IMPLICIT DOUBLE PRECISION (A-H,O-Z)
  DIMENSION E(100),D(100)
  COMMON/PERMC/ PERMZ(100)
  COMMON/DIAG/ IDIAG(8),IPLOT,IDT
  COMMON/PRIM/ U(100),US(100),P(100),SIGMA(100),
1    AA(100),BB(100),CC(100),DD(100)
  COMMON/POR/ DT,DZ,AREA,DVIS,K,EE(100),SO,TIM,TEMP
1    EI,PAPP,RM,DL,NFIL,NSOL,FACT,EYLD
  COMMON/PAR/ VO,E0
  COMMON/DOMN/ DIST(100),EET(100),UST(100)
C
C RECOMPUTE DOMAIN AND NEW DZ
C
C DIST:DIST FROM POROUS PLATE CORRESPONDING TO EE
C
C DURING NHOLD=1 NO DOMAIN HEIGHT CHANGE
C
  IF(NHOLD.EQ.1)GO TO 678
  DH=VO*DT*EE(1)
  DL=DL-DH
  KK=0
  SK1=(DL/DZ)+0.5
  SK2=SK1-INT(SK1)
  IF (SK2 .NE. 0.0)KK=1
  K=INT(SK1)+KK
  DIST(K+1)=DL
  DIST(K+2)=DL+(DIST(K+1)-DIST(K))
C
C CREATE LARGER CELL AT UPPER BOUNDARY IF DZ GETS TOO SMALL
C
  DZ1=DIST(K+1)-DIST(K)
  DZ2=DZ/4.
  IF(DZ1.LT.DZ2)GO TO 897
  GO TO 898
897 CONTINUE
  K=K-1
  DIST(K+1)=DL
  DIST(K+2)=DL+(DIST(K+1)-DIST(K))
898 CONTINUE
  CALL INTER(DIST(K+1),4,E1)
  EET(K+1)=E1
  CALL INTER(DIST(K+2),4,E1)
  EET(K+2)=E1
678 DO 3 J=1,K+2
3    EE(J)=EET(J)
C
  IF(NSOL.EQ.0)GO TO 50
C
50 RETURN
C END

```

```

C*****
C      SUBROUTINE INIT(E0,THETA)
C*****
C
C      INIT READS IN INPUT DATA AND INITIALIZES POROSITY ARRAY
C
C      IMPLICIT DOUBLE PRECISION (A-H,O-Z)
C      COMMON/DOMN/ DIST(100),EET(100),UST(100)
C      COMMON/POR/ ETERM(50),T2(50),NETERM
C      COMMON/POR/ DT,DZ,AREA,DVIS,K,EE(100),SO,TIM,TEMP,
1      EI,PAPP,RM,DL,NFIL,NSOL,FACT,EYLD
C      COMMON/OUT/ TIML,NPR,NITL,INPOR
C      COMMON/VOLUME/ V(50),T1(50),NVOL
C      COMMON/DIAG/ IDIAG(8),IPLOT,IDT
C      COMMON/AVCAL/ AVA,AVB,EL
C      COMMON/PERMCAL/ PKA1,PKB1,NKC,PKA2,PKB2,EKP,A
C
C      DEFINITION OF VARIABLES:
C      A: MEAN PARTICLE DIAMETER IN CM
C      AREA:AREA OF FILTRATION CELL IN CM**2
C      AVA,AVB:PARAMETERS USED IN AV CALCULATION IN AVV SUBROUTINE
C      (NOTE:AVA IN UNITS OF GM/CM/S/S)
C      EE:POROSITY AT EACH SPATIAL STEP FROM THE MEDIA
C      EKP:POROSITY AT WHICH PKA1,PKB1 IS VALID IN PERM SUBROUTINE
C      EI:INITIAL POROSITY OF THE SUSPENSION
C      DL:LENGTH OF DOMAIN(CM)
C      DT:TIME STEP IN SECONDS
C      DVIS:DYNAMIC VISCOSITY IN GM/CM/SEC
C      DZ:VERTICAL SPATIAL STEP IN CM
C      EL:LIMITING POROSITY BETWEEN PARTICLE/PARTICLE CONTACT AND NO
C      CONTACT
C      FACT:SAFETY FACTOR FOR TIME STEP STABILITY ANALYSIS 1.0>FACT>0.0
C      IDIAG:DIAGNOSTIC FLAGS THAT PRINT INTERMEDIATE CALCULATIONS
C      IDT:IF IDT=1, TIME STEP IS SET TO DT IN INPUT DATA FILE
C      IPLOT:IF EQUAL TO '1' AN OUTPUT FILE SUITABLE FOR PLOTTING IS MADE
C      K:NUMBER OF SPATIAL STEPS IN VERTICAL DOMAIN
C      NETERM:NUMBER OF TERMINAL POROSITY WITH TIME DATA
C      NITL:TIME LIMIT IN TIME STEPS FOR RUN TO CEASE
C      NKC:FLAG THAT USES CARMEN-KOZENY PERM IF NKC=1
C      NPR:FULL OUTPUT PRINTED EVERY NPR TIME CYCLES
C      NSOL:PARAMETER TO TURN ON(=1)OR OFF(=0)THE CALCULATION
C      OF VS,VL,P,SIGMA
C      NVOL:NUMBER OF FILTRATE VOLUME WITH TIME DATA
C      PAPP:APPLIED PRESSURE DIFFERENTIAL IN PASCALS(N/M**2)
C      PKA,PKB:PARAMETERS USD IN PERM VS POROSITY CALCULATION IN PERM
C      (NOTE:PKA IN UNITS OF CM*CM)
C      SO:SPECIFIC SURFACE(1/CM)(USED IN PERM IF NKC=1)
C      SYLD:EFFECTIVE STRESS AT WHICH SOLID PHASE YIELDS(PASCALS)
C      TEMP:TEMPERATURE OF THE SUSPENSION IN DEGREES CELSIUS
C      TIM:TIME SINCE BEHINNING OF THE RUN UPDATED IN MAIN SEC
C      TIML:TIME LIMIT IN SEC TO STOP CALCULATIONS
C
C      OPEN(UNIT=10, FILE='CAKEIN.DAT', STATUS='OLD')
C      OPEN(UNIT=11, FILE='CKFWGOUT.1', STATUS='NEW')
C      OPEN(UNIT=12, FILE='CKFWGOUT.2', STATUS='NEW')
C      OPEN(UNIT=13, FILE='CKFWGOUT.3', STATUS='NEW')
C      OPEN(UNIT=14, FILE='CKFWGOUT.4', STATUS='NEW')
C      OPEN(UNIT=15, FILE='CKFWGOUT.5', STATUS='NEW')
C      OPEN(UNIT=16, FILE='CKFWGOUT.6', STATUS='NEW')
C      OPEN(UNIT=17, FILE='CKFWGOUT.7', STATUS='NEW')
C      OPEN(UNIT=18, FILE='CKFWGOUT.8', STATUS='NEW')
C      OPEN(UNIT=19, FILE='CKFWGOUT.9', STATUS='NEW')
C      OPEN(UNIT=20, FILE='CKFWGOUT.10', STATUS='NEW')
C      OPEN(UNIT=21, FILE='AVV.OUT', STATUS='NEW')
C      READ(10,200)
C      READ(10,100)DL,AREA,TEMP,EI,PAPP,A,TIML,SYLD
C      READ(10,200)
C      READ(10,100)AVA,AVB,PKA1,PKB1,EL,FACT,THETA,PKB2
C

```

```

C CALCULATE DVIS BASED ON TEMP
  CALL INTER(TEMP,3,DVIS)
C
C CONVERT TO CGS SYSTEM, PASCALS(KG/M/SEC/SEC) TO (GM/CM/SEC/SEC)
  SYLD=10.*SYLD
C
C COMPUTE POROSITY AT WHICH CRACKING BEGINS...FILTRATION CEASES
  EYLD=(-1./AVB)*LOG((EXP(-AVB*EO ))+AVA*AVB*SYLD)
C
C IF INPOR=1,INITIAL POROSITY DISTRIBUTION IS GIVEN TO ALLOW FOR
C SEDIMENTATION
  READ(10,200)
  READ(10,101)INPOR,NVOL,NETERM,K,NPR,NITL,NFIL,NKC
  READ(10,200)
  READ(10,101)IPLOT,NSOL,IDT,IETERM
  READ(10,200)
  READ(10,101)IDIAG
C
C INITIALIZE POROSITY ARRAY
  DO 10 I=1,K
10  EE(I)=EI
  READ(10,200)
  IF(INPOR.NE.1)GO TO 11
    DO 13 J=1,K
13  READ(10,103)DIST(J),EE(J)
11  READ(10,200)
C
C TERMINAL POROSITY AS A FUNCTION OF TIME
  IF(IETERM.EQ.1)GO TO 14
  DO 12 J=1,NETERM
12  READ(10,103)ETERM(J),T2(J)
  E0=ETERM(1)
  GO TO 15
C COMPUTE ETERM FROM MV RELATIONSHIP
14  continue
  E0=(-1./AVB)*LOG((PAPP*AVA*AVB)+EXP(-AVB*EI))
  ETERM(1)=E0
15  CONTINUE
C  IF(IDIAG(1).EQ.1)WRITE(17,201)SYLD,EYLD,E0
  RETURN
C
C FORMAT STATEMENTS
C
100  FORMAT(8F10.5)
101  FORMAT(8I10)
103  FORMAT(2F10.5)
200  FORMAT(1X)
END

```

```

C*****
SUBROUTINE INTER(T,N,Z)
C*****
C
C INTER INTERPOLATES INPUT DATA TO OBTAIN DYNAMIC VISCOSITY, LIQUID
C VELOCITY AT Z=0, TERMINAL POROSITY
C
C T..TIME IN SEC OR TEMP IN DEG C OR POROSITY
C N..SPECIFIC VARIABLE TO INTERPOLATE:1=TERM POR
C                                     2=LIQ VEL
C                                     3=DVIS
C                                     4=NEW POROSITY
C Z..RETURNED VARIABLE
C IMPLICIT DOUBLE PRECISION (A-H,O-Z)
C DIMENSION VIS(15),VTEMP(15),X(100),Y(100)
C COMMON/DIAG/ IDIAG(8),IPLOT,IDT
C COMMON/PORTEM/ ETERM(50),T2(50),NETERM
C COMMON/POR/ DT,DZ,AREA,DVIS,K,EE(100),S0,TIM,TEMP,
1 EI,PAPP,RM,DL,NFIL,NSOL,FACT,EYLD
C COMMON/VOLUME/ V(50),T1(50),NVOL
C COMMON/DOMN/ DIST(100),EET(100),UST(100)
C
C THE FOLLOWING VISCOSITY(GM/CM/SEC)-TEMP(C) DATA IS FROM G. K.,
C BATCHELOR, AN INTRODUCTION TO FLUID DYNAMICS P.595,1967
C
DATA VIS/1.781,1.514,1.304,1.137,1.002,0.891,0.798,
1 0.720,0.654,0.548,0.467,0.405,0.355,0.316,
1 0.283/
DATA VTEMP/0.,5.,10.,15.,20.,25.,30.,35.,40.,50.,60.,
1 70.,80.,90.,100./
10 IF(N-2)10,20,30
NY=NETERM
DO 1 J=1,NY
X(J)=T2(J)
1 Y(J)=ETERM(J)
GO TO 5
20 NY=NVOL
DO 2 J=1,NY
X(J)=T1(J)
2 Y(J)=V(J)
GO TO 5
30 IF(N.EQ.4)GO TO 40
NY=15
DO 3 J=1,NY
X(J)=VTEMP(J)
3 Y(J)=VIS(J)*0.01
GO TO 5
40 NY=K+1
DO 4 J=1,NY
Y(J)=EET(J)
4 X(J)=DIST(J)
5 CONTINUE
C
C LINEAR INTERPOLATION
C
IF(N.EQ.1.AND.NETERM.EQ.1)GO TO 204
IF(T.LE.X(1))GO TO 206
IF(T.GE.X(NY))GO TO 207
C
DO 6 J=1,NY
IF(T.EQ.X(J))GO TO 201
6 IF(T.LT.X(J))GO TO 50
C
50 CONTINUE
DX=X(J-1)-X(J)
DY=Y(J-1)-Y(J)
SLOPE=DY/DX
Z=Y(J-1) + SLOPE*(T-X(J-1))
IF(N.EQ.2)Z=SLOPE/AREA
GO TO 202
C
201 Z=Y(J)

```

```

C AVERAGE SLOPE ON EITHER SIDE OF THE POINT
  IF(N.EQ.2)Z=((Y(J+1)-Y(J))/(X(J+1)-X(J))*0.5 +
1      (Y(J)-Y(J-1))/(X(J)-X(J-1))*0.5)/AREA
  GO TO 202
206 Z=Y(1)
  IF(N.EQ.2)Z=(Y(1)-Y(2))/(X(1)-X(2))/AREA
  GO TO 202
207 Z=Y(NY)
  IF(N.EQ.2)Z=(Y(NY-1)-Y(NY))/(X(NY-1)-X(NY))/AREA
  GO TO 202
204 Z=ETERM(1)
202 IF(IDIAG(7).EQ.1)WRITE(11,101)N,NY,T,Z,SLOPE
  RETURN
C
C FORMAT STATEMENTS
101 FORMAT(1X,'N=',I2,1X,'NY=',I2,1X,'T=',E10.3,1X,'Z=',E10.3,
1      1X,'SLOPE=',E10.3)
  END

```

```

C*****
FUNCTION AVV(EE)
C*****
IMPLICIT DOUBLE PRECISION (A-H,O-Z)
COMMON/AVCAL/ AVA,AVB,EL
avv=ava*exp(avb*ee)
go to 21
E=EE
IF(E.GT.EL.or.e.lt.0.55) GO TO 20
c BI-SECTION ROOT-FINDING TECHNIQUE
c This is an iterative root-finder for E=f( $\sigma$ ). After an
c initial guess ( $\sigma_0$ ),  $\sigma$  is halved or doubled until  $\sigma_1$ 
c is on the left and  $\sigma_2$  on the right of the root for
c the passed variable, E. Iterations are begun by interpo-
c lating for new  $\sigma$ s, assuming a linear relationship. E and
c  $\sigma_0$  are compared until they are very close.
SIGMA0=100.0
ZETA=0.54
EPI=2.0
11 E0=SIGMA0**((ZETA/(SIGMA0-EPI))-(1-ZETA))
12 DIFF0=E-E0
IF((DIFF0.GE.-0.000001).AND.(DIFF0.LE.0.000001))GO TO 20
IF(DIFF0.LT.0.0)THEN
13 SIGMA1=SIGMA0
SIGMA2=2.0*SIGMA0
SIGMA0=SIGMA2
E1=E0
E2=SIGMA2**((ZETA/(SIGMA2-EPI))-(1-ZETA))
E0=E2
DIFF1=DIFF0
DIFF2=E-E2
DIFF0=DIFF2
IF((DIFF0.LT.0.0).AND.(DIFF2.LT.0.0))GO TO 13
END IF
IF(DIFF0.GT.0.0)THEN
14 SIGMA2=SIGMA0
SIGMA1=0.5*SIGMA0
SIGMA0=SIGMA1
E2=E0
E1=SIGMA1**((ZETA/(SIGMA1-EPI))-(1-ZETA))
E0=E1
DIFF2=DIFF0
DIFF1=E-E1
DIFF0=DIFF1
IF((DIFF0.GT.0.0).AND.(DIFF1.GT.0.0))GO TO 14
END IF
c Find  $\sigma_0$  for new iteration:
SIGMA0=SIGMA2-(SIGMA2-SIGMA1)*(E2-E)/(E2-E1)
GO TO 11
20 CONTINUE
IF(E.GT.EL)then
AVV=1.E20
go to 21
end if
c next line is only for kaolin, very important!!!!
if(e.lt.0.55)then
avv=2.9e-9
go to 21
end if
c Compute coefficient of volume compressibility, mv in units of kPa-1
avv=-(E0*(ZETA*((SIGMA0-EPI)**(-1)))/SIGMA0
1 -ZETA*((SIGMA0-EPI)**(-2))*dLOG(SIGMA0))
c change of units to (gm/cm/s/s)^-1, conversion factor is *10^-4
avv=avv/(10.**4)
21 continue
RETURN
END

```

```

C*****
FUNCTION PERM(E)
C*****
  IMPLICIT DOUBLE PRECISION (A-H,O-Z)
  COMMON/PERMCAL/PKA1,PKB1,NKC,PKA2,PKB2,EKP,A
  COMMON/AVCAL/ AVA,AVB,EL
  COMMON/POR/ DT,DZ,AREA,DVIS,K,EE(100),SO,TIM,TEMP,
1    EI,PAPP,RM,DL,NFIL,NSOL,FACT,EYLD
  EKP=.65
  PKA2=PKA1*EXP((PKB1-PKB2)*EKP)
  IF(E.LE.EKP)PERM=PKA1*EXP(PKB1*E)
  IF(E.Gt.EKP)PERM=PKA2*EXP(PKB2*E)
  if(e.gt.ei.and.e.le.ekp)perm=PKA1*EXP(PKB1*ei)
  if(e.gt.ei.and.e.gt.ekp)perm=PKA2*EXP(PKB2*ei)
  RETURN
  END
C*****
SUBROUTINE SMASS(X)
C*****
C COMPUTES THE MASS IN THE DOMAIN
C [THE CALCULATION IS REALLY THE VOLUME OCCUPIED BY SOLIDS,
C TO OBTAIN THE MASS MULTIPLY BY THE MASS DENSITY OF SOLIDS]
C
  IMPLICIT DOUBLE PRECISION (A-H,O-Z)
  COMMON/DOM/ DIST(100),EET(100),UST(100)
  COMMON/POR/ DT,DZ,AREA,DVIS,K,EE(100),SO,TIM,TEMP
1    ,EI,PAPP,RM,DL,NFIL,NSOL,FACT,EYLD
C
  X=0.0
  DO 10 J=1,K
  DZZ=DIST(J+1)-DIST(J)
  E5=(EE(J+1)+EE(J))*0.5
10  X=X+DZZ*(1.-E5)*AREA
  RETURN
  END
C*****
SUBROUTINE THOMAS (IL,IU)
C*****
C THOMAS SOLVES A TRIDIAGONAL SYSTEM OF EQUATIONS BY ELIMINATION
C IL=SUBSCRIPT OF FIRST EQUATION
C IU=SUBSCRIPT OF LAST EQUATION
C BB=COEFFICIENT BEHIND DIAGONAL
C DD=COEFFICIENT ON DIAGONAL
C AA=COEFFICIENT AHEAD OF DIAGONAL
C CC=ELEMENT OF CONSTANT VECTOR
  IMPLICIT DOUBLE PRECISION (A-H,O-Z)
  COMMON/PRIM/ U(100),US(100),P(100),SIGMA(100),
1    AA(100),BB(100),CC(100),DD(100)
C
C ESTABLISH UPPER TRIANGULAR MATRIX
C
  LP=IL+1
  DO 10 I=LP,IU
  R=BB(I)/DD(I-1)
  DD(I)=DD(I)-R*AA(I-1)
10  CC(I)=CC(I)-R*CC(I-1)
C
C BACK SUBSTITUTION
C
  CC(IU)=CC(IU)/DD(IU)
  DO 20 I=LP,IU
  J=IU-I+1L
20  CC(J)=(CC(J)-AA(J)*CC(J+1))/DD(J)
C
C SOLUTION STORED IN CC
C
  RETURN
  END

```

APPENDIX B

SAMPLE INPUT FILE

DL	AREA	TEMP	EI	PAPP	A	TIML	SYLD
3.925	26.325	24.0	0.9465	117.60	1.0E-4	1525.	1.7E5
AVA	AVB	PKA1	PKB1	EL	FACT	THETA	PKB2
2.04E-13	28.9	2.70E-16	20.0	0.84	1.0	0.0	24.
INPOR	NVOL	NETERM	K	NPR	NITL	NFIL	NKC
0	0	1	079	95500	1001100	0	0
IPLLOT	NSOL	IDT	IETERM				
1	0	0	1				
IDIAG(1)	IDIAG(2)	IDIAG(3)	IDIAG(4)	IDIAG(5)	IDIAG(6)	IDIAG(7)	IDIAG(8)
1	0	0	0	0	0	0	0
INITPOR							
.025	.725						
.07500	.75900						
.12500	.78550						
.17500	.81820						
.22500	.84470						
.27500	.86430						
.32500	.87380						
.37500	.87740						
.42500	.88000						
.47500	.88150						
.52500	.88150						
.57500	.88150						
.62500	.88150						
.67500	.88150						
.72500	.88150						
.77500	.88150						
.82500	.88150						
.87500	.88150						
.92500	.88150						
.97500	.88150						
1.02500	.88150						
1.07500	.88150						
1.12500	.88150						
1.17500	.88150						
1.22500	.88150						
1.27500	.88150						
1.32500	.88150						
1.37500	.88150						
1.42500	.88150						
1.47500	.88150						
1.52500	.88150						
1.57500	.88150						
1.62500	.88150						
1.67500	.88150						
1.72500	.88150						
1.77500	.88150						
1.82500	.88150						
1.87500	.88150						
1.92500	.88150						
1.97500	.88150						
2.02500	.88150						
2.07500	.88150						
2.12500	.88150						
2.17500	.88150						
2.22500	.88150						
2.27500	.88150						
2.32500	.88150						
2.37500	.88150						
2.42500	.88150						
2.47500	.88150						
2.52500	.88150						
2.57500	.88150						
2.62500	.88150						
2.67500	.88150						
2.72500	.88150						
2.77500	.88150						
2.82500	.88150						
2.87500	.88150						
2.92500	.88150						
2.97500	.88150						
3.02500	.88150						
3.07500	.88150						

3.12500	.88150
3.17500	.88150
3.22500	.88150
3.27500	.88150
3.32500	.88150
3.37500	1.0
3.42500	1.0
3.47500	1.0
3.52500	1.0
3.57500	1.0
3.62500	1.0
3.67500	1.0
3.72500	1.00
3.77500	1.00
3.82500	1.00
3.87500	1.00
3.92500	1.00
ETERM	TIME

APPENDIX C

FORTRAN COMPUTER CODES FOR PROCESSING DATA AND MODEL OUTPUT

FORTRAN CODE TO SORT POROSITY DATA (DATA-EE.FOR)

```

C DATA-EE.FOR
C SORTS POROSITY DATA FROM "DATA.EE3" TO *.DT
  DIMENSION EE(40,40)
  CHARACTER*20 FN
  OPEN(1,FILE='1.DT',STATUS='NEW')
  OPEN(2,FILE='2.DT',STATUS='NEW')
  OPEN(3,FILE='3.DT',STATUS='NEW')
  OPEN(4,FILE='4.DT',STATUS='NEW')
  OPEN(5,FILE='5.DT',STATUS='NEW')
  OPEN(6,FILE='6.DT',STATUS='NEW')
  OPEN(7,FILE='7.DT',STATUS='NEW')
  OPEN(8,FILE='8.DT',STATUS='NEW')
  OPEN(9,FILE='9.DT',STATUS='NEW')
  OPEN(10,FILE='10.DT',STATUS='NEW')
  OPEN(11,FILE='11.DT',STATUS='NEW')
  OPEN(12,FILE='12.DT',STATUS='NEW')
  OPEN(13,FILE='13.DT',STATUS='NEW')
  OPEN(14,FILE='14.DT',STATUS='NEW')
  OPEN(15,FILE='15.DT',STATUS='NEW')
  OPEN(16,FILE='16.DT',STATUS='NEW')
  OPEN(17,FILE='17.DT',STATUS='NEW')
  OPEN(18,FILE='18.DT',STATUS='NEW')
  OPEN(19,FILE='19.DT',STATUS='NEW')
  OPEN(20,FILE='20.DT',STATUS='NEW')
  OPEN(21,FILE='21.DT',STATUS='NEW')
  OPEN(22,FILE='22.DT',STATUS='NEW')
  OPEN(23,FILE='23.DT',STATUS='NEW')
  OPEN(24,FILE='24.DT',STATUS='NEW')
  OPEN(25,FILE='25.DT',STATUS='NEW')
  OPEN(26,FILE='26.DT',STATUS='NEW')
  OPEN(27,FILE='27.DT',STATUS='NEW')
  OPEN(28,FILE='28.DT',STATUS='NEW')
  OPEN(29,FILE='29.DT',STATUS='NEW')
  OPEN(30,FILE='30.DT',STATUS='NEW')
  open(31,file='data.ee3')
  DO 200 J=1,40
    read(31,201)(ee(j,i),i=1,40)
200  CONTINUE
201  FORMAT(1X,20F6.4)
    DZ=0.5
    DO 100 IWR=1,22
    DO 100 J=1,39
      Z=(REAL(J)*DZ)-0.25
      Z1=Z/10.
      X=2.616*(1.0-EE(J,IWR))
      IF(EE(J,IWR).EQ.0.0)GO TO 100
      if(x.eq.0.0)go to 100
      if(x.lt.0.1)go to 100
202  FORMAT(1X,F10.5,4X,F10.5)
      WRITE(IWR,202)Z,X
100  CONTINUE
C
  STOP
  END

```

FORTRAN CODE TO CALCULATE SOLID VELOCITY FROM THE POROSITY DATA SET (SOLVEL.FOR)

```

c   program solvel
c
c   parameter(m=40,m1=m-1)
c
c   real zero,half,one,
1   dt,dz,ee1t,ee1,ee2,
1   ee(m,m),vs(m,m)
c
c   data zero,half,one/0.0,0.5,1.0/
c
c   dt=60.
c   dz=0.5
c   do 10 n=1,40
10  vs(1,n)=zero
c
c   open(10,file='data.ee3',status='old')
c   open(11,file='solvel.out', status='new')
c
c   READ IN POROSITY DATA:
c
c   do 100 i=1,m
100  read(10,'((1X,20f6.4))',end=101) (ee(i,n),n=1,m)
101  continue
c   close (10,status='keep')
c
c   COMPUTE SOLID VELOCITY:
c   Note: The i in the vs terms in this code is actually i+1
c   (in the gravcul1 code), and the i-1 in this code is i
c   do n=1,m1
c   do 301 i=2,m1
c   ee1t=(ee(i-1,n+1)+ee(i,n+1))*half
c   ee1=(ee(i,n)+ee(i+1,n))*half
c   if (ee1.eq.one) ee1=.99
c   ee2=(ee(i-1,n)+ee(i,n))*half
c   vs(i,n)=
1   ((ee(i,n+1)-ee(i,n))/dt)*dz+(one-ee2)*vs(i-1,n))/(one-ee1)
301  continue
c   end do
c
c   WRITE OUT SOLID VELOCITY DATA:
c
c   do i=1,m1
c   write(11,3000) (vs(i,n),n=1,m1)
c   end do
3000  format((1X,20e12.4))
c   close (11,status='keep')
c
c   stop
c   end

```

FORTRAN CODE TO SORT SOLID VELOCITY DATA (DATA-US.FOR)

```

C DATA-US.FOR
C SORTS SOLID VELOCITY DATA FROM "SOLVEL.OUT" TO *.DT
  DIMENSION US(40,40)
  OPEN(1,FILE='1.DT',STATUS='NEW')
  OPEN(2,FILE='2.DT',STATUS='NEW')
  OPEN(3,FILE='3.DT',STATUS='NEW')
  OPEN(4,FILE='4.DT',STATUS='NEW')
  OPEN(5,FILE='5.DT',STATUS='NEW')
  OPEN(6,FILE='6.DT',STATUS='NEW')
  OPEN(7,FILE='7.DT',STATUS='NEW')
  OPEN(8,FILE='8.DT',STATUS='NEW')
  OPEN(9,FILE='9.DT',STATUS='NEW')
  OPEN(10,FILE='10.DT',STATUS='NEW')
  OPEN(11,FILE='11.DT',STATUS='NEW')
  OPEN(12,FILE='12.DT',STATUS='NEW')
  OPEN(13,FILE='13.DT',STATUS='NEW')
  OPEN(14,FILE='14.DT',STATUS='NEW')
  OPEN(15,FILE='15.DT',STATUS='NEW')
  OPEN(16,FILE='16.DT',STATUS='NEW')
  OPEN(17,FILE='17.DT',STATUS='NEW')
  OPEN(18,FILE='18.DT',STATUS='NEW')
  OPEN(19,FILE='19.DT',STATUS='NEW')
  OPEN(20,FILE='20.DT',STATUS='NEW')
  OPEN(21,FILE='21.DT',STATUS='NEW')
  OPEN(22,FILE='22.DT',STATUS='NEW')
  OPEN(23,FILE='23.DT',STATUS='NEW')
  OPEN(24,FILE='24.DT',STATUS='NEW')
  OPEN(25,FILE='25.DT',STATUS='NEW')
  OPEN(26,FILE='26.DT',STATUS='NEW')
  OPEN(27,FILE='27.DT',STATUS='NEW')
  OPEN(28,FILE='28.DT',STATUS='NEW')
  OPEN(29,FILE='29.DT',STATUS='NEW')
  OPEN(30,FILE='30.DT',STATUS='NEW')
  open(31,file='solvel.out')
  DO 200 i=1,39
  read(31,201)(us(i,n),n=1,39)
200 CONTINUE
201 FORMAT((1X,20E12.4))
  DZ=0.5
  DO 100 IWR=1,30
  DO 100 I=1,39
  Z=(REAL(I)*DZ)-0.25
  X=US(I,IWR)
  if(x.eq.0.0)x=1.E-6
202 FORMAT(1X,E12.4,4X,F10.5)
  WRITE(IWR,202)abs(X),Z
100 CONTINUE
  STOP
  END

```

FORTRAN CODE TO SORT POROSITY OUTPUT FROM MODEL (MODEL+EE.FOR)

```

c      CHARACTER*20 FN
      OPEN(1,FILE='1.MD',STATUS='NEW')
      OPEN(2,FILE='2.MD',STATUS='NEW')
      OPEN(3,FILE='3.MD',STATUS='NEW')
      OPEN(4,FILE='4.MD',STATUS='NEW')
      OPEN(5,FILE='5.MD',STATUS='NEW')
      OPEN(6,FILE='6.MD',STATUS='NEW')
      OPEN(7,FILE='7.MD',STATUS='NEW')
      OPEN(8,FILE='8.MD',STATUS='NEW')
      OPEN(9,FILE='9.MD',STATUS='NEW')
      OPEN(10,FILE='10.MD',STATUS='NEW')
      OPEN(11,FILE='11.MD',STATUS='NEW')
      OPEN(12,FILE='12.MD',STATUS='NEW')
      OPEN(13,FILE='13.MD',STATUS='NEW')
      OPEN(14,FILE='14.MD',STATUS='NEW')
      OPEN(15,FILE='15.MD',STATUS='NEW')
      OPEN(16,FILE='16.MD',STATUS='NEW')
      OPEN(17,FILE='17.MD',STATUS='NEW')
      OPEN(18,FILE='18.MD',STATUS='NEW')
      OPEN(19,FILE='19.MD',STATUS='NEW')
      OPEN(20,FILE='20.MD',STATUS='NEW')
      OPEN(21,FILE='21.MD',STATUS='NEW')
      OPEN(22,FILE='22.MD',STATUS='NEW')
      OPEN(23,FILE='23.MD',STATUS='NEW')
      OPEN(24,FILE='24.MD',STATUS='NEW')
      OPEN(25,FILE='25.MD',STATUS='NEW')
      OPEN(26,FILE='26.MD',STATUS='NEW')
      OPEN(27,FILE='27.MD',STATUS='NEW')
      OPEN(28,FILE='28.MD',STATUS='NEW')
      OPEN(29,FILE='29.MD',STATUS='NEW')
      OPEN(30,FILE='30.MD',STATUS='NEW')
      OPEN(31,FILE='CKFWGOUT.2',STATUS='OLD')
900    read(31,900)
      format(1x)
      IWR=1
      DO 100 I=1,6000
      IF(I.EQ.1)GO TO 25
      ZZ=Z
25     READ(31,200,END=250)Z,X
      Z=Z*10.
      X=2.616*(1.0-X)
200    FORMAT(1X,F12.7,4X,E10.4)
      IF(I.EQ.1)GO TO 26
      IF(Z.LT.ZZ)IWR=IWR+1
      if(x.eq.0.0)go to 100
26     IF(Z.GT.40.0)GO TO 100
      WRITE(IWR,200)Z,X
100    CONTINUE
c
250    CONTINUE
      x=1.0
      z=0.0
      do 500 i=iwr+1,30
      write(i,200)z,x
500    continue
      STOP
      END

```

FORTRAN CODE TO SORT SOLID VELOCITY OUTPUT FROM MODEL (MODEL-US.FOR)

```

OPEN(1,FILE='1.MD',STATUS='NEW')
OPEN(2,FILE='2.MD',STATUS='NEW')
OPEN(3,FILE='3.MD',STATUS='NEW')
OPEN(4,FILE='4.MD',STATUS='NEW')
OPEN(5,FILE='5.MD',STATUS='NEW')
OPEN(6,FILE='6.MD',STATUS='NEW')
OPEN(7,FILE='7.MD',STATUS='NEW')
OPEN(8,FILE='8.MD',STATUS='NEW')
OPEN(9,FILE='9.MD',STATUS='NEW')
OPEN(10,FILE='10.MD',STATUS='NEW')
OPEN(11,FILE='11.MD',STATUS='NEW')
OPEN(12,FILE='12.MD',STATUS='NEW')
OPEN(13,FILE='13.MD',STATUS='NEW')
OPEN(14,FILE='14.MD',STATUS='NEW')
OPEN(15,FILE='15.MD',STATUS='NEW')
OPEN(16,FILE='16.MD',STATUS='NEW')
OPEN(17,FILE='17.MD',STATUS='NEW')
OPEN(18,FILE='18.MD',STATUS='NEW')
OPEN(19,FILE='19.MD',STATUS='NEW')
OPEN(20,FILE='20.MD',STATUS='NEW')
OPEN(21,FILE='21.MD',STATUS='NEW')
OPEN(22,FILE='22.MD',STATUS='NEW')
OPEN(23,FILE='23.MD',STATUS='NEW')
OPEN(24,FILE='24.MD',STATUS='NEW')
OPEN(25,FILE='25.MD',STATUS='NEW')
OPEN(26,FILE='26.MD',STATUS='NEW')
OPEN(27,FILE='27.MD',STATUS='NEW')
OPEN(28,FILE='28.MD',STATUS='NEW')
OPEN(29,FILE='29.MD',STATUS='NEW')
OPEN(30,FILE='30.MD',STATUS='NEW')
OPEN(31,FILE='CKFWGOUT.8',STATUS='OLD')
900  read(31,900)
    format(1x)
    IWR=1
    DO 100 I=1,6000
    IF(I.EQ.1)GO TO 25
    ZZ=Z
25    READ(31,200,END=250)Z,X
    Z=Z*10.
    x=10.*abs(x)
    if(x.eq.0.0)x=1.e-6
200  FORMAT(1X,E10.4,4X,F12.7)
    IF(I.EQ.1)GO TO 26
    IF(Z.LT.ZZ)IWR=IWR+1
26    IF(Z.GT.40.0)GO TO 100
    WRITE(IWR,200)X,Z
100  CONTINUE
    C
250  CONTINUE
    do 500 i=iwr+1,30
    write(i,200)x,z
500  continue
    STOP
    END

```

FORTRAN CODE TO COMPARE MODEL-DATA POROSITIES AND GIVE STATISTICS (STAT-EE.FOR)

```

c      STAT-EE.FOR
c      STATISTICS COMPARING POROSITY DATA TO MODEL PRED.
      DIMENSION CONC(150),DDIST(150)
      DIMENSION PDIST(150),PCONC(150),DCONC(150),X(1000)
      OPEN(65,FILE='stat.out',STATUS='new')
      L=1
      SUMM=0.0
      SUMR=0.0
      do 6000 iwr=1,22
      IF (IWR.EQ.1)OPEN(1,FILE='1.DT')
      IF (IWR.EQ.2)OPEN(2,FILE='2.DT')
      IF (IWR.EQ.3)OPEN(3,FILE='3.DT')
      IF (IWR.EQ.4)OPEN(4,FILE='4.DT')
      IF (IWR.EQ.5)OPEN(5,FILE='5.DT')
      IF (IWR.EQ.6)OPEN(6,FILE='6.DT')
      IF (IWR.EQ.7)OPEN(7,FILE='7.DT')
      IF (IWR.EQ.8)OPEN(8,FILE='8.DT')
      IF (IWR.EQ.9)OPEN(9,FILE='9.DT')
      IF (IWR.EQ.10)OPEN(10,FILE='10.DT')
      IF (IWR.EQ.11)OPEN(11,FILE='11.DT')
      IF (IWR.EQ.12)OPEN(12,FILE='12.DT')
      IF (IWR.EQ.13)OPEN(13,FILE='13.DT')
      IF (IWR.EQ.14)OPEN(14,FILE='14.DT')
      IF (IWR.EQ.15)OPEN(15,FILE='15.DT')
      IF (IWR.EQ.16)OPEN(16,FILE='16.DT')
      IF (IWR.EQ.17)OPEN(17,FILE='17.DT')
      IF (IWR.EQ.18)OPEN(18,FILE='18.DT')
      IF (IWR.EQ.19)OPEN(19,FILE='19.DT')
      IF (IWR.EQ.20)OPEN(20,FILE='20.DT')
      IF (IWR.EQ.21)OPEN(21,FILE='21.DT')
      IF (IWR.EQ.22)OPEN(22,FILE='22.DT')
      IF (IWR.EQ.23)OPEN(23,FILE='23.DT')
      IF (IWR.EQ.24)OPEN(24,FILE='24.DT')
      IF (IWR.EQ.25)OPEN(25,FILE='25.DT')
      IF (IWR.EQ.26)OPEN(26,FILE='26.DT')
      IF (IWR.EQ.27)OPEN(27,FILE='27.DT')
      IF (IWR.EQ.28)OPEN(28,FILE='28.DT')
      IF (IWR.EQ.29)OPEN(29,FILE='29.DT')
      IF (IWR.EQ.30)OPEN(30,FILE='30.DT')

c      IF (IWR.EQ.1)OPEN(31,FILE='1.MD')
      IF (IWR.EQ.2)OPEN(32,FILE='2.MD')
      IF (IWR.EQ.3)OPEN(33,FILE='3.MD')
      IF (IWR.EQ.4)OPEN(34,FILE='4.MD')
      IF (IWR.EQ.5)OPEN(35,FILE='5.MD')
      IF (IWR.EQ.6)OPEN(36,FILE='6.MD')
      IF (IWR.EQ.7)OPEN(37,FILE='7.MD')
      IF (IWR.EQ.8)OPEN(38,FILE='8.MD')
      IF (IWR.EQ.9)OPEN(39,FILE='9.MD')
      IF (IWR.EQ.10)OPEN(40,FILE='10.MD')
      IF (IWR.EQ.11)OPEN(41,FILE='11.MD')
      IF (IWR.EQ.12)OPEN(42,FILE='12.MD')
      IF (IWR.EQ.13)OPEN(43,FILE='13.MD')
      IF (IWR.EQ.14)OPEN(44,FILE='14.MD')
      IF (IWR.EQ.15)OPEN(45,FILE='15.MD')
      IF (IWR.EQ.16)OPEN(46,FILE='16.MD')
      IF (IWR.EQ.17)OPEN(47,FILE='17.MD')
      IF (IWR.EQ.18)OPEN(48,FILE='18.MD')
      IF (IWR.EQ.19)OPEN(49,FILE='19.MD')
      IF (IWR.EQ.20)OPEN(50,FILE='20.MD')
      IF (IWR.EQ.21)OPEN(51,FILE='21.MD')
      IF (IWR.EQ.22)OPEN(52,FILE='22.MD')
      IF (IWR.EQ.23)OPEN(53,FILE='23.MD')
      IF (IWR.EQ.24)OPEN(54,FILE='24.MD')
      IF (IWR.EQ.25)OPEN(55,FILE='25.MD')
      IF (IWR.EQ.26)OPEN(56,FILE='26.MD')
      IF (IWR.EQ.27)OPEN(57,FILE='27.MD')
      IF (IWR.EQ.28)OPEN(58,FILE='28.MD')
      IF (IWR.EQ.29)OPEN(59,FILE='29.MD')
      IF (IWR.EQ.30)OPEN(60,FILE='30.MD')

```

c

```

JWR=IWR+30
NMOD=0
DO 2000 J=1,100
  READ(JWR,3000,END=2001)PDIST(J),PCONC(J)
  NMOD=NMOD+1
2000  CONTINUE
2001  CONTINUE
3000  FORMAT(1X,F12.7,4X,E10.4)
c
IF(L.EQ.0)CI=PCONC(NMOD)
NDAT=0
DO 2500 I=1,100
  READ(IWR,2700,END=2501)DDIST(I),DCONC(I)
  NDAT=NDAT+1
2500  CONTINUE
2501  CONTINUE
2700  FORMAT(1X,F10.5,4X,F10.5)
c
N=NDAT
K=2
c
DO 4000 J=1,N
5  CONTINUE
  IF (DDIST(J).GT.PDIST(K)) THEN
    K=K+1
    IF (K .GT. NMOD)GO TO 4010
    GO TO 5
  ENDIF
9998 WRITE(65,9998)L,J,K,DDIST(J),PDIST(K)
  FORMAT(1X,3(1X,I3),2(1X,F8.4))

  IF(DDIST(J).EQ.PDIST(K)) THEN
    CONC(J)=PCONC(K)
    GO TO 19
  ENDIF
  Z=DDIST(J)
  ZLOW=PDIST(K-1)
  ZHI=PDIST(K)
  CLOW=PCONC(K-1)
  CHI=PCONC(K)
  CONC(J)=CLOW+((CHI-CLOW)*(Z-ZLOW))/(ZHI-ZLOW)
  IF (CONC(J).EQ.CI)GOTO 4010
c L: # OF COMPARISONS X: ERROR
19 IF(DCONC(J).EQ.0.0.OR.CONC(J).EQ.0.0)GO TO 4000
  X(L)=(DCONC(J)-CONC(J))
  SUMM=SUMM+X(L)
  SUMR=SUMR+(X(L))**2
9999 WRITE(65,9999)L,J,K,DCONC(J),CONC(J),X(L),SUMM,SUMR
  FORMAT(1X,3(1X,I3),5(1X,F8.4))
  L=L+1
4000 CONTINUE
4010 CONTINUE
  CLOSE(IWR)
  CLOSE(JWR)
6000 CONTINUE
NOBS=L
XMEAN=SUMM/NOBS
RMS=(SUMR/NOBS)**0.5
IF(NOBS.LT.50)STD=((SUMR-SUMM**2/NOBS)/(NOBS-1))**0.5
IF(NOBS.GE.50)STD=((SUMR/NOBS)-XMEAN**2)**.5
c
K=25
  WRITE(65,5500)L,XMEAN,RMS,STD
5500  FORMAT(1X,I5,3(1X,F10.6))
  close(unit=65)
STOP
END

```

FORTRAN CODE TO COMPARE MODEL-DATA SOLID VELOCITIES AND GIVE STATISTICS (STAT-US.FOR)

```

c      STAT-US.FOR
c      STATISTICS COMPARING SOLID VEL. DATA TO MODEL PRED.
      DIMENSION VS(150),DDIST(150)
      DIMENSION PDIST(150),PVS(150),DVS(150),X(1000)
      OPEN(65,FILE='stat.out',STATUS='new')
      SUMM=0.0
      SUMR=0.0
      L=1
      do 6000 iwr=1,21
      IF (IWR.EQ.1)OPEN(1,FILE='1.DT')
      IF (IWR.EQ.2)OPEN(2,FILE='2.DT')
      IF (IWR.EQ.3)OPEN(3,FILE='3.DT')
      IF (IWR.EQ.4)OPEN(4,FILE='4.DT')
      IF (IWR.EQ.5)OPEN(5,FILE='5.DT')
      IF (IWR.EQ.6)OPEN(6,FILE='6.DT')
      IF (IWR.EQ.7)OPEN(7,FILE='7.DT')
      IF (IWR.EQ.8)OPEN(8,FILE='8.DT')
      IF (IWR.EQ.9)OPEN(9,FILE='9.DT')
      IF (IWR.EQ.10)OPEN(10,FILE='10.DT')
      IF (IWR.EQ.11)OPEN(11,FILE='11.DT')
      IF (IWR.EQ.12)OPEN(12,FILE='12.DT')
      IF (IWR.EQ.13)OPEN(13,FILE='13.DT')
      IF (IWR.EQ.14)OPEN(14,FILE='14.DT')
      IF (IWR.EQ.15)OPEN(15,FILE='15.DT')
      IF (IWR.EQ.16)OPEN(16,FILE='16.DT')
      IF (IWR.EQ.17)OPEN(17,FILE='17.DT')
      IF (IWR.EQ.18)OPEN(18,FILE='18.DT')
      IF (IWR.EQ.19)OPEN(19,FILE='19.DT')
      IF (IWR.EQ.20)OPEN(20,FILE='20.DT')
      IF (IWR.EQ.21)OPEN(21,FILE='21.DT')
      IF (IWR.EQ.22)OPEN(22,FILE='22.DT')
      IF (IWR.EQ.23)OPEN(23,FILE='23.DT')
      IF (IWR.EQ.24)OPEN(24,FILE='24.DT')
      IF (IWR.EQ.25)OPEN(25,FILE='25.DT')
      IF (IWR.EQ.26)OPEN(26,FILE='26.DT')
      IF (IWR.EQ.27)OPEN(27,FILE='27.DT')
      IF (IWR.EQ.28)OPEN(28,FILE='28.DT')
      IF (IWR.EQ.29)OPEN(29,FILE='29.DT')
      IF (IWR.EQ.30)OPEN(30,FILE='30.DT')

c      IF (IWR.EQ.1)OPEN(31,FILE='1.MD')
      IF (IWR.EQ.2)OPEN(32,FILE='2.MD')
      IF (IWR.EQ.3)OPEN(33,FILE='3.MD')
      IF (IWR.EQ.4)OPEN(34,FILE='4.MD')
      IF (IWR.EQ.5)OPEN(35,FILE='5.MD')
      IF (IWR.EQ.6)OPEN(36,FILE='6.MD')
      IF (IWR.EQ.7)OPEN(37,FILE='7.MD')
      IF (IWR.EQ.8)OPEN(38,FILE='8.MD')
      IF (IWR.EQ.9)OPEN(39,FILE='9.MD')
      IF (IWR.EQ.10)OPEN(40,FILE='10.MD')
      IF (IWR.EQ.11)OPEN(41,FILE='11.MD')
      IF (IWR.EQ.12)OPEN(42,FILE='12.MD')
      IF (IWR.EQ.13)OPEN(43,FILE='13.MD')
      IF (IWR.EQ.14)OPEN(44,FILE='14.MD')
      IF (IWR.EQ.15)OPEN(45,FILE='15.MD')
      IF (IWR.EQ.16)OPEN(46,FILE='16.MD')
      IF (IWR.EQ.17)OPEN(47,FILE='17.MD')
      IF (IWR.EQ.18)OPEN(48,FILE='18.MD')
      IF (IWR.EQ.19)OPEN(49,FILE='19.MD')
      IF (IWR.EQ.20)OPEN(50,FILE='20.MD')
      IF (IWR.EQ.21)OPEN(51,FILE='21.MD')
      IF (IWR.EQ.22)OPEN(52,FILE='22.MD')
      IF (IWR.EQ.23)OPEN(53,FILE='23.MD')
      IF (IWR.EQ.24)OPEN(54,FILE='24.MD')
      IF (IWR.EQ.25)OPEN(55,FILE='25.MD')
      IF (IWR.EQ.26)OPEN(56,FILE='26.MD')
      IF (IWR.EQ.27)OPEN(57,FILE='27.MD')
      IF (IWR.EQ.28)OPEN(58,FILE='28.MD')
      IF (IWR.EQ.29)OPEN(59,FILE='29.MD')
      IF (IWR.EQ.30)OPEN(60,FILE='30.MD')

```

```

JWR=IWR+30
NMOD=0
DO 2000 J=1,100
  READ(JWR,3000,END=2001)PVS(J),PDIST(J)
  NMOD=NMOD+1
2000 CONTINUE
2001 CONTINUE
3000 FORMAT(1X,E10.4,4X,F12.7)
C
IF(L.EQ.0)VSI=PVS(NMOD)
NDAT=0
DO 2500 I=1,100
  READ(IWR,2700,END=2501)DVS(I),DDIST(I)
  NDAT=NDAT+1
2500 CONTINUE
2501 CONTINUE
2700 FORMAT(1X,E12.4,4X,F10.5)
C
N=19
K=2
C
DO 4000 J=1,N
  CONTINUE
  IF (DDIST(J).GT.PDIST(K)) THEN
    K=K+1
    IF (K .GT. NMOD)GO TO 4010
    GO TO 5
  ENDIF
  WRITE(65,9998)L,J,K,DDIST(J),PDIST(K)
9998 FORMAT(1X,3(1X,I3),2(1X,F8.4))
C
  IF(DDIST(J).EQ.PDIST(K)) THEN
    VS(J)=PVS(K)
    GO TO 19
  ENDIF
  Z=DDIST(J)
  ZLOW=PDIST(K-1)
  ZHI=PDIST(K)
  VSLOW=PVS(K-1)
  VSHI=PVS(K)
  VS(J)=VSLOW+((VSHI-VSLOW)*(Z-ZLOW))/(ZHI-ZLOW)
  IF (VS(J).EQ.VSI)GOTO 4010
C L: # OF COMPARISONS X: ERROR
IF(DVS(J).EQ.1.0.OR.VS(J).EQ.1.0)GO TO 4000
19 X(L)=(DVS(J)-VS(J))
  SUMM=SUMM+X(L)
  SUMR=SUMR+(X(L))**2
  WRITE(65,9999)L,J,K,DVS(J),VS(J),X(L),SUMM,SUMR
9999 FORMAT(1X,3(1X,I3),5(1X,E12.4))
  L=L+1
4000 CONTINUE
4010 CONTINUE
  CLOSE(IWR)
  CLOSE(JWR)
6000 CONTINUE
  NOBS=L
  XMEAN=SUMM/NOBS
  RMS=(SUMR/NOBS)**0.5
  IF(NOBS.LT.50)STD=((SUMR-SUMM**2/NOBS)/(NOBS-1))**0.5
  IF(NOBS.GE.50)STD=((SUMR/NOBS)-XMEAN**2)**.5
  WRITE(65,5500)L,XMEAN,RMS,STD
5500 FORMAT(1X,I5,3(1X,F10.6))
  close(unit=65)
  STOP
  END

```